universität wien

DISSERTATION / DOCTORAL THESIS

Titel der Dissertation /Title of the Doctoral Thesis

„Manipulation of Wnt signaling in tumorcells with antisense molecules“

verfasst von / submitted by

Matthias Vonbrüll, Bakk. MSc

angestrebter akademischer Grad / in partial fulfilment of the requirements for the degree of

Doctor of Philosophy (PhD)

Wien, 2018 / Vienna 2018

Studienkennzahl lt. Studienblatt / degree programme code as it appears on the student record sheet:	A 794685437
Dissertationsgebiet lt. Studienblatt / field of study as it appears on the student record sheet:	Doctor of Philosophy-Doktoratsstudium NAWI Bereich Lebenswissenschaften UG200
Betreut von / Supervisor:	Ao. Univ.- Prof. Dipl.- Biol. Dr. Angela Witte
Mitbetreut von / Co-Supervisor:	Dr. Czerny Thomas

Contents

Danksagung

Diese Arbeit wurde erst durch die Unterstützung und Motivation vieler Menschen möglich. In erster Linie möchte ich mich bei meinen Eltern bedanken. Ohne deren finanzielle Unterstützung und motivierenden Gespräche hätte ich dieses Projekt in den letzten Jahren nicht beenden können. Speziell in Bezug auf meine persönliche Motivation hat mir auch mein Bruder Simon sehr geholfen. Dank auch an meine Freunde und das Chelsea, die mich ab und zu dem Laboralltag entreißen konnten.

Sehr großer Dank geht an Dr. Thomas Czerny von der FH Campus Wien, der mir in seinem Team die Chance gegeben hat, an diesem spannenden Projekt zu arbeiten. Er hat mit seiner besonnenen Art und interessanten Diskussionen immer positiv eingewirkt. Dann möchte ich meine Laborkollegen erwähnen, die über die Jahre auch zu Freunden wurden. Elisabeth Riegel stand mir immer mit ihrer Erfahrung und ihrem Humor zur Seite. Dank meinen PhD Kolleginnen und Kollegen Sarah, Nini, Christoph und Stefan war oft eine gute Stimmung im Labor und beim Mittagessen.

Danke an meine Betreuerin Frau Ao. Univ.- Prof. Dipl.- Biol. Dr^{in}. Angela Witte die mich stets in allen Belangen unterstützt hat.

Des Weiteren möchte ich mich bei der Firma ugichem bedanken, die das Projekt ermöglicht hat.

1 Abstract

Since the invention of antisense molecules there have been numerous attempts to apply them therapeutically[1]. The FDA approvals of Fomivirsen[2], Pegaptanib[3] and Mipomersen[4] point out the great potential of antisense molecules. However, compared to the efforts made the output has been modest[5], but since new modifications to the molecules are developed permanently there is a demand on reliable assays to test them. Further, it is important to improve targeting strategies. Meaning, since it is theoretically possible to target any gene it is important to know the best way to do that once a powerful antisense molecule is available.
When it comes to potential new tumor therapies the canonical wnt signaling pathway is of great importance, since it involves an array of interesting target genes[6]. Among these, β-catenin plays a key role. This gene is not only the main player of wnt signaling but also overexpressed in many cancer types[7,8]. In order to test a new antisense strategy, with peptide nucleic acids (PNAs) targeting β-catenin within tumor cells, a splice based reporter assay was designed and optimised in this project. After the essay enabled a reliable quantification of the antisense effect of antisense molecules, we used it to screen different PNAs targeting multiple sites within β-catenin. These candidates revealed a nouveau strategy. Targeting of the splice donor of exon 13 of β-catenin is ideal, because it leads to a truncated version of the protein that retains its important interaction with Tcf/Lef proteins. Therefore, it competes with the wildtype β-catenin protein resulting in a dominant negative effect. That strategy is applicable with different kinds of antisense molecules given that they are suitable for a splice blockade. This offers great potential for future projects including β-catenin as a target gene.

One of the big challenges in optimising antisense molecules is the improvement of their binding affinity. Simple extension of oligonucleotide length does improve the binding affinity, but only to a certain degree[9]. In a second project, I investigated whether a new design with linked short oligonucleotides (Catemer Subunits) could improve binding affinity without losing specificity. The principal was tested, using fluorescence marked oligonucleotides and melting point analysis. Binding affinity was indeed improved, because of a higher degree of interaction between the catemer subunits.

Taken together this thesis presents a nouveau reporter assay capable of accurate detection of antisense effects within cancer cells and an interesting targeting strategy for ß-catenin that would be applicable in future projects. Further, first steps were done to improve binding affinity of antisense molecules representing a potential idea for further research.

2 List of abbreviations

$(NH_4)_2SO_4$ ..... *ammonium sulfate*
µl ..... *microliter*
µM ..... *micromolar*
7-AAD ..... *7-Aminoactinomycin D*
A2780 ..... *human ovarian cancer cell line*
acpcPNA ..... (2S)-amino-cyclopentane-(1S)- carboxylic acids *PNA*
aegPNA ..... N-(2-aminoethyl) glycine*PNA*
AIDS ..... acquired immunodeficiency syndrome
AMD ..... *age-related macular degeneration*
AP ..... *alkaline phosphatase*
APC ..... *adenomatous polyposis coli*
ARM ..... *armadillo repeats*
ASOs ..... *antisense oligonuleotides*
ASSP ..... *alternative splice site prediction*
ATCC ..... *American Type Culture Collection*
ATP ..... *adenosine triphosphate*
BRG1 ..... *brahma-related gene 1*
BSA ..... *bovine serum albumin*
CaCl ..... *calcium chloride*
CBP ..... *cyclic AMP response-element binding protein binding protein*
cDNA ..... *complementary DNA*
CK1α ..... *casein kinase1α*
CPP ..... *cell penetrating peptide*
CRISPR-Cas9 ..... *clustered regularly interspaced short palindromic repeats*
CtBP ..... *carboxy-terminal binding protein*
DEPC ..... *diethyl pyrocarbonate*
dH_2O ..... *destilled water*
DMEM ..... *Dulbecco's Modified Eagle's Medium*
dNTP ..... *deoxynucleoside triphosphates*
DsiRNAs ..... *Dicer-substrate short interfering RNAs*
DTT ..... *dithiothreitole*
E. Coli ..... *Escherichia coli*
ECL ..... *enhanced chemiluminescence*
EDTA .....*ethylenediaminetetraacetic acid*
EGFP ..... *enhanced GFP*
ESEs ..... *exonic splicing enhancers*
ESSs ..... *exonic splicing silencers*
EtOH ..... *ethanol*
FACS ..... *fluorescence-activated cell sorting*
FAP ..... *familial adenomatous polyposis*
FBS ..... *fetal bovine serum*

FCS ..... *fetal calf serum*
FDA ..... *food and drug administration*
FITC ..... *fluorescein isothiocyanate*
Fluc ..... *firefly luciferase*
FR ..... *folate receptor*
fz ..... *frizzled*
GAPDH ..... *glyceraldehyde 3-phosphate dehydrogenase*
GFP ..... *green fluorescent protein*
Gluc ..... gaussia luciferase
GPNA ..... *guanidine-based peptide nucleic acid*
GSK3β ..... *glycogen synthase kinase 3* β
h ..... *hours*
H_2O ..... *water*
HCC ..... *hepatocellular carcinoma*
HEK 293 T-REx ..... *human embryonic kidney cell line expressing a tetracycline repressor protein*
HeLa ..... *human cervical cancer cell line*
HEPES ..... *(4-(2-hydroxyethyl)-1-piperazineethanesulfonic acid buffer)*
hnRNPs ..... *heterogeneous nuclear ribonucleoproteins*
HoFH ..... *homozygous familial hypercholesterolaemia*
HSA ..... *human alpha-skeletal actin*
IPTG ..... *isopropyl-β-D-thiogalactopyranosid*
ISE ..... *intronic splicing enhancers*
ITS ..... *insulin-transferrin-selenium*
KCl ..... *potassium chloride*, *potassium chloride*
kDa ..... *kilo dalton*
KH_2PO_4 .....*potassium dihydrogen phosphate*
LB ..... *lysogeny broth*
LiCl ..... *lithium chloride*
LNA ..... *locked nucleic acid*
LNCaP ..... *human prostate carcinoma cell line*
LNPs ..... *lipid nanoparticles*
LRP ..... *low density lipoprotein receptor-related protein*
Lys ..... *lysine*
M ..... *molar*
m2h ..... *mammalian-two-hybrid*
Met-tRNAi ..... *methionyl tRNA specialised for initiation*
mg ..... *milligramm*
$MgCl_2$ ..... *magnesium chloride*
MgSO4 ..... *magnesium sulfate*
min ..... *minutes*
ml ..... *milliliter*
mM ..... *millimolar*

MO ..... *morpholino*
MOPS ..... *(3-(N-morpholino)propanesulfonic acid)*
mRNA ..... *messenger RNA*
ms ..... *milliseconds*
Na_2HPO_4 ..... *sodium hydrogen phosphate*
NaCl .....*sodium chloride*
NaOH ..... *sodium hydroxide*
ng ..... *nanogramm*
Nluc ..... *nano luciferase*
ODN ..... *oligodeoxynucleotide*
oligos..... *oligonucleotides*
PBS ..... *phosphate buffered saline*
PC-3 ..... *grade IV, adenocarcinoma human cell line*
PCP ..... *planar cell polarity*
PCR ..... *polymerase chain reaction*
PEG..... *polyethylene glycol*
pePNA ..... *phosphonic ester PNAs*
PIC ..... *pre-initiation complex*
pmol ..... *picomol*
PMSF ..... *phenylmethylsulfonyl fluoride*
PNA ..... *peptide nucleic acid*
PNK ..... *polynucleotide kinase reaction buffer*
POLR2A ..... *RNA polymerase II*
qPCR ..... *quantitative polymerase chain reaction*
RISC ..... *RNA induced silencing complex*
Rluc ..... *renilla luciferase*
RNA ..... *ribonucleic acid*
RNAi ..... *RNA interference*
RNase ..... *ribonuclease*
RNP ..... *ribonucleoprotein*
RT ..... *room temperature*
s ..... *seconds*
SD ..... *splice donor*
SDmut ..... *splice donor mutated*
SDS ..... *sodium dodecylsulfate*
siRNA ..... *small interfering RNA*
SNP ..... single nucleotide polymorphism
snRNA ..... *small nucleolar RNAs*
SW480 ..... *Dukes' type B, colorectal adenocarcinoma human cell line*
TAMRA ..... *tetramethylrhodamine*
TBP ..... *TATA box binding protein*
TBS-T ..... *tris-buffered saline with tween20*
Tbx5 ..... *T-box transcription factor 5*

Tcf3 ..... *transcription factor 3*
TLE ..... *transducin-like enhancer of split protein*
Tris ..... *tris(hydroxymethyl)aminomethane*
UV ..... *ultra violett*
VEGF ..... *vasular endothelial growth factor*
XGal *5-bromo-4-chloro-3-indolyl-β-D-galactopyranoside*

3 Introduction

Inhibition of gene expression

After the human genome sequence was published, it has been theoretically possible to inhibit the expression of almost any gene[1]. This is especially interesting in context of treatment of genetic diseases. Over the years a variety of reagents and strategies have been developed[10]. Among the favourite approaches are RNA interference and antisense oligonucleotides. While RNA interference (RNAi) uses the RNA interference pathway, which is present in all eukaryotic cells[11], antisense strategies are based on externally added oligo nucleotides which block translation initiation[12] or splicing[13].

3.1 RNA interference

Small interfering RNA (siRNA)

These synthetic 20 to 25 base pair double stranded RNAs use the RNAi pathway, and were first described in 1999 by the group of Baulcombe[14]. The inhibition or degradation of mRNA is caused by the antisense active strand being complementary to the target sequence. Explained in more detail this means that after entering the cell, siRNA is loaded, assisted by the enzyme dicer, to the endogenous RNA induced silencing complex (RISC). One strand of the siRNA - the so-called guide strand - is inserted into the RISC. The guide strand binds to the target mRNA and subsequently allows the RNase argonaute 2 sequence specific cleavage[11,15]. This endogenous gene silencing mechanism is present in all eukaryotic cells and can be used as a knockdown strategy.

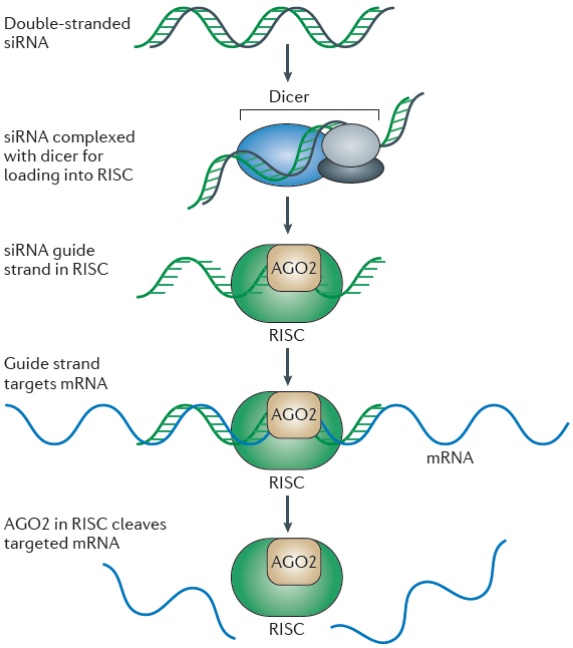

Figure 1. siRNA mechanism for down regulation of gene expression (from Kole et al. 2012)[15].

.

Intracellular delivery of siRNA oligonucleotides has been problematic due to their negative charges. Once the siRNA molecule manages to enter the cell, it is stable in the RISC for weeks being able to target multiple transcripts. But it is diluted with every cell division. Being not in complex with other molecules, siRNAs are small enough to be filtered in the kidney, they are quickly excreted. In order to circumvent delivery issues multiple strategies have been tested. One option is represented by incorporating siRNAs into lipid nanoparticles (LNPs). Whereas these can be easily delivered to cell culture cells by incubation[16], *in vivo* these complexes tend to accumulate in the liver and other filtering organs. Thereby the effect on other organs that may need delivery is decreased. Hence the focus of siRNA drug development has been focused on hepatic genes or treatment of liver tumors[17]. Wittrup et al. document that there is potential in LNP delivery to leaky or permeable vasculature, but delivery to solid tumors remains problematic[11]. More promising is targeted delivery to selected tissues or cells. Favourable for this strategy are aptamers, high affinity antibodies/antibody fragments or receptor ligands. These show better efficiency at lower doses combined with reduced toxicity. Targeting moieties can be bound covalently or non-covalently to siRNAs as well as co-delivered within LNPs. For example Ohyama et al. developed folate-PEG-appended dendrimer (G4)/α-cyclodextrin conjugates for better delivery. As tumors progress the expression level of folate receptor (FR) increases. It turned out to be a promising marker and a target protein for therapy. Experiments *in vitro* showed good endocytosis mediated uptake, better endosomal escape (siRNA can be trapped and degraded in endosomes - enhanced escape improves cytosolic delivery[18]), intracellular stability as well as low cytotoxicity. *In vivo* the siRNA conjugate resulted in stronger effects, longer blood circulating ability and serum stability[19].

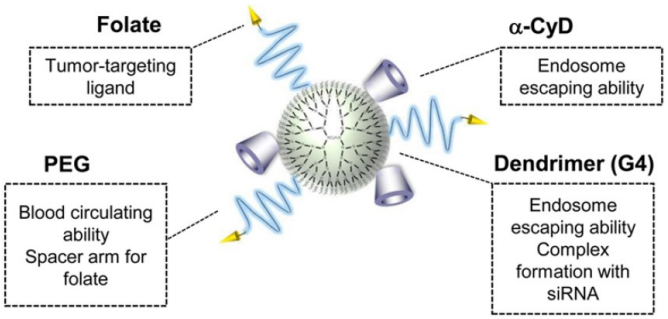

Figure 2. Folate-PEG-appended dendrimer (G4)/α-cyclodextrin conjugates for better siRNA delivery (from Ohyama et al. 2015)[19].

Bäumer et al. designed a complex of cell surface receptors internalising antibodies coupled to the siRNA carrier peptide protamine. As a result efficient binding and internalisation of siRNA into receptor positive cells was possible[20].
In summary, looking at studies from the last 2 years, it seems that siRNA enables a safe knockdown of liver genes. However it bears the risk of unintended clinical toxicity, favouring cautious development of siRNA therapies.
But new techniques based on modified mRNAs or CRISPR-Cas9 benefit from experiences with siRNA according to intracellular delivery. Since the hurdles of delivery are even greater for these techniques, siRNA should have an impact in the future[11].

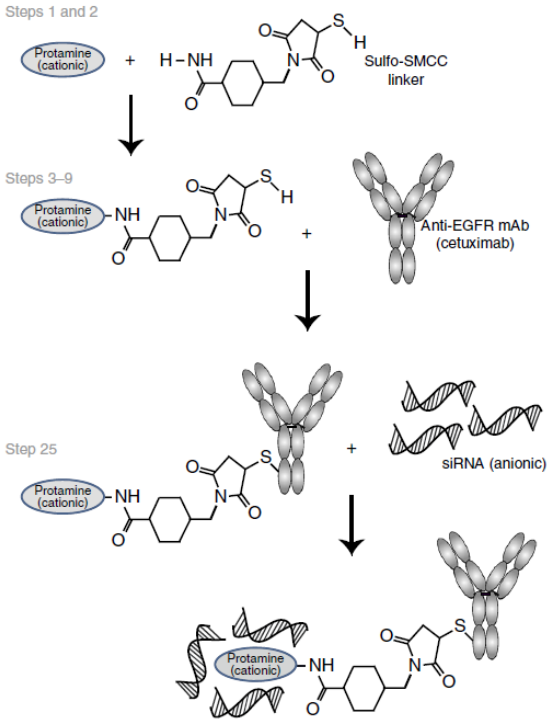

Figure 3. Example for an antibody-siRNA complex (from Bäumer et al. 2016)[20].

3.2 Discovery of antisense oligonucleotides

Antisense oligonucleotides (ASOs) are macromolecules designed to bind complementary to mRNA by Watson-Crick base pairing[21]. These synthetically engineered strands of deoxynucleotide sequences usually show a length between 18-21 nucleotides[1]. Translational processes may be arrested in different ways. Either cleavage mechanisms involving endogenous cellular nucleases like RNase H are activated, or enzymes involved in target gene expression are sterically blocked. Since the first appearance of antisense oligonucleotides in 1978 there has been a keen interest in improving their properties for therapeutic applications[1]. Zamecnik and Stephensen used a synthetic tridecamer oligodeoxyribonucleotide targeting Rous sarcoma virus RNA. Introduced to chick embryo fibroblasts blocking of viral protein translation was possible[22]. This idea brought huge potential for therapeutic use, hence gene specific knockdown seemed realistic, once ASOs would be refined sufficiently[5]. This would be interesting especially concerning treatment of genetic diseases[21].
So far three drugs have been FDA (Food and Drug Administration) approved:

1) In 1998 Fomivirsen was approved for the treatment of cytomegalovirus retinitis in AIDS patients. It is a phosphorothioate modified DNA oligonucleotide being intraocularly injected[2].

2) For treating neovascular (wet) age-related macular degeneration (AMD) a pegylated RNA aptamer called Pegaptanib was generated, and FDA approved in 2004[3]. By specifically binding the 165 isoform of VEGF it can reduce the elevated growth of blood vessels, typically for neovascular AMD[23].

3) Mipomersen a drug FDA approved in 2013 is targeting ApoB100 for treatment of homozygous familial hypercholesterolaemia (HoFH). This second generation antisense oligonucleotide contains a phosphorothioate modified backbone as well as 2'O-metoxyethyl modifications at the ends and is administered via intravascular injection.[4]

Successful use of these reagents in the clinic shows the great potential of antisense oligonucleotides for therapeutical use, but progress has been hampered due to issues as solubility, degradation by intracellular nucleases as well as cellular delivery. These have partially been resolved, and will be discussed in the following section with more detailed descriptions of commonly used antisense reagents[5].

3.3 Antisense strategies

Working with antisense reagents, there are two main strategies:

1) Steric hindrance of ribosome assembly can prevent translation. Therefore the start codon is targeted[12,24].
2) In order to achieve a splicing modulation, splice sites (either the splice donor or acceptor) are targeted resulting in a splice block. Reading frames can be either restored or shifted, making this option attractive for therapeutic approaches .[13,25,26]

Both strategies and their underlying mechanisms are described in this section.

1) Translation initiation and block

Regulation of gene expression takes place at different levels, one of them being the translation of mRNA into proteins. Since the reading frame of the message depends on it, the starting point needs to be determined accurately. Therefore the startcodon AUG is identified by a scanning mechanism. A small (40S) ribosomal subunit binds to mRNA near the 5'end in a so-called pre-initiation complex (PIC) with the methionyl tRNA specialised for initiation (Met-tRNAi), and scans the mRNA for complementarity with the Met-tRNAi[27]. AUG recognition is followed by joining a 60S ribosomal subunit to receive an elongation-competent 80S ribosome[28,29]. That's where antisense reagents[30,31] can interfere: targeting the 5' region by the AUG progression of the initiation complex can be physically blocked, thereby inhibiting ribosome assembly and subsequently translation of a certain protein[32]. This strategy has been shown to be very effective. For example morpholino oligonucleotides targeted in proximity of the AUG have been shown to be very effective[33].

2) Splicing mechanism and splicing modulation

For evolutionary benefits, e.g. improvement of mutation buffering or coding capacity, eukaryotic genes contain protein coding (exon) and non-coding (intron) sequences[34].There is need for a mechanism to excise the introns, before mRNA can be translated into protein. This step called splicing is executed by a large ribonucleoprotein (RNP) machine called the spliceosome. It takes place at conserved sequences called splice sites. These "consensus sequences" have been shown to be critical, since a change of these sequences results in an inhibition of splicing[35]. Within coding regions a single mutation can result in a frame shift and subsequent nonsense-mediated decay of the transcript[34]. Splice sites can be targeted and subsequently mechanically blocked with antisense molecules. As a result gene expression can be inhibited. Also reading frames can be restored in order to decrease the damage resulting of point mutations. Since

our splice assay as well as our targeting strategy depend on splicing modulations using PNAs there is a more in depth description of the topic in the section Peptide nucleic acids (see p. 18).

3.4 Intracellular delivery and different antisense reagents

Over the years lots of different approaches have been tested to improve reagents concerning the above mentioned issues (see p. 12)[1]. After discussing delivery options applicable to numerous reagents, the most important ones are listed with more detailed information.

3.4.1 Methods for intracellular delivery

Since the structure of antisense reagents does not always favour cell membrane permeability, different methods have been established to enable intracellular delivery. Herein the ones tested for my project are described.

3.4.1.1 Scraping

This method was developed for macromolecule delivery to adherent cells. After growing cells on a cell culture plate, they are scraped off the surface with a cell scraper. As a result perturbations of the membrane occur, subsequently leading to holes enabling macromolecule delivery. After the procedure the membrane is restored and the molecule trapped[36,37,38]. Efficiencies depend on cell type and exact protocol. In fibroblasts efficiencies of about 40% positive cells have been detected 18 h after scraping, with a viability from 50 to 60 %[36]. This method is very cheap hence it is not dependent on complex equipment, but in terms of transfection efficiency and reproducibility other methods (e.g. electroporation[39]) are better.

3.4.1.2 Electroporation

As scraping, electroporation also results in pores within the cell membrane making it permeable for macromolecules. Application of an electric field causes reorientation of the lipid molecules within the lipid bilayer, forming hydrophilic pores. Additionally the conduct current causes local joule heating, which induces thermal phase transitions of the bilayer[40,41]. Depending on the equipment efficiencies can reach from 70%[42] to more than 90%[39] and cell viability varies strongly as reported by Canatella and Prausnitz, who summed up results from 39 studies. Most showed around 50% viability, but fluctuation was high (29 ± 28%). Thanks to the good efficiency, this delivery method has become the standard method for transfection of various cell lines, over the years[43].

3.4.1.3 Transfection with poly-cations or cationic lipids

Poly-anionic oligo nucleotides as DNA, RNA, siRNA and Ribozymes can be delivered with poly-cations (e.g. polyethyleneimine) or cationic lipids. In both cases electrostatic complexes are formed that favour intracellular delivery of the oligonucleotides. Additionally these complexes protect the nuclease-sensitive oligo nucleotides from degradation[44]. This method is very popular due to the simple use and high reproducibility[45].

3.4.1.4 Co-transfection of synthetic oligonucleotide/DNA hybrids

This strategy has been first described by Hamilton et al. especially for PNAs which lack the backbone charges used for cationic lipid transfer of DNA and RNA. They used PNAs for inhibition of human telomerase and wanted to circumvent intracellular delivery issues. A PNA strand is hybridised with a partially overlapping DNA strand. Due to the negatively charged phosphodiester backbone of the DNA strand the hybrid can be transfected using cationic lipids (Fig. 11)[46]. Tested with a splice based luciferase assay, this method showed 85% correction of aberrant splicing at ≥ 400 nM concentrations[47]. In comparison with other options the method is cheap.

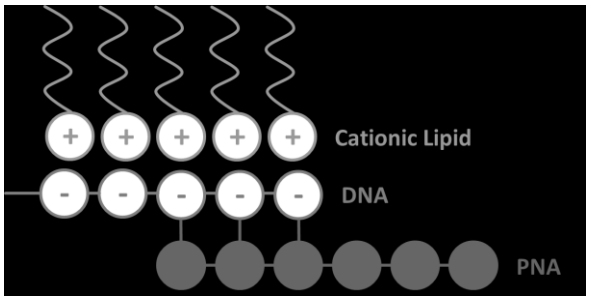

Figure 4. Principle of PNA/DNA-hybrid co-transfection.

3.4.1.5 CPPs (cell penetrating peptides)

CPPs are short peptides originating from proteins that are naturally able to cross cell membranes, or artificially designed to do so. Delivery of various biomolecules can be improved, ranging from low molecular weight drugs to nano particles[48]. CPPs have been successfully used in combination with PNA delivery. For this strategy cell penetrating peptides are conjugated to a PNA[49]. CPPs showed high potential *in vivo*. For example hematopoietic stem cell therapy experiments in mice[50] or successful induction of targeted exon skipping, to restore a reading frame of mutated dystrophin mRNA in mdx mouse muscles[13].

Figure 5. CPP principle

Summing up methods for intracellular delivery, it strongly depends on the exact application which delivery method works best. Reagent's characteristics as well as the tissue or cell type targeted are crucial. Preferably, antisense reagents show modifications within the molecule, which already favor intracellular delivery. History, characteristics as well as individual delivery options of different antisense molecules, are discussed in the following chapter.

3.4.2 Phosphorothioate oligodeoxynucleotides

First developed in 1966 by Eckstein et al. these new modifications to oligodeoxynucleotides have been of great importance for the progression of antisense strategies[51]. Since normal DNA is quickly digested by nucleases, it could not be used for antisense approaches[52]. Unmodified oligodeoxynucleotides in serum or living cells have shown half-lives of only 5 min or 30 min, respectively. Therefore modifications of the natural backbone were indispensable, in order to achieve stability in biological systems[53]. Phosphorothioate modified oligonucleotides show thiophosphate group modifications of phosphates[51]. These nucleotide analogues are insensitive to nucleases and can cause activation of RNase H. Thanks to their negative charges intracellular delivery by cationic lipids is possible[54]. An example for a phosphorothioate oligodeoxynucleotide successfully used in therapy is the - before mentioned - drug Fomivirsen. But while the negatively charged backbone is no problem for intraocular delivery, it can cause poor intracellular uptake being an issue for other applications[15]. Therefore, development of reagents with further modifications, determined to solve that problem, was pushed after the first breakthrough.

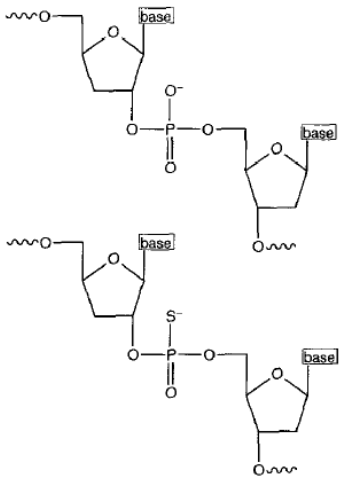

Figure 6. Comparison of DNA structure and nuclease resistant phosphorothioate linkage used in antisense oligonucleotides (from Stein 1996)[52].

3.4.3 Morpholino oligonucleotides

First developed by Summerton and his team in 1985, morpholino oligonucleotides are a DNA analogue with major modifications. 6-membered morpholine rings replace ring sugars present within naturally occurring nucleic acids. Further, negatively charged phosphate linkages of DNA and RNA have been replaced by phosphorodiamidate intersubunit linkages. Therefore morpholino oligonucleotides are stable in biological systems, their affinity for complementary RNA sequences is exceptional (due to the non-ionic phosphorodiamidate linkages) and morpholino oligonucleotides show excellent solubility in aqueous solution (about 100 mg/ml). Resulting from their unnatural backbone structure interactions with naturally occurring proteins are not common at a significant extent[55].

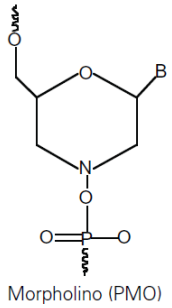

Figure 7. Phosphorodiamidate morpholino oligonucleotide structure (from Moreno et al. 2014)[4].

The minimum inhibitory length for morpholino oligonucleotides is about 14 to 15 bases. Meaning that morpholino oligonucleotides at this length are effective at inhibiting expression of their targeted mRNA. A longer morpholino oligonucleotide, including a contiguous stretch of 14 to 15 bases matching to a complementary RNA sequence, would also work. Most morpholino oligonucleotides for research use even show lengths of about 25. This, as well as the before mentioned high affinity, provides ability to invade most secondary structures common in RNA[55]. Due to the non-ionic nature of morpholino oligonucleotides, delivery to cell culture

cells with poly-cations or cationic lipids is impossible[44]. There are different other options including scraping[56,57], electroporation[58] or endocytosis based systems such as Endo-Porter[44]. For in vivo applications microinjection at the one cell stage of embryonic development[59,60] and electroporation[61], have shown to be efficient. In order to find miRNAs being under the influence of T-box transcription factor 5 (Tbx5) Chiavacci et al. injected specific morpholino oligonucleotides against this gene into one cell stage zebrafish embryos. As a result 70% of the embryos showed typical cardiac and fin defects[59]. Another example for successful gene targeting by injection of morpholino oligonucleotides to one cell stage zebrafish embryos would be Macaulay et al. They injected morpholino oligonucleotides for successful thyroid receptor β knockdown[60]. Munoz et al. combined injection of morpholino oligonucleotides targeting Sox2/3 to the spinal cord of *Xenopus laevis* with electroporation. This resulted in a clear reduction of Sox2 protein after the treatment[61]. During the last 15 years morpholino oligonucleotides played a big role within developmental biology studies. New tools like CRISPR are gaining relevance. Nonetheless, according to Blum et al. the importance of morpholino oligonucleotides as a gold standard will remain. Mainly due to the experience gained in the past, especially in developmental biology[62].

3.4.4 Locked nucleic acids (LNAs)

Synthesised simultaneously by Takeshi Imanishis[63] and Jesper Wengels[64] groups in 1997, LNAs are bicyclic nucleoside analogues containing
a methylene bridge connecting the 2′-oxygen of ribose with the 4′-carbon [65].

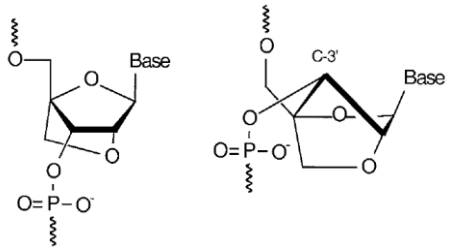

Figure 8. LNA (locked nucleic acid) structure (from Wahlestedt et al. 2000)[66].

As a result of this structure the melting temperature of oligonucleotides, with introduced LNA, bound to a matching RNA sequence, has been shown to be increased compared to standard oligonucleotides. Further biological stability, good efficiency as well as a lack of toxicity have been reported[65]. Most common antisense strategies pursued with LNAs include induction of RNase H cleavage[65], translational inhibition[67] and splicing inhibition[68]. For example Wahlestedt et al. showed in *in vivo* experiments that DNA/LNA co-polymers were better for RNase H mediated knock down of rat δ opioid receptor, than classic DNA ODNs (oligodeoxynucleotides)[66]. Another *in vivo* study by Fluiter et al. proved successful inhibition of tumor growth using another strategy. In this case LNAs were designed

to target the gene coding for the large subunit of RNA polymerase II (POLR2A)[69]. LNAs targeted for splicing inhibition were used to treat myotonic dystrophy in cell lines as well as in a mouse model by Wojtkowiak-Szlachcic et al. Further LNAs proved good stability within proliferating cells. Meaning the duration of a useful effect lasted about 20 days, significantly longer than a standard ODN. Therapeutic effects in muscle fibres of HSA^{LR} mice lasted 14 days - twice as long as siRNA activity in the same model. Further in vivo experiments may confirm the therapeutic potential of this reagent[68].

3.4.5 Peptide nucleic acids (PNAs)

Since PNAs were the main subject of our studies, they are described in more detail here.

3.4.5.1 General introduction, structure

PNAs first developed by Nilsen et al. in 1991 are a DNA analogue with unique properties. Their aim was to design an analogue that should be structurally similar to the DNAs deoxyribose phosphate backbone and easily be synthesised.[2] It was important to keep the number of backbone bonds and the distance to the nucleobases similar to DNA. The backbone of the resulting molecule consists of N-(2-aminoethyl) glycine subunits. Nucleobases are attached to glycine nitrogen by a methylene carbonyl linker[2]. As a result the neutrally charged backbone reduces electrostatic repulsion between the PNA strand and a target RNA or DNA strand, causing exceptional thermal stability and ionic strength of resulting hybrid complexes [70,71]. Another advantage is the insensitivity to enzymatic degradation due to the synthetic backbone[72]. Selective binding between oligonucleotide and target can be achieved using short oligonucleotide lengths of 13 to 18 bases[71,12]. With these properties PNAs have shown to be interesting for different applications including microRNA sensing[73], detection of SNPs[74], PCR clamping[75,76], on microarrays[77,78], for diagnostics[75,79] and also as a candidate for gene therapy[70].

3.4.5.2 Modifications of PNA structure

Progress with *in vivo* applications of PNAs has been delayed. Mainly due to low solubility of PNAs, with unmodified neutrally charged backbones, as well as poor cellular uptake[80]. Hence a lot of work has been done during the last years to resolve these issues by introducing different PNA modifications[72,81,82] as well as delivery strategies like cell penetrating peptides (CPPs)[13,49,50].

3.4.5.2.1 Modifications of the backbone

- A substitution of the backbone by 4’ proline units with (2’R, 4’R) configuration combined alternating with (2S)-amino-cyclopentane-(1S)-carboxylic acids (acpcPNA) was tested by Bohländer et al. In this case in-vitro experiments were made showing good strand invasion ability of acpcPNA. Hence the authors suggest use of acpcPNA/DNA hybrids for better intracellular delivery[83].

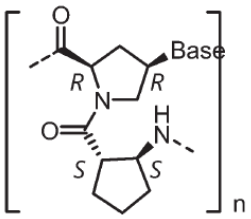

Figure 9. Monomeric unit of acpcPNA (from Bohländer et al. 2015)

- Another modification of Cα was tested by Zhou et al. They incorporated an arginine side chain (guanidinium functional group) into the backbone at Cα, creating a GPNA (Guanidine-Based Peptide Nucleic Acid). Improved intracellular delivery after incubation was verified by fluorescence microscope images. UV spectroscopy showed that, despite the modifications, binding ability to DNA had not decreased [84].

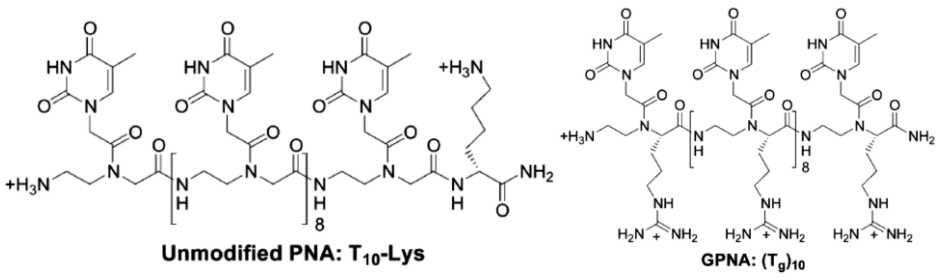

Figure 10. Chemical structure of GPNA (from Zhou et al. 2003)

- Addition of the side-chain can also take place at cγ of the side-chain (γGPNA). Sahu et al. synthesised γGPNAs and executed melting point analysis in order to determine binding affinity to target DNA strands. Resulting melting points were similar to unmodified PNA. Getting an impression of uptake efficiency was achieved by incubating TAMRA labelled γGPNA compared to unmodified, labelled PNA as well as TAT transduction domain. According to FACS analysis intracellular uptake was similar between TAT transduction domain and γGPNA. Both being about 2 orders of magnitude higher than uptake of unmodified PNA [85].

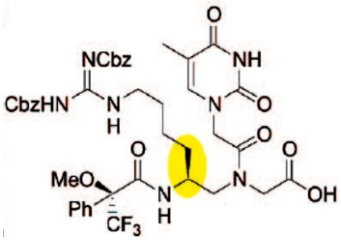

Figure 11. γGPNA (from Sahu et al. 2009)

- Modifications were further extended by Kumar through substitution of three carbon amino-propylene (amp) side chains at the γ-position to receive a Cγ-Aminopropylene peptide nucleic acid (amp-PNA). They did conformational analysis with circular dichroism studies of PNA:DNA and PNA:RNA duplexes. After comparing amp-PNA and control aeg-PNA, the modified amp-PNA showed more stable duplexes than the control ones. Further, analysis of tagged amp-PNAs by confocal microscopy showed good intracellular uptake [82].

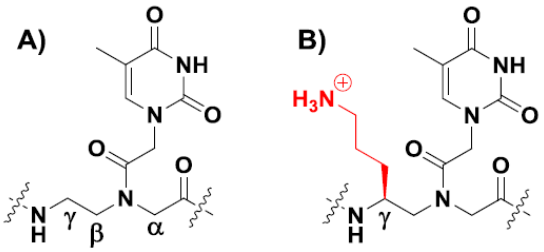

Figure 12. Chemical structure of Cγ-Aminopropylene peptide nucleic acid (amp-PNA) (from Kumar 2015)

- Similar to the two modifications first listed here (by Bohländer and Zhou), PNAs used for our studies include a modification of the Cα. For the synthesis, the company ugichem used an Ugi reaction. Among multi component reactions (MCRs) the Ugi 4-component reaction has become the most famous and versatile for PNA synthesis[86]. Thereby an amine, a carbonyl compound, a carboxylic acid and an isocyanide react in one process[87]. Being given the chance to combine such a large number of components, the Ugi 4-component reaction is ideal for generating large libraries and has also been favoured for PNA synthesis[87]. PNAs used in our experiments were modified by introducing phosphonic ester side chains into the backbone of aminoethyl glycine PNAs (aegPNAs), receiving phosphonic ester PNA variants (pePNA). As a result the structure is similar enough to aegPNA to keep their advantageous characteristics as high binding affinity and specificity, but with improved water solubility[88]. These modifications were tested successfully *in vivo* by injection into Medaka (Oryzias latipes) embryos. Efficient down regulation of the six3 gene as well as a block of gfp expression was demonstrated[88].

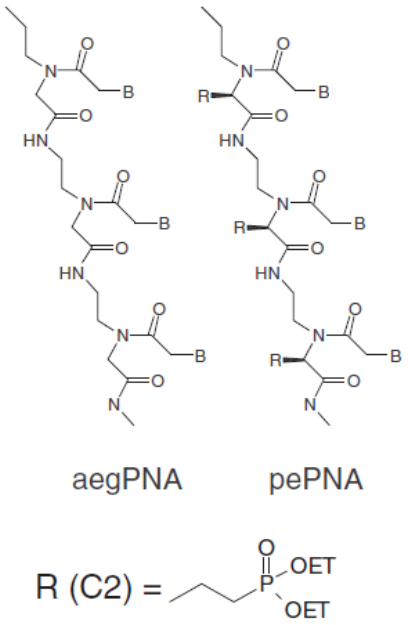

Figure 13. Chemical structure of PNAs (from Dorn et al. 2012)

Therefore a number of modifications have successfully been introduced into PNAs, most of them improved intracellular delivery without affecting binding strength to DNA or RNA.

3.4.5.3 Antisense strategies for PNAs

As with other antisense reagents it is most common to design PNAs either for a translation block or a splicing modulation. These mechanisms are described under “antisense strategies” (page 12/13). Due to its importance for the successful design of the splice based assay I herein describe the splicing mechanism and modulation in more detail. In order to successfully design PNAs specifically targeting splice sites the knowledge of the consensus sequence is of great importance. For human 5’ splice sites the sequence is MAG|GURAGU (M is A or C; R is purine)[35]. A spliceosome includes five U snRNPs called U1, U2, U4, U5 and U6. Complexes consisting of different snRNPs are distinguished and termed complex A, B and C. For first intron recognition the U1 snRNA base-pairs with the 5’splice site. Meanwhile U2 snRNA base-pairs with the branch point sequence of the intron[89]. This branchpoint sequence is conserved in yeast and mammalian pre-mRNAs. Within this sequence occurs an adenosine with a 2’-OH that forms the lariat intermediate during the first step of splicing. Besides the importance in splicing chemistry the branchpoint is also essential for splicing complex-formation[90]. Then complex B1 is formed by recruitment of tri-snRNP U4/U6.U5. Recently cryo-electron microscopy revealed the structure of this complex[91]. Once the spliceosome is assembled intron excision includes two major steps: first the 5’ splice site is cleaved and the intron is rearranged to a lariat structure. Subsequently the 3’ splice site is cleaved and the exons are ligated. Once splicing is completed the spliceosome is completely disassembled and its components can reunite to build another spliceosome.

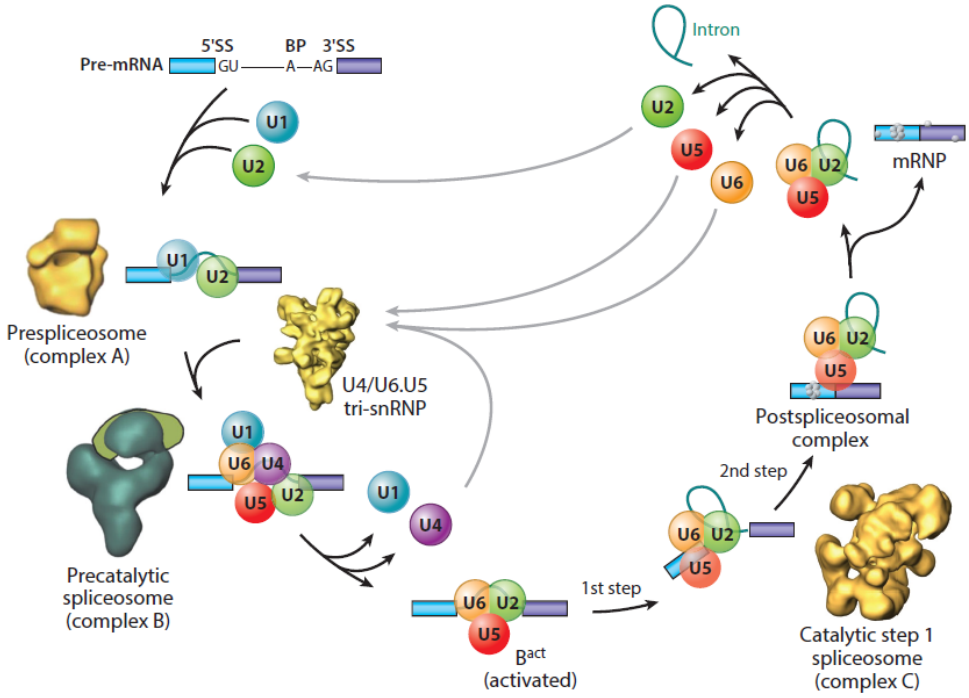

Figure 14. Spliceosome assembly and disassembly cycle (from Lee et al. 2015)

Alternative pre-mRNA splicing further increases the form and function of proteomes by making a single gene code for multiple proteins[89]. Which exons end up in the mature mRNA depends on cis-acting elements and trans-acting factors. Positive trans-acting factors as SR proteins (serine/arginine-rich family of nuclear phosphoproteins) bind to cis acting elements as exonic splicing enhancers (ESEs) and intronic splicing enhancers (ISE). Contrary to that, negative factors like heterogeneous nuclear ribonucleoproteins (hnRNPs) form exonic splicing silencers (ESSs). Interaction of these components subsequently leads to inhibition or promotion of spliceosome assembly[92]. Splice site selection differs between stronger and so-called cryptic splice sites. Cryptic ones are suppressed by nearby stronger ones - which is sequence dependant. These sites are either totally inactive or used at low levels. Activation of cryptic sites most likely happens after mutation of a nearby authentic or advantageous site[93]. Alteration of splicing patterns is not only dependant on splice sites. Disruptions of the before mentioned regulatory elements (ESEs, ISEs and ESs), alterations in the secondary structure of mRNA[94] as well as mutations within the spliceosome[95] can interfere with the splicing machinery. These mechanisms have to be taken into account, using ASOs designed to block splicing at defined sites. Because blocking of one splice site may activate a cryptic one next to it[96]. Consequences of blocking a splice site can be tested via PCR using specific primers[97].

Splicing dysregulation in disease

Dysregulation of splicing has shown to be the cause of a variety of diseases[34]. For treatment of splice based disease gene therapy shows great potential[98, 99, 100,101]. In order to show examples for the principle of splice based diseases, two well investigated ones with interesting therapeutic options using antisense molecules are described in detail here:

β-Thalassaemia

β-Thalassaemias are hereditary diseases caused by a variety of mutations (over 300) on the β-globin gene. Among these mutations were the first splicing mutations described [102,98]. Depending on the exact locus of the mutation follows a more or less severe reduction of β globin and adult haemoglobin subsequently leading to severe anemia and even death[103,102]. Distorted erythropoiesis and apoptosis within the erythroid lineage makes it necessary to treat patients lifelong with transfusion therapy and blood transfusion. During the last years, there have been great efforts to establish alternative therapies, mainly in the field of gene therapy. In order to restore correct splicing, phosphorothioate 2'-O- methyl-oligoribonucleotides[104] and PNAs were tested in cell culture experiments[105,106]. But

clinically most advanced approaches include use of lentiviral vectors for insertion of normal β-globin gene[98].

Duchenne muscular dystrophy (DMD)

DMD is an x-linked hereditary, lethal, neuromuscular disorder. Point mutations within the dystrophin gene are causing a disruption of the correct mRNA reading frame or generate a stop codon. This subsequently leads to shortened versions of the dystrophin protein (in-frame mutations e.g. Becker muscular dystrophy) or a total lack thereof (DMD). In healthy muscle cells dystrophin is important for membrane stability by linking the mobile actin filaments with the extracellular matrix (Fig. 15) [107]. A loss of connection means that the muscle fibres are very likely to get damaged during contraction. This causes chronic muscle damage accompanied by inflammation. As a result fat and fibrotic tissue replace muscle fibres and cause loss of muscle function[108].

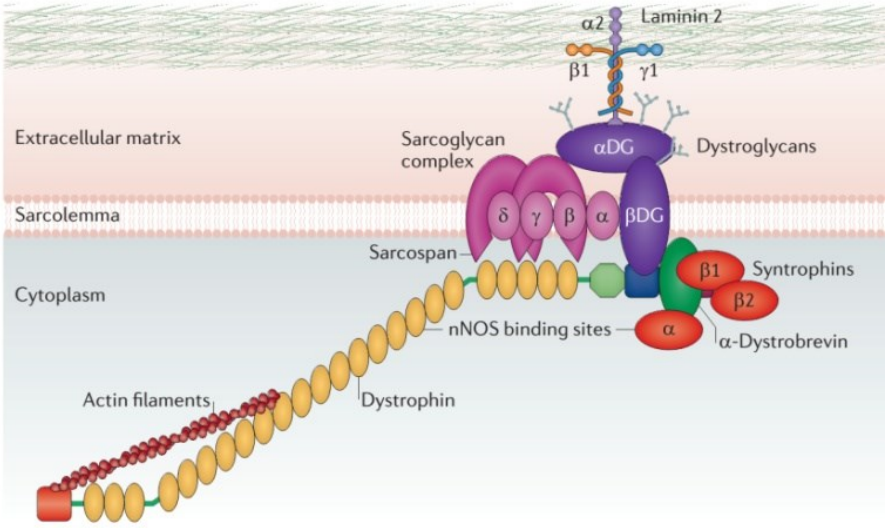

Figure 15. Dystrophin associated protein complex (from Fairclough et al. 2011)[107]

For treatment gene therapy seems very promising[107]. Antisense molecules could help restore the disrupted dystrophin pre-mRNA reading frame as proposed by Goyenvalle et al. They tested different snRNA constructs in a way that deletion of exons responsible for the frame shift, is prevented (Fig. 16). For example a deletion at exon 50 leads to a disrupted reading frame. In this case targeting exon 51 subsequently led to a skipping of this exon (51) and restored the reading frame. This produces a deleted but functional dystrophin, as it is typical for the less severe Becker's syndrome.

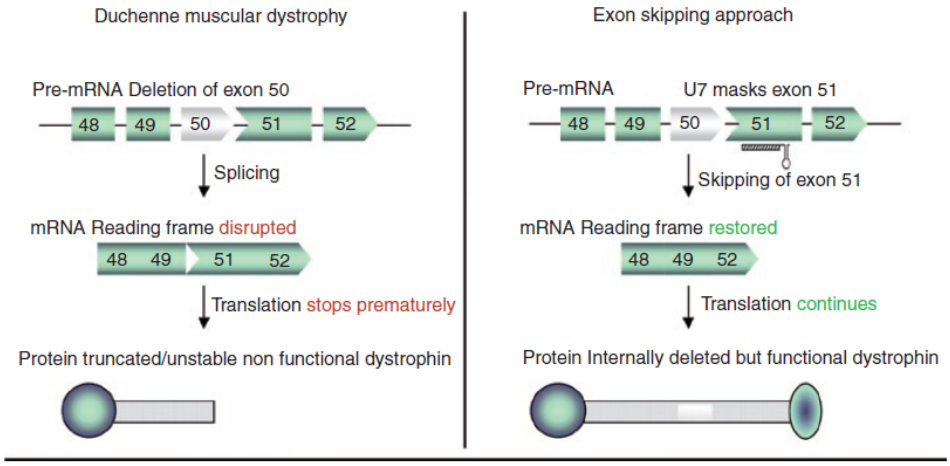

Figure 16. Example for restoring exon skipping for Duchenne muscular dystrophy (DMD) (from Goyenvalle et al. 2012)[99]

Following this principle the group tested 11 different exons relevant for DMD patients as well as in vivo experiments for a multi exon skipping approach. Thereby exon 45 to 55 were skipped, covering an area where most deletions within DMD patient genomes occur [99]. Recently a breakthrough was possible by using CRISPR/Cas9 for genome editing mediated restoring of dystrophin expression in a mouse model. CRISPR/Cas9 uses short RNA to direct degradation of foreign nucleic acids within bacteria and archaea. By creating custom guide RNAs the system can be used for function in mammal cells[109]. Using adeno-associated virus-9 enabled Long et al. and Tabebordbar et al. to deliver the components of CRISPR/Cas9 to mdx mice, which are a model for DMD. As a result dystrophin protein expression was restored to varying degrees in cardiac and skeletal muscle[100,101]. Besides adeno-virus associated delivery, Xu et al. also successfully electroporated CRISPR/Cas9 constructs to the flexor digitorum longus muscles of adult mdx mice[110]. Depending on the progress of development, antisense molecules may have the potential to be of importance for treatment of diseases as β-thalassemia or DMD, but the alternatives seem promising, too.

4 How to test antisense reagents

4.1 Reporter assays

In order to determine where and when a gene is expressed, reporter assays have shown to be a useful technique. Gene expression is determined by specific cis-regulatory DNA sequences. These can be studied by putting them next to a reporter gene, which stands under their control subsequently. Recombinant molecules can be introduced into cells enabling studies of expression patterns of genes. Additionally the influence of the tested regulatory cis-sequence can be monitored. There are different options to be chosen from reporter genes. Most prominent are fluorescent proteins as GFP (green fluorescent protein) or different

kinds of luciferases[111]. Here reporter genes used for my studies are described in more detail:

4.1.1 Luciferases

Luciferase enzymes catalyse light emitting reactions based on various substrates. These (reactions) lead to the emission of photons which can be measured. A main advantage compared to fluorescence is, that there is no need for excitation light energy[112].
Many bioluminescent organisms have been described as a source for luciferases. Such as luciferases from the North american firefly (*Photinus pyralis*)[113], Sea pansy (*Renilla Reniformis*)[114], the Copepod *Gaussia princeps*[115] as well as the deep sea shrimp *Oplophorus gracilirostris*[116] have been used for reporter assays successfully.
Assays can be designed using two different luciferases. The Emission of one luciferase is being determined for detection of target gene activity, and the second one as a control for normalisation. Normalisation helps to account for differences in cell number, cytotoxicity and transfection efficiency.[112]

4.1.1.1 Firefly luciferase (Fluc)

It has been isolated from the North american firefly (*Photinus pyralis*) and is one of the best described luciferases. First cloned by de Wet et al. 1985, Firefly luciferase (Fluc) has a molecular weight of 62 kDa. It requires luciferin, O_2 and ATP as substrates for the two reactions it catalyses:

$$\text{Firefly luciferase + luciferin + ATP} \overset{Mg^{2+}}{\leftrightarrow} \text{Firefly luciferase} \cdot \text{luciferyl-AMP + } PP_i$$

$$\text{Firefly luciferase} \cdot \text{luciferyl-AMP + } O_2 \rightarrow \text{Firefly luciferase + oxyluciferin + AMP + } CO_2 + h\nu$$

Finally a yellow-green light is emitted with a peak emission wavelength at 560 nm[113].

4.1.1.2 Renilla luciferase

Renilla luciferase (Rluc) was isolated from the sea pansy (*Renilla Reniformis*) and first cloned by Lorenz et al. in 1991. The molecular weight is 36 kDa and as substrates Rluc needs coelenterazine and O_2. Decarboxylation of coelenterazine produces coelenteramide and blue light emission at a wavelength of 480 nm[114].

4.1.1.3 Gaussia luciferase (Gluc)

Cloning of the cDNA encoding luciferase of *Gaussia princeps* was achieved in 2002 by Bryan et al. (Gluc) has a molecular weight of 19.9 kDa and uses coelenterazine and O_2 as substrates to produce the excited state coelenteramide. During relaxation to the ground state coelenteramide emits blue light at 470 nm[117]. Contrary to the before mentioned luciferases, Gluc is secreted by the cells leading to a significantly longer protein half live (once protein is secreted from cells)[112]. Subsequently it accumulates in the cell culture medium and increases the signal brightness[116].

4.1.1.4 Nano luciferase (Nluc)

In order to create a bioluminescence system with better chemical characteristics and higher light emission Hall et al. presented Nluc in 2002. A luciferase from the deep sea shrimp *Oplophorus* showed good potential. It consists of two 19 kDa and two 35 kDa subunits. Finally, the researchers realised that only the smaller subunit (Oluc-19) provides bioluminescent activity. The new Nluc produces luminescence signals about 150-fold higher than that of Fluc or Rluc. In mammalian cells no posttranslational modifications have been reported. Further Nluc shows improved physical stability and retaining activity up to 55°C. Taken together Nluc shows advantageous properties compared to other luciferases[116].

4.1.2 Splice based reporter assays

As mentioned above, splice blocking is one option for gene knockdown with antisense reagents. In order to quantify the knock down effect of antisense reagents, splicing based test systems can be integrated into reporter essays[118,119,48,49]. This brings several advantages. Typically cell based systems to test antisense activity are based on inhibited protein synthesis. Kang et al. mention drawbacks as a low signal-to-noise ratio and a delayed response due to dependence on protein stability (of protein translated from the mRNA targeted). Further contribution of cytotoxicity from a strategy to global protein synthesis, and the site of the antisense activity within the cell (nuclear or cytoplasmic) are unknown.
Using systems, wherein the antisense oligonucleotide activity results in an activation of luciferase gene expression, avoids such drawbacks[118]. First antisense oligonucleotides were used to restore reading frames, searching for new options within gene therapy. This was described by Sierakowska and her team, who restored splicing of the DMD gene in a cell culture model[104]. Here the main goal

was development of treatment strategies for β-globin. This knowledge could also be used for assay design. Therefore an intron from β-globin carrying a point mutation (IVS2-705) was inserted into a luciferase plasmid[118]. Regular splicing results in a non-functional luciferase protein, due to the shifted reading frame. Treatment with antisense reagents, targeted specifically to aberrant splice sites, prevents aberrant splicing. As a result the reading frame for the luciferase gene is restored resulting in EGFP translation, enabling a sensitive, positive readout of the antisense activity[118]. A similar approach was used by Sazani et al. after insertion of the human β-globin intron IVS2-654 into EGFP cDNA[120] or Younis et al. who inserted a chimeric β-globin/immunoglobulin intron into firefly luciferase. This system allowed fast screens for regulators of splicing [121].

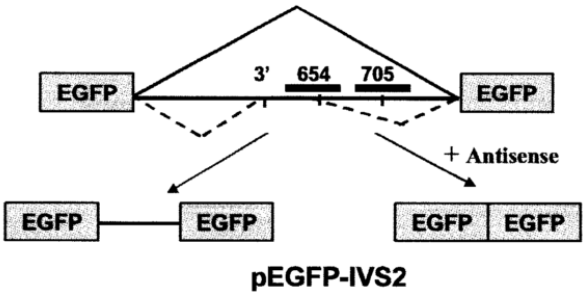

Figure 17. Splicing of IVS2-654 EGFP pre-mRNA (from Sazani et al. 2001)[120].

5 Cancer related targets: Wnt-signaling

5.1 General introduction

During the last decade the Wnt-signaling pathway showed to be of importance in development as well as disease. First discovery of the mouse wnt1 gene (originally int1) was made 1982 by Nusse and Varmus[122]. After sequencing it's description as a homolog of the Drosophila wingless (wg) was possible (Rijsewijk et al., 1987)[123].
Further studies verified the importance of Wnt signaling in development throughout the animal kingdom. Injection of mouse Wnt1 into Xenopus blastomeres even lead to a duplication of the body axis, showing how strongly conserved the pathway is within vertebrates. In 1991 the groups of Kinzler and Nishisho discovered the adenomatous polyposis coli (APC) gene in familial adenomatous polyposis (FAP). That discovery was followed by a confirmation of an interaction of APC with β-catenin, representing the first connection of Wnt pathway and human cancer[122].
So far three pathways have been described to be dependent on wnt receptor activation: The Wnt/Ca^{2+} pathway, the noncanonical planar cell polarity (PCP) pathway and the canonical Wnt/β-catenin cascade. Canonical Wnt/β-catenin

signaling is best described and will be discussed in detail, due to its relevance for cancer development[122].

5.1.1 Canonical Wnt/β-catenin signaling

In order to understand the dynamics of the pathway it is advantageous to first know what happens in the inactive state:
Without binding of Wnt proteins to frizzled (fz)/LRP5/6 co-receptors, a so-called destruction box is built in the cytosol and captures the transcriptional activator β-catenin. This complex consists of adenomatous polyposis coli (APC), Axin, glycogen synthase kinase 3 (GSK3β) and casein kinase1α (CK1α). While APC and Axin catch β-catenin, the two kinases GSK3β and CK1α phosphorylate its amino terminus. As a result β-TRCP binds and mediates the ubiquitinylation and subsequent proteasomal degradation of the protein. Due to the lack of β-catenin within the nucleus DNA-binding proteins from the Tcf/Lef transcription factor family repress target genes. This takes place mainly by recruitment of co-repressors as Groucho/TLE[122,124,125].

In contrast to that the active state is reached after proteins of the Wnt family are secreted and bind to fz receptors on the surfaces of target cells. Binding of Wnt proteins to fz/LRP5/6 co-receptors leads to a phosphorylation of LRP5/6 by casein kinase1γ (CK1γ). This causes the relocation of Axin towards the membrane and disturbs the formation of the destruction box. As a result β-catenin is not degraded and accumulates, being able to enter the nucleus. There it interacts with members of the Tcf/Lef family. Groucho/TLE proteins are replaced from Tcf/Lef and co-activator proteins like cyclic AMP response-element binding protein binding protein (CBP)[126], TBP, BRG1, Mediator or Hyrax are recruited[122,124,125].

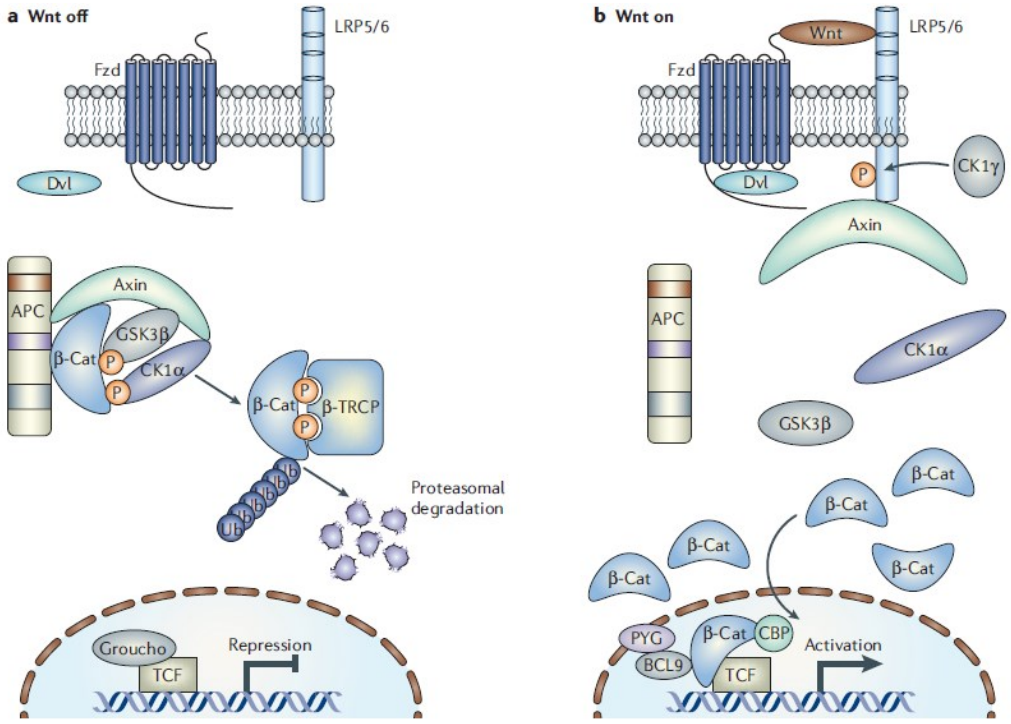

Figure 18. Overview: Wnt signaling pathway.
a) Without Wnt, β-catenin is bound by a destruction box composed of axin, GSK3β and CK1α. Phosphorylation leads to ubiquitinylation resulting in proteasomal degradation.
b) Binding of Wnt to Fzd/LRP5/6 receptors leads to translocation of axin. As a result the destruction box is not build and β-catenin can enter the nucleus. Binding of Tcf7Lef subsequently attracts transcriptional co-activators. (from Barker et al. 2006)[124].

5.2 The role of Wnt signaling in cancer

Different components of the Wnt signaling pathway, including APC, Axin, Tcf and β-catenin have shown mutations related to human cancer[6,127].

Mutations of APC cause a heritable form of colorectal cancer called familial adenomatous polyposis (FAP). Further they have been detected in a majority of sporadic colorectal cancers[128,129]. Most APC mutations are frame shift and deletion mutations causing a truncation of the protein. Hence proper building of the β-catenin destruction box is hindered, subsequently leading to β-catenin overexpression[6, 130] followed by onset of tumorigenesis[131].

Axin1 and *Axin 2*, other negative regulators of Wnt signaling, have been shown to be mutated in numerous human cancers. Most mutations lead to an inhibition of Axin 1 function as a scaffold within the destruction box[130]. Some variants described in detail showed inability of proper binding with GSK[132]. *Axin 2* mutations have been shown to be very common in tumors, that also show either an APC or β-catenin mutation[6].

Further mutations occur in the transcriptional factor TCF4. All known mutations cause a frame shift within the final exon. Functional TCF4 binds to β-catenin, but the consequences of the mutations are still discussed[6,133]. A loss of the interaction between TCF4 and the transcriptional repressor carboxy-terminal binding protein (CtBP) has been shown by Cuillere-Dartigues et al[134].

β-catenin degradation by the destruction box is also circumvented as a result of mutations within β-catenin. These are more common than APC mutations within non-colon related cancers[6,135] and have also been described frequently existing beside APC mutations in colon cancer[127]. Looking at different colon cancer cells, mutations within regions of the protein showing potential for functional modification are very common. For example in HCT116 and SW480 colon carcinoma cell lines mutations concern GSK-3β phosphorylation sites positioned at β-catenin residues 20 to 31[131], disrupting proper β-catenin destruction box assembly[129]. 1997 Ilyas et al. investigated 23 human colorectal cancer cell lines for mutations within β-catenin. In 26% of the cases mutations were found; mostly at codon 33 within exon 3 [136]. Exon 3 has also shown to be affected in other cancer types as human hepatocellular carcinoma (human HCC). β-catenin mutations are common in 20-40% of the cases. A study came to the conclusion that besides phosphorylation site related mutations in exon 3 non-phosphorylation sites lead to activation of β-catenin as well. Both, conventional and non-phosphorylated sites cause equal up regulation of β-catenin[137]. Besides these most common examples, mutations within β-catenin also appear in various other forms of cancer[138,139,140].

5.3 β-catenin as a target for therapeutic applications

Since β-catenin is the main player of Wnt signaling, shown to be affected regularly in different cancers, the idea of directly targeting the protein with antisense reagents came up[7,8]. Although the question whether one can target Wnt signaling safely raised by Kahn 2014[141] has not been answered yet, targeting β-catenin showed a potential therapeutic benefit in a variety of studies applying different reagents. Grossmann et al. developed a hydrocarbon-stapled peptide directly targeting β-catenin interfering with its ability to interact with TCF. Thereby β-catenin mediated transcriptional activity could be inhibited in cell culture experiments[142,143]. In another study systemic administration of antisense ODNs to human colon cancer xenografts in nude mice showed proper down regulation of β-catenin expression, accompanied by inhibition of tumor growth (to total eradication in some cases)[7]. Targeting β-catenin with lipid nanoparticle-delivered DsiRNAs (Dicer-substrate short interfering RNAs) could also help to reduce liver tumor growth in a xenograft- mouse model, demonstrating β-catenin to be a good target for treatment of liver cancers[17]. This was confirmed in a study using LNAs for treatment of hepatocellular carcinoma in C3H/He mice, also showing a potential

therapeutic benefit[144]. In order to point out the best options where and how to target β-catenin a closer look at the structure is provided below.

5.4 Structure of β-catenin

β-catenin is a 781 amino acid protein. It consists of an amino-terminal domain, a prominent central structure containing 12 armadillo (ARM) repeats and a carboxy-terminal domain. The central armadillo region stretching from residue 138 to 664 is very important for the main interactions of β-catenin with other proteins. N- and C-terminal domains are less conserved, but are also of importance, mediating some of the protein-protein interactions. An example for the N-terminus is the connection of the β-catenin/E-cadherin complex to α-catenin, one major structural regulator of the cytoskeleton. Further degradation of cytosolic β-catenin is dependent on recognition of phosphorylations within the N-terminus by β-TrCP ubiquitin ligase[145,146]. Interaction domains of many binding proteins stretch through the C-terminal region of β-catenin[147].

5.4.1 Binding partners

Herein, the binding partners investigated in our studies are described with focus on their interaction domains with β-catenin:

APC

Being part of the destruction box, this tumor suppressor is a negative regulator of the Wnt pathway[124]. Mutations leading to truncated versions of APC cause strong β-catenin overexpression and accumulation[148,129]. APC contains a conserved central region of 20 amino acids. It binds mainly to armadillo repeats 1 to 5 of β-catenin. Regions of APC N-terminal to the central region bind to β-catenin within armadillo repeats 5 to 12[148].

α-catenin

Within adherens junctions the Cadherin-catenin complex connects Cadherin to the cytoskeleton through binding β-catenin which is itself bound to α-catenin (Fig. 19)[149]. For the connection with β-catenin it does interact with amino acid 118-149 of β-catenin[150].

Cadherin

Cadherin is a major component of the adherens junction complex (Fig. 19). As mentioned above its cytoplasmic domain recruits a variety of proteins including β-catenin. In context with Wnt pathway this means - given the situation that the pathway is off - only Cadherin bound β-catenin is safe from degradation. Tumor progression often leads to a down regulation of Cadherin expression, going hand in hand with invasiveness of carcinoma cells[151]. Interaction with β-catenin takes place within five main regions. Region I spans armadillo repeats 7 to 9, region II ARM 12 and 11, region III ARM 9 to 4, region IV ARM 4 and 3 where the chain turns and finally region V which continues towards the N-terminus of β-catenin[152].

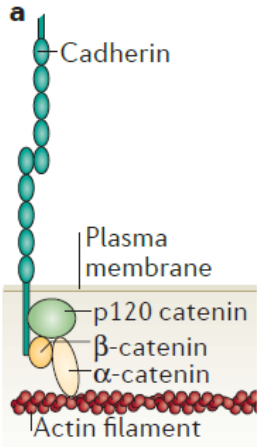

Figure 19. The Cadherin-catenin complex (changed after Ratheesh et al. 2012)[149].

CBP/P300

By regulation of binding transcription factors[153], CBP and P300 also play an important role in Wnt signaling[154]. Direct interaction with β-catenin leads to activation of gene expression. Binding of β-catenin takes place from ARM 10 to the C-terminus[155].

Tcf/Lef

As mentioned, in cells with inactivated Wnt pathway, Tcf/Lef proteins are placed at Wnt/β-catenin target gene promoters. Their task is suppression of basal transcription by forming complexes with co-repressor proteins. Once β-catenin enters the nucleus as a result of an active Wnt pathway, it binds to Tcf/Lef and blocks its interaction with repressors. Subsequently the promoter can be activated[156]. Binding between Tcf and β-catenin covers an extended region from β-catenin ARM repeats 3 to 4 over ARM 5 to 8 and finally the interaction with the central binding domain within ARM 9 and 10[131,157]. As the hotspot of interaction between β-catenin and Lef-1/Tcf factors Kries et al. described the region of ARM

8[158]. A structural characterisation of β-catenin Lef-1 interaction showed binding regions on β-catenin covering ARM 2 to 5 as well as ARM 5 to 10[159].

6 Material and Methods

6.1 Cloning

6.1.1 Plasmids constructed

6.1.1.1 Splice based reporter assay

In order to construct the splice based reporter assay for testing antisense reagents, we started with a pKCF backbone [160] that has been complemented with a Flag-tag. Subsequently pKCFintron luc was constructed. This version could be modified by introducing splice donors of interest into the reporter. First constructs were made with Fluc as a reporter gene, later ones with Nluc in order to improve light emission as previously described[110].

construct	Vector	vector digest	intron	intron digest
pKCFluc	pKCF	Cla, EcoRV	pKC2luc2a	Cla, EcoRV
pGemTintron	as template: pKW 2T		primer foreward: GACGCGTAGCTCAGCTGCAACCGCCTATAGAGTCT primer reverse: GGCTAGCCCTCTGTGGAGAGAAAGGCAAAGTGGATCCGTCAGA TTGTAGCCGCGTTC	
pGemTlucΔATG part	as template: pKC2luc2a		primer foreward: GGCTAGCTGAAGACGCCAAAAAC primer reverse: TAGGCTGCGAAATGCCCATAC	
pGemTinron luc Δ	pGemTlucΔATGpart	NheI, PstI	pGemTintron	NheI, PstI
pKCFintron luc	pKCFluc	Mlu, Bsp119	pGemTintron lucΔ	Mlu, Bsp119
pKCFintronTcf3	pKCFintron luc	Mlu, Bpu	5'CGCGTAACAGCAGCTCGTCTGACTCCGAGGTAAATTGTTATTC AATGCTCCGC3' 3'TGAGCGGAGCATTGAATAACAATTTACCTCGGAGTCAGACGAG CTGCTGTTA5'	
pKCTcf3intron mut	pKCFintron luc	Mlu, Bpu	5'CGCGTAACAGCAGCTCGTCTGACTCCGAAGCGAACTGTTATTC AATGCTCCGC3' 3'TGAGCGGAGCATTGAATAACAGTTCGCTTCGGAGTCAGACGAG CTGCTGTTA5'	
pKCTcf3intron spliced	pKCFintron luc	Mlu, Bpu	5'CGCGTAACAGCAGCTCGTCTGACTCCGAGGTAAATTGTTATTA AATGCTCCGC3' 3'TGAGCGGAGCATTTAATAACAATTTACCTCGGAGTCAGACGAG CTGCTGTTA5'	
pKCFintron basis1	pKCFintron luc	Mlu, Bpu	5'CGCGTTCAAACTCTCAGGTAAGTATCAAGGCTACGAGACAGGT TAGC3' 3'TGAGCTAACCTGTCTCGTAGCCTTGATACTTACCTGAGAGTTTG AA5'	
pKCFintron SDmut	pKCFintron luc	Mlu, Bpu	5'CGCGTTCAAACTCTCAAGTCTCCATCAAGGCTACGAGACAGGT TAGC3'	

			3'TGAGCTAACCTGTCTCGTAGCCTTGATGGAGACTTGAGAGTTTGAA5'	
pKCFintron SDspliced	pKCFintron luc	Mlu, Bpu	5'CGCGTTCAAACTCTCAGGG3' 3'CTAGCCCTGAGAGTTTGAA5'	
pKCluc hGHpaSV40pa	pKC2luc2a	Acc65, Not	pGEMThGHpolyA	Acc65, Not
pGVLΔlucTATA	pGVLΔluc	Acc64	5'GTACGTATATATGCATAGCTCGTTTAGTGAACCGCCAGTCTATCGATG3' 3'GTACCATCGATAGACTGGCGGTTCACTAAACGAGCTATGCATATATAC5'	
pGVL4	pGVLΔlucTATA	Cla, Acc	pKcLuc hGHpA SV40pA	Cla, Acc
pGVL4Gluc	pGVL4	Cla, Acc	pGemTGlucS	Cla, Acc
pGVL4GlucΔeco	pGVL4Gluc	EcoRI part	5'AATTGCGC3'	Sma, EcoRV
pSplice basis1	pPBEFSGfpRluc puro	Bsp1407 T4blunt Sma	pKCFintron luc basis1	Sma, EcoRV
pSplice2 basis1	pGVL4GlucΔeco	EcoRI,PstI	psplice basis1	EcoRI,PstI
pSplice Tcf3	pPBEFSGfpRluc puro	Bsp1407 T4blunt Sma	pKCFintronTcf3	Sma, EcoRV
pSplice2 Tcf3	pGVL4GlucΔeco	EcoRI,PstI	pSplice Tcf3	EcoRI,PstI

Table 1. Constructs for splice based reporter assay with Fluc. The ones in bold letters were tested transient or used for generating a stable cell line.

For transient tests of the assay, mutated versions that represent a situation without splicing (mut) and completely spliced (spliced) ones, were made for all splice donors. Splice donors included one version simply for testing the principle called “basis1”, Tcf3 as well as a ß-catenin construct (pSplice3ßcat ex13SD).

construct	vector	vector digest	intron	intron digest
pGemTNuc (-ATG)	as template: pKCNluc		primer foreward: GGCTAGCTGTCTTCACACTCGAAGATT primer reverse: CGATATCCTGCAGCGCCAGAATGCGTTCGCACA	
pSplice2luc	pSplice2 Tcf3	Cla, EcoRV	pKC2luc2a	Cla, EcoRV
pKCFintron Nluc basis1	pKCFintron basis1	NheI, EcoRV	pGemTNluc (-ATG)	NheI, EcoRV
pKCFintron Nluc SDmut	pKCFintron SDmut	NheI, EcoRV	pGemTNluc (-ATG)	NheI, EcoRV
pKCFintron Nluc SDspliced	pKCFintron SDspliced	NheI, EcoRV	pGemTNluc (-ATG)	NheI, EcoRV
pSplice3	pSplice2luc	Nhe, PstI	pKCFintron Nluc basis1	Nhe, PstI
pSplice3 basis1	pSplice3	Mlu, PstI	pKCFintron Nluc basis1	Mlu, PstI
pSplice3 SDmut	pSplice3	Mlu, PstI	pKCFintronNluc SDmut	Mlu, PstI
pSplice3 SDspliced	pSplice3	Mlu, PstI	pKCFintronNluc SDspliced	Mlu, PstI
pKCFβcat ex13SD	pKCFluc intron	Mlu, Bpu1102	5'CGCGTACAGAGCCAATGGCTTGGAATGAGGTAGGGAAATGTGAGCAGTTATGC3' 3'TGAGCATAACTGCTCACATTTCCCTACCTCATTCCAAGCCATTGGCTCTGTA5'	
pSplice3βcat ex13SD	pSplice3 basis1	Mlu, BamHI	pKCFßcatex13 SD	Mlu, BamHI
pEFSFβcat ex13SDmut	pEFSFluc intron	Mlu, Bpu1102	5'CGCGTACAGAGCCAATGGCTTGGAATGAACTCGCCAAATGTGAGCAGTTATGC3'	

			3'TGAGCATAACTGCTCACATTTGGCGAGTTCATTCCAAGCCATTG GCTCTGTA5'	
pSplice3βcat ex13SDmut	pSplice3 basis1	BglII, NheI	pEFSFßcat ex13SDmut	BglII, NheI

Table 2. Constructs for splice based reporter assay with Nluc. The ones in bold letters were tested transient or used for generating a stable cell line.

6.1.1.2 Modified β-catenin versions

These were designed to test a dominant negative knock-down strategy. All constructs are based on pKCDPβcat containing a full length human β-catenin cDNA in the pKC expression vector.

Construct	vector	vector digest	intron	intron digest
pGemTβcat (1-694)	as template: pKCDPβcat		primer foreward: GTTCGAAATCTTGCCCTTTGTCCCGCAAATCATGCACCT primer reverse: GTCTAGACTACCAGATAAATAACTGCTCACATTTCCCTACCTCATTCCAAG CCATTGGCTCTGTT	
pGemTβcat (1-653)	as template: pKCDPβcat		primer foreward: GTTCGAAATCTTGCCCTTTGTCCCGCAAATCATGCACCT primer reverse: GTCTAGATTAGCAGTCCACACCTTCATTCCTAGAGTGA	
pGemTβcat (exon6skip)	as template: pKCDPβcat		primer foreward: CTTGATTAACTATCAAGATGATGCAGAACTT primer reverse: CATCGATTCTAGATTAAAGCTTGGGGTCCACCACTAGCCAGTATGATGAG CCAAGCATTTTCACC	
pGemTβcat (plus intron6)	as template: pKCDPβcat		primer foreward: CTTGATTAACTATCAAGATGATGCAGAACTT primer reverse: CATCGATTCTAGATTAAAGCTTGGGGTCCACCACTAGCCAGTATGATGAG CCAAGCATTTTCACC	
pKCβcat (1-694)	pKCDPβcat	Bsp119, NotI	pGemTβcat(1-694)	Bsp119, NotI
pKCβcat (1-653)	pKCDPβcat	Xba, Bsp119	pGemTβcat(1-653)	Xba, Bsp119
pKCDPβcat (exon6skip)	pKCDPβcat	Eco72I, ClaI	pGemTβcat (exon6skip)	Eco72I, ClaI
pKCDPβcat (plus intron6)	pKCDPβcat	Eco72I, ClaI	pGemTβcat (plus intron6)	Eco72I, ClaI
pKCDPβcat (134-487)				
pKCDPβcat (134-756)				

Table 3. β-catenin constructs for dominant negative knock-down strategy. The ones in bold letters were tested transient or used for generating a stable cell line.

6.1.1.3 Mammalian-two-hybrid (m2h)

As a backbone for the constructs needed for the m2h experiments pMC65 was used. Modified shortened ß-catenin versions were integrated as shown in Table 4.

construct	vector	vector digest	intron	intron digest
pMC65gDPβcat	pMC65	Cla, NotI	pMC anFKgDPβcat	Cla, NotI

pGemTβcat (exon6skip)	as template: pKCDPβcat		primer foreward: CTTGATTAACTATCAAGATGATGCAGAACTT primer reverse: CATCGATTCTAGATTAAAGCTTGGGGTCCAC CACTAGCCAGTATGATGAGCCAAGCATTTTC ACC	
pGemTβcat (plus intron6)	as template: pKCDPβcat		primer foreward: CTTGATTAACTATCAAGATGATGCAGAACTT primer reverse: CATCGATTCTAGATTAAAGCTTGGGGTCCAC CACTAGCCAGTATGATGAGCCAAGCATTTTC ACC	
pMCβcatS (exon6skip)	pMCDPβcatS	Eco72I, XbaI	pGemTβcat (exon6skip)	Eco72I, XbaI
pMCβcatS (plus intron6)	pMCDPβcatS	Eco72I, XbaI	pGemTβcat (plus intron6)	Eco72I, XbaI
pMCDPβcatS (1-694)	pMCDPβcatS	Bsp 119, XbaI	pGemT βcat (1-694)	Bsp 119, XbaI
pMCDPβcatS (1-653)	pMCDPβcatS	Bsp 119, XbaI	pGemT βcat (1-653)	Bsp 119, XbaI
pMC65gDPβcat (1-694)	pMC65gDPβcat	Bsp 119, NotI	pMCDPβcatS (1-694)	Bsp 119, NotI
pMC65gDPβcat (1-653)	pMC65gDPβcat	Bsp 119, NotI	pMCDPβcatS (1-653)	Bsp 119, NotI

Table 4. pMC65 based constructs for m2h reporter assay.

These other constructs used were already in the laboratory stock and not modified by the author:

pKC luc

pMCGlucS

pMCGFP

pBsMHisH4

pMCBtrans

pMlucF6lefcons (lef cons)

pMlucM6lefmyc (lef myc)

pMlucF Spe Nhe.

6.1.2 Reagents and buffers

Gels: depending on the size of the investigated construct a 1% or 2% agarose (Biozym) gel was made with 1x SB gel running buffer. For staining, peqGREEN (peqlab) was added in a 1:20 000 dilution. As standard we used DNA ladder λ-mix (Thermo Scientific).

SB gel running buffer:	volume: 1 l, 20x NaOH (Roth): 8 g Boric Acid (Roth): 45 g
Loading dye:	volume: 100 ml Ficoll 400 (Roth): 20 g EDTA (Serva) 0.5 M, pH 8.0: 20 ml SDS (Roth) 20% Bromphenol blue (Roth): 0.1 g adjusted to pH 8.0

Restriction enzymes used were supplied by Thermo Scientific and are listed for each cloning experiment (Tables 1, 2, 3 and 4).

LB medium:	volume: 2 l Peptone from casein (Roth): 20 g Yeast extract (Roth): 10 g NaCl (Roth): 10 g NaOH (Roth) 1 M: 2 ml Final pH: 7.2 to 7.5
LB agar plates:	volume: 500 ml LB medium: 500 ml Agar agar (Roth)
P1:	volume: 500 ml Tris (Roth) 1M (pH 8.0): 25 ml EDTA (Serva) 0.5M (pH 8.0): 10 ml RNase A: 1 ml freshly added per 100 ml
RNase A:	volume: 20 ml RNase A (Sigma-Aldrich): 200 mg Tris (Roth) 1M, pH 7.5: 200 µl NaCl (Roth) 5M: 60 µl
P2:	volume: 500 ml NaOH (Roth) 5M: 20 ml SDS (Roth) 20%: 25 ml
P3:	$C_2H_3KO_2$ (Roth): 147.15 g Glacial acetic acid (Roth): 58 ml pH 5.5

PEG: volume: 500 ml
PEG6000 (Merck): 120 g
NaCl (Roth): 87.7 g
Stirred at 70°C

XGal (Fermentas): diluted in N'N-dimethylformamid (Roth)

Isopropyl-β-D-thiogalactopyranosid (IPTG, Fermentas)

CaCl solution: volume: 500 ml
$CaCl_2.2H_2O$ (Merck): 4.41 g
Glycerol 100% (Roth): 75 g
MOPS (Sigma): 1.05 g

6.1.3 Protocol for competent Top 10 F' E. Coli

Top 10 F' E. coli (Invitrogen) were plated on a LB agar plate and grown at 37°C overnight.
Next day one colony was picked from the plate and inoculated into 50 ml LB medium overnight. 4 ml of this suspension were used the next day to inoculate 400 ml LB medium and grown to an optic density (OD) of 0.35 to 0.40. In the next step the suspension was transferred to 50 ml tubes and left 5min on ice followed by a centrifugation for 7 min at 4000 rpm at 4°C. Resulting pellets were suspended in 10 ml ice cold 60 mM CaCl solution using a 10 ml glass pipette.
A centrifugation for 5 min at 4000 rpm at 4°C followed. Pellets were once again suspended in 10 ml ice cold 60 mM CaCl solution and then put on ice for 30 min. After centrifuging for 5 min at 4000 rpm at 4°C pellets were suspended in 2 ml ice cold 60 mM CaCl solution and aliquots of 330 µl within pre-cooled 1.5 ml tubes were stored at -80°C until further use.

6.1.4 Preparation of vectors and inserts

Preparation of the vector:

Digestion of 1 µg DNA was performed in 100 µl total volume including restriction enzyme buffer (as recommended by the supplier, Thermo Scientific), 4 µl of each restriction enzyme (Thermo Scientific) and water at 37°C for at least 4 h or overnight.

Dephosphorylation using FastAP (Thermo Scientific):

After adding 1µl FastAP the vector was incubated in a heating block (Eppendorf, Thermo Scientificmixer compact) for 10 min at 37°C. In order to inactivate the enzyme, 1 µl 500 mM, pH 8 EDTA (Serva) was added followed by incubation at 80°C.

DNA purification using Gene JET Gel Extraction Kit (Thermo Scientific):
First 500 µl of binding buffer was added to the digestion. After mixing gently 602 µl were transferred to a 2ml collection tube including a column and centrifuged for 1 min at 10 000 rpm (Eppendorf, mini spin). Then the flow through was discarded and 750 µl of wash buffer were added and the tube was spun 1 min at 10 000 g. This washing step was repeated once.
In order to dry the column the flow through was discarded once again and the column put to the emptied 2 ml collection tube and centrifuged at 13 400 rpm for 4 min. Subsequently the filter was placed in a fresh 1.5 ml tube and 10 µl of H_2O (preheated to 70°C) were added to the centre of the filter followed by centrifugation for 1 min at 13 400 g.
This procedure was repeated once more providing a final yield of 15 µl.

Preparation of the insert:

5 µg DNA were digested in a total volume of 100 µl supplemented with restriction enzyme buffer (as recommended by the supplier, Thermo Scientific), 4 µl of each enzyme and water at 37°C for at least 4 h or overnight.
After adding 20 µl DNA loading buffer, the whole amount of digested insert was run on a gel and the required band excised. In order to completely dissolve the gel slice for subsequent DNA purification with Gene JET Gel Extraction kit (Thermo Scientific), the equivalent volume of binding buffer was added and the slice was incubated shacking for 10 min at 55 to 65°C in the heating block (Eppendorf, Thermo Scientificmixer compact). Starting with the transfer of the solution to the 2 ml tube including a column, the rest of the procedure is in accordance with the DNA purification protocol for the vector.

Checking appropriate size of vector and insert was achieved by running 1 µl of each purified product on a gel.

6.1.4.1 Plasmid cloning using PCR and pGem-T Easy vector system (Promega)

First, in order to amplify the desired insert, a PCR with Phusion Polymerase (Thermo Scientific) was performed. Therefore 10 ng plasmid DNA, 25 pmol of each primer (Mycrosynth), 1 µl 10 mM dNTPs (Thermo Scientific), 0.5 U Phusion Polymerase (Thermo Scientific), 10 µl 5x HF-Buffer (Thermo Scientific) were combined with dH_2O up to a total reaction volume of 50 µl.
PCR was run with the following program: denaturation at 98°C for 30 sec followed by 25 cycles with denaturation at 98°C for 10 sec, primer annealing at 55°C for 30 sec and elongation at 72°C for 15 sec. Once products were ready agarose gel electrophoresis was performed and the desired band cut out with a razor blade. Purification of the gel was done using Gene JET Gel Extraction Kit (Thermo Scientific) as described above (p. 40). Subsequently another gel was made to verify the size of the resulting product.

A-tailing:

For A-tailing 6 µl PCR product, 1 µl SB buffer with tween, 0.5 µl 25 mM $MgSO_4$ (Thermo Scientific), 0.5 µl Taq polymerase (Agrobiogen) and 2 µl 0.1 µM ATP (Roth) were combined and incubated for 20 min at 72°C in a heating block.

Ligation with pGem- TEasy Kit (Promega):

3 µl of the A-tailed product, 1 µl pGem-TEasy vector, 1 µl T4 DNA ligase (Thermo Scientific), 1µl T4 DNA ligase buffer (Thermo Scientific) and 4 µl dH_2O were added to one reaction and incubated at least 4 h or overnight at RT. In case of incubating 4 h, ligase was inactivated at 65°C for 20 min.

Transformation of the plasmids into competent E.coli was done according to the protocol below (p. 42) additionally adding 10 µl Isopropyl-β-D-thiogalactopyranosid (IPTG, Fermentas) and X-Gal (Fermentas) for blue-white staining.

6.1.4.2 Oligonucleotide cloning

This was either performed with or without kinasing.

Without kinasing:

The vector was prepared according to the protocol on p. 39, but not dephosphorylated. For ligation (as described below) 0.5 µl 100 pm/µl of each oligo (Microsynth) were added and before

transformation the ligation was put on 80°C for 10 min and cooled down to RT slowly.

With kinasing:

We added 20 pmol of the oligo nucleotides, 3 ml 10 mM ATP (Roth), 3 µl T4 Polynucleotide Kinase Reaction Buffer (PNK, Thermo Scientific), 10 U (1µl) T4 kinase (Thermo Scientific) and up to 30 µl dH_2O to a reaction and incubated for 1 h at 37°C.
In order to inactivate the kinase the mixture is incubated for 5 min in a beaker with boiling water and slowly cooled down to RT.
2 µl of the kinased oligonucleotides were used for ligation which was performed as follows.

6.1.5 Ligation

For ligation 50 to 100 ng of vector and the double amount of insert were incubated together with T4 DNA ligase (Thermo Scientific) and T4 DNA ligase buffer (Thermo Scientific) in a total volume of 10 µl for at least 4 h or overnight. If incubation was executed for 4 h inactivation of ligase was achieved by incubation for 20 min at 65°C. As a control a 1.5 ml reaction tube without insert was prepared.

6.1.6 Transformation of plasmids into E.coli

Starting transformation the whole volume of the ligation was put on ice for 10 min after adding 100 µl of competent Top 10 F'. After a heat shock at 42°C for 1 min 30 sec the tubes were put on ice for 2 min followed by adding 1 ml LB medium and incubation at 37°C for 30 min while shaking on a heating block (Eppendorf, Thermo Scientific mixer comfort). Subsequently tubes were spun 4 min at 5000 rpm and the supernatant was removed leaving about 100 µl in the tubes. Remaining 100 µl were re-suspended and plated on LB agar with 100 µg/ml ampicillin (Roth). In order to provide optimal growth plates were incubated at 37°C overnight.

Re-transformation:

For re-transformation from Minis or Midis a shortened version of this protocol including directly plating the suspension after the 42°C heatshock was used. This leaded to a 5x reduced efficiency, being negligible due to the high concentrations of plasmid provided by Minis and Midis.

6.1.7 Mini-preparation

Single colonies were picked from the plates using pipette tips followed by inoculation in 14 ml tubes containing 2 ml LB medium with 100 µg/ml ampicillin (Roth). These were put to the incubator for overnight growth at 37°C.
Next day the bacteria suspension was transferred to 2 ml tubes. Since transfer was done by pouring, a little rest remained in the tubes that could later be used for inoculation of Midi-prep. Before mentioned 2 ml tubes were spun for 2 min at 6000 rpm (Eppendorf,) before the supernatant was removed completely. The pellet was re-suspended thoroughly in 100 µl buffer P1 by vortexing. After adding 200 µl lysis buffer P2 the suspension was mixed by manually shaking and left at room temperature for 5 min.
In order to stop lysis 200 µl buffer P3 was added and the samples shook manually followed by centrifugation for 20 min at 14680 rpm (full speed). Subsequent PEG precipitation was performed by transferring the supernatant after the centrifugation to a fresh 2 ml tube adding 500 µl 24% PEG. Reaction tubes were incubated on a shaker for 15 min, shaking. A pre-cooled centrifuge was use to spin the tubes for 15 min at maximum speed at 4°C. Then pellets were washed adding 500 µl 70 % EtOH followed by spinning them for 5 min at RT. Finally, the supernatant was removed completely and after drying for 5 to 10 min the pellets were dissolved in 20 µl H_2O.
In order to distinguish positive mini-preps from others a control digestion of 2 µl Mini with enzyme buffer (as recommended by the supplier, Thermo Scientific), 0.4 µl of enzyme (Thermo Scientific) and up to 10 µl water was performed. Standard control digestion lasted for 1 h at 37°C followed by running a gel with the products.

6.1.8 Midi-preparation using JetStar® 2.0 Plasmid Purification Kit (Genomed)

75 ml of LB medium were inoculated with 10 µl of a single colony from the miniprep culture and incubated overnight at 37°C.
After 16 h 50 ml of the E. coli culture were transferred to a 50 ml falcon and centrifuged at 4000 g for 7 to 10 min. In the next step the supernatant was removed and 4 ml cell suspending buffer E1 (Genomed) was added to the pellet which was subsequently thoroughly resuspended using a 10 ml glass pipette. Next, 4 ml of lysis buffer E2 (Genomed) was supplemented, everything mixed immediately by manually inverting the tubes 5 times. After incubation for 5 min at RT 3 ml of buffer E3 (Genomed) was added and mixed by inverting the tubes 5 times manually. In the next step the lysate was centrifuged for 20 min at 4500 g at RT. In the meantime columns (Genomed) were pre-equilibrated with 10 ml buffer E4 (Genomed). After centrifugation finished the supernatant was transferred to the columns where it drained by gravity flow. In order to wash the columns 10 ml wash

buffer E5 (Genomed) was added. This step was repeated once, then elution of plasmids into fresh 15 ml tubes, was achieved adding 5 ml elution buffer E6 (Genomed) to the columns. Subsequently 3.5 ml isopropanol were added and mixed well, before centrifuging at 4500 rpm at 4°C for 30 min in a pre-cooled centrifuge. Resulting pellets were washed with 1 ml 70% EtOH and spun 5 min with 4500 rpm (maximum speed) followed by removal of the supernatant. Pellets were air-dried for 5 to 10 min before they were dissolved carefully in 100 µl dH_2O and transferred to a 1.5 ml tube. Purified DNA was left 1 h at 65°C shaking and then spun for 5 min with 13 400 rpm. Finally the supernatant was transferred to fresh screw tubes. Plasmids were verified making a control digestion. Resulting products were run on an agarose electrophoresis gel.

6.1.9 Sequencing

Sequencing reactions were performed by the Microsynth GmbH.

6.2 Cell culture

Reagents and buffers

Complete medium:

Complete medium: 1% Penicillin/Streptomycin (Thermo Scientific) and 10% FBS (Thermo Scientific) were added to 500 ml DMEM (GE).

PBS:	volume: 1l concentration: 10x NaCl (Roth): 80 g KCl (Sigma): 2 g $Na_2HPO_4x2H_2O$ (Roth): 7.7 g KH_2PO_4 (Merck): 2 g
PEI[161]	
Lysis Buffer:	0.03% Triton X-100 25 mM Tris (Roth) pH7.5

Injection solutions for luciferase measurement:

Solution 1:	50 µl 10mM Luciferin 62,5 µl 0,2M ATP (Roth)

31,25 µl 1M Tris (Roth) pH 7,5
46,88 µl 1M $MgCl_2$ (Roth)
4,8 ml H_2O

Solution 2: 5 ml 210M DCTA (Roth)
31,25 µl 1M Tris (Roth) pH 7,5
3,125 µl Coelentherazine (Synchem OHG)

Stop solution: 0,3 M H_2SO_4

Scraping:
Loading solution: volume: 50 ml
KH_2PO_4 (Merck) 10 mM: 68 mg
D-Glucosemonohydrate (Merck): 50 mg
EDTA (Serva) 0.5 M: 10 µl
KCl (Sigma) 140 mM: 2.3 ml

6.2.1 Cell lines

HeLa, SW480, PC-3, A2780, LNCaP were propagated as described below using medium and split ratios as indicated on Table 5.

cell line	spec	medium	culture additions	split ratio	special characteristics
HeLa	human cervix adenocarcinoma	DMEM complete	+ FCS (10%) + PenStrep 1%)	1/10	
SW480	human colon carcinoma	DMEM complete	+ FCS (10%) + PenStrep 1%)	1/4	clump at low densities
PC-3	human prostate cancer	RPMI-1640	+ FCS (10%) + PenStrep (1%)	1/3	
		RPMI-1640	+ FCS(10%) + PenStrep (1%)+ 2 mM L-glutamine		
A2780	human ovarian cancer cell line	RPMI-1640	+ FCS (10%) + PenStrep (1%)	1/3	
		RPMI-1640	+ FCS (10%) + PenStrep (1%)+ 2 mM L-glutamine		
LNCaP	human prostate adenocarcinoma cells	RPMI-1640 (corrected to ATCC-medium)	+ 5 ml HEPES 1M+ 2.8 ml 45% glucose, 5 ml Pyruvat (100x)	1/4	can grow as "towers"

Table 5. Mediums, culture additions, split ratios and special characteristics of cell lines in use (from ATCC).

6.2.1.1 Stable cell lines

All stable cell lines were generated from HeLa cells. Table 6 shows the constructs they were based on as well as their purpose.

Transfection of 10 cm dishes

First 10 cm dishes were seeded with $0.3x10^6$ HeLa cells/dish. Cells were grown over night. The next day 5 µg/dish of the construct was transfected together with 2.5 µg/dish pMC PBtrans (Piggy bac transposase[162]). Therefore the desired plasmid amount was mixed with 1.5 ml DMEM incomplete and transferred to a 15 ml falcon. In a separate tube another 1.5 ml DMEM incomplete including 20 µl turbofect were prepared and finally mixed in the plasmid containing 15 ml tube resulting in a total volume of 3 ml. This mix was left for 30 min. at RT. Subsequently medium was evacuated from the 10 cm dishes and the transfection mix added followed by 2 h incubation at 37°C. In order to stop the transfection 7 ml DMEM complete were added to each 10 cm dish.

6.2.1.2 Selection and picking of clones

Selection was started 3 d after transfection by adding 1µg/ml puromycin (Santa Cruz) to fresh DMEM complete. Medium with puromycin was renewed at least once a week. As soon as colonies had grown big enough to pick, not yet overlapping, these single clones were picked and put to growth following this procedure:
First cloning discs (Sigma Aldrich) were quartered and rinsed in trypsin. Medium was evacuated from the 10 cm dish with the clones and cells were washed once with 1x PBS. After removal of PBS a cloning disc was cautiously put on a single colony using forceps. After an incubation time of 5 min, the disc with the cells was transferred to a fresh 24-well plate and 1 ml DMEM complete was added. As soon as single clones had attached in the 24-well plate and grown to confluency, cells could be tested for reporter function.

stable cell line	integrated construct	purpose
HeLa pSplice2 basis1	psplice2 basis1	splice based reporter assay basis construct for first tests
HeLa pSplice2 tcf3	pSplice2 Tcf3	splice based reporter assay tcf3 splice donor with Fluc
HeLa pSplice3 basis1	pSplice3 basis1	splice based reporter assay optimised basis version with Nluc
HeLa pSplice3 βcat ex13SD	pSplice3 βcat ex13SD	splice based reporter assay β-catenin splice donor with Nluc

Table 6. Stable cell lines.

6.2.1.3 Propagation of cell lines

In order to avoid contaminations the UV light in the laminar flow was turned on for 15 min. before use. After turning on the motor/blower for a warm up time of 15 min. the flow was ready to use. Medium (GE) and 1x PBS were pre-warmed at 37°C for 15 min in a water bath (Grant). Used medium was removed from the cell culture flasks (GBO) and cells were washed with 10 ml pre warmed 1x PBS.

Subsequently to completely removing 1x PBS, cells were incubated with 1 ml Trypsin at 37°C in the incubator (Sanyo) for 10 min. Cells were re-suspended with 3 ml DMEM complete by pipetting up and down 10 to 15 times with a 10 ml glass pipette. Depending on the cell line, different split ratios were applied (Table 5, p.45) and 10 to 15 ml complete medium was added to the cells. In order to distribute cells evenly the flask was moved circular before putting it back to the incubator.

6.2.2 Transfection protocol

Transfection 96-well plate

Plates were coated with PEI (Sigma): therefore 50 µl PEI (2.5 µg/ml) were added per well and incubated at 37°C for 30 min. After evacuating PEI the plates were washed once with 50µl 1x PBS and stored at 4°C (for immediate use plates were incubated for 15 min at 4°C).

Seeding:
Cells were split as described (p. 45) and excess cells were counted under a Nikon Eclipse TS100 microscope using a Neubauer chamber (Marienfeld). Cell density optimal for transfection was chosen dependent on the cell line. Cells were seeded in 100 µl DMEM complete per well using an electronic multichannel pipette (Biohit or Hirschmann) and incubated for 24 h.

Transfection:

Prior to transfection DNA amount for 6 wells was prepared in a batch in 1.5 ml Eppendorf tubes. In order to get the optimal DNA concentration of 90 ng per well pBSMHistoneH4 construct was added to each tube.
Then 20 µl per well (total 120 µl per tube) DMEM incomplete (serum free) were added.
In separate tubes 120 µl DMEM incomplete (serum free) containing 0.84 µl Turbofect (Thermo Scientific) were prepared and finally mixed to a transfection mix with the 120 µl from the DNA containing tubes and incubated at room temperature for 30 min.
Medium was removed from the cells and 40 µl transfection mix was added per well. After an incubation for 2 h at 37°C the reaction was stopped by adding 100 µl DMEM complete per well.

6.2.3 Single or dual luciferase measurements of 96-well plates with plate reader

Medium was aspirated from the 96-well plate with the cells and cells were washed once with 40 µl PBS. Subsequently 25 µl lysis buffer were added per well and plates put on a shaker for 10 minutes. Meanwhile injection solutions with firefly luciferase (solution 1) and renilla luciferase (solution 2) were prepared.
As soon as solutions were ready the tubes of the machine were emptied and primed two times with the according solution before the measurement was started using the following settings:

Plate acceleration: 10
Settle delay: 0
Blanking time (0 – 100%) of integration time: 100

Dispenser 1:
Luciferase:
Volume: 40 µl
Step time (hh:mm:ss.s): 00:00:30.0
Interval: 0 sec
Measurement type: Single
Integration time (ms): 3000s (less sensitive measuring), 10 sec (sensitive measuring)
Lag time (hh:mm:ss.s): 00:00:00.0

Dispenser 2:
Renilla luciferase:
Volume: 40 µl
Step time (hh:mm:ss.s): 00:00:30.0
Interval: 0 sec
Measurement type: Single
Integration time (ms): 1000s
Lag time (hh:mm:ss.s): 00:00:16.0

Dispenser 3:
H_2SO_4
Volume: 100 µl
Step time (hh:mm:ss.s): 00:00:30.0
Interval: 0 sec
Measurement type: Single

6.3 Different protocols for PNA delivery

6.3.1 Incubation

HeLa pSplice2 basis1 were seeded on a 96-well plate at a density of 0.5 x 10^4 cells/well. Next day the medium was evacuated and 4, 8, 16, 32 or 64 µM PNA327 were added to the wells in 50 µl DMEM complete. All were done in triplicates, except for 32 µM (duplicates) and 64 µM (single) samples; in order to save material. Incubation until luciferase measurement lasted 24, 48 or 72 h.

6.3.2 Scraping

First cells (HeLa) were seeded with 0.3 x 10^5 cell /well in complete medium on a 24 well plate and incubated at 37°C overnight. For experiments with transiently transfected reporter constructs, cells were transfected the next day and scraping was conducted one day later. For stable cell lines scraping was performed one day after seeding. Therefore medium was removed from each well and 30 µl loading solution including the antisense reagent (morpholino oligonucleotide or PNA) as well as 0.1 mg/ml Fluorescein isothiocyanate-dextran (FITC-dextran, Sigma-Aldrich) was added. FITC-dextran was used in order to check if the scraping worked. Subsequently wells were scraped 5 x clockwise and 5 x counter clockwise followed by transferring the whole volume to a fresh 24-well plate. Finally 500 µl DMEM were added to the previously scraped well to wash off remaining cells and then transferred to the fresh plate, too. This method was first tested by delivering 0.1 mg/ml FITC to cells via scraping followed by analysis via fluorescence microscope (Nikon) and cytometer (CytoFLEX, Beckman Coulter).

6.3.3 Co-transfection of PNAs with annealed oligonucleotides

HeLa psplice3basis1 cells were seeded at a density of 0.55x10^4 cells/well and incubated for 24 h.
PNAs and according oligonucleotides (Table 7, p. 50) were annealed in a PCR cycler (Thermo Scientific, Arktik) using the following program:
95°C 10 min for denaturation, 91 cycles for 0.05 min followed by cooling to 4°C.
siRNA protocol (DharmaFECT Transfection Reagents, GE Healthcare) was tested for PNA/oligonucleotide co-transfection on 96-well plate:
1.5 ml tubes (Sarstedt) containing the annealed PNA/oligonucleotide composition were mixed with 10 µl DMEM with 1% FCS and 1% ITS (Insulin-Transferrin-Selenium, Thermo Scientific) per well and left at RT for 5 min. 10 µl per well DMEM with 1% FCS and 1% ITS were mixed with 0.4 µl Turbofect (Thermo

Scientific) and added to the tubes containing PNA/olgigonucleotide mix and incubated at RT for 20 min.
Next DMEM with 1% FCS and 1% ITS was added up to a total volume of 50 µl per well, mixed and the 96-well plate was transfected (see transfection protocol p. 47). In contrast to the standard transfection protocol thanks to the FCS already used within transfection process, no adding of DMEM complete was necessary.

Oligonucleotide No.	description	Oligonucleotide sequence
TP1814	complementary to PNA393	AATAGGAATGAGGTAGG
TP1815	complementary to PNA393	AATAGGAATGAGGTA
TP1816	complementary to PNA393	AATAGGAATGAGG
TP1817	complementary to PNA394	AATATTGGAATGAGGTA
TP1818	complementary to PNA394	AATATTGGAATGAGG
TP1819	complementary to PNA394	AATATTGGAATGA
TP1820	complementary to PNA327 (SD Basis) 13 bp overlap	AATAACTCTCAGGTAAG
TP1821	complementary to PNA327 (SD Basis) 12bp overlap	AATAACTCTCAGGTAA
TP1822	complementary to PNA327 (SD Basis) 11 bp overlap	AATAACTCTCAGGTA
TP1823	complementary to PNA327 (SD Basis) 10 bp overlap	AATAACTCTCAGGT
TP1824	complementary to PNA327 (SD Basis) 12bp overlap	AATAATAATAATAATAATAATAATAATAATAACTCTCAGGTAA
TP1825	complementary to PNA327 (SD Basis) 12bp overlap	AATAATAATAATAATAATAATAATAATAATAACTCTCAGGT

Table 7. Sequences of oligonucleotides used for PNA co-transfection.

6.3.4 Electroporation

For electroporation the following instruments were joined: a power supply from Voltcraft (PPS-6515), Philips function generator (PM5133), Grundig electronic oszilloscope (MO100), worldwide precision instruments A310 Accupulser as well as a cuvette holder from a Biorad gene pulser II electroporation system.
Cells were trypsinised, counted and diluted in DMEM incomplete to $3x10^7$ cells/ml. A setup for electroporation was chosen depending on the cell line (Table 8).

cell line	cell density (cells/ml)	volume (cuvette)	medium	pulse width	pulse interval	train duration	Voltage/wave form	frequency
SW480	$3x10^7$	30 µl	DMEMinc	12 ms	20 msec	0,5 sec	AC 60 V/AC	1 kHz
HeLa	$3x10^7$	30 µl	DMEMinc	12 ms	20 msec	0,25 sec	AC 60 V/AC	1 kHz

Table 8. Conditions for electroporation with different cell lines.

Then 30 µl of cell suspension were pipetted to a 1mm gap electroporation cuvette (VWR) precooled on ice and electroporated, followed by transfer to a 24 well plate. Therefore, the electroporation cuvette was flushed with 500 µl DMEM complete and everything transferred to a 24 well plate (Sarstedt). Another 500 µl DMEM complete were added and cells were divided to two wells to avoid overgrowth. Due to the extensive protocol the procedure is rather time consuming. In order to

reduce cell stress the plate was placed on a digital hotplate (Stuart) adjusted to 37°C until electroporation was finished and the 24 well plate was incubated. Survival rates verified by FACS (Cytoflex, Beckman Coulter) were about 58%, hence it was necessary to pool 3 electroporations in order to get enough cells for RNA extraction.

6.4 Cell Cytometry

In these studies cell cytometry was mainly used in order to distinguish between positive, negative as well as living and dead cells after various delivery methods as scraping or electroporation were applied. After executing the protocols for these methods (see scraping p. 48 or electroporation p. 50) the following steps were performed for analyses with the cytometer.
For sample preparation cells were washed once with PBS and incubated for 5 to 15 min at 37°C until they were completely detached. Subsequently cells were resuspended in 1 ml DMEM complete and centrifuged for 5 min at 900 rpm. Then cells were washed 2x with 1 ml PBS followed by a centrifugation for 5 min at 900 rpm. After these washing steps cells were resuspended once more in 1 ml PBS and 1 µl 7-AAD (1µg/µl stock, BioLegend) was added and cells were incubated for 20 min at RT in the dark. Finally cells were analysed with the flow cytometer. Using forward and side scatter living and dead cells were discriminated and total cell number was counted. Then the percentage of dead cells was compared between treated and untreated cells.

6.5 RNA extraction and cDNA synthesis

RNA extraction was done using GeneJET RNA Purification Kit (Thermo Scientific) following the instructions in the product information.

cDNA synthesis

DNaseI digestion was performed using 8 µl purified RNA adding 1 µl 10x Reaction buffer with $MgCl_2$ (Roth) for DNaseI (Thermo Scientific), 1 µl DNaseI (Thermo Scientific) to a 10 µl reaction which was incubated at 37°C for 30 min. After adding 1 µl 25 mM EDTA (Thermo Scientific) samples are incubated 10 min at 65°C and then put on ice immediately, before starting first strand cDNA synthesis.

First strand cDNA synthesis

Therefore 10 µl of the DNaseI digested RNA were added to 1 µl random primer (Thermo Scientific) mixed in an RNase-free 1.5 ml

tube on ice and spun down three to five seconds in a centrifuge. Subsequently samples were incubated at 70°C for 5 min followed by short incubation on ice. In order to collect drops samples were centrifuged three to five seconds and kept on ice before adding 4 µl 5x buffer for reverse transcriptase (Thermo Scientific), 2 µl 10mM dNTPs (Thermo Scientific) and 1µl ribonuclease inhibitor (Thermo Scientific). After mixing the reagents on ice drops were collected by short centrifugation and samples were incubated at 25°C for 5 min. Then 1 µl reverse transcriptase (Thermo Scientific) was added (for negative control 1 µl DEPC water (Thermo Scientific) was used) and reaction tubes were incubated for 10 min at 25°C followed by incubation at 42°C for 1h. Inactivation of reverse transcriptase was performed for 10 min at 70°C. Finally, samples were put on ice, then stored at -20°C or used for qPCR.

6.6 qPCR

Reagents and buffers

Buffer B: volume: 50 ml, 10x
Tris (Roth) 1M (pH 8.0): 40 ml
$(NH_4)_2SO_4$ 2M: 5 ml
Tween20 10%: 1 ml

dNTPs (Thermo Scientific)
BSA (Roth)
$MgCl_2$ (Thermo Scientific)
Taqman Polymerase (Agrobiogen)
Sybrgreen (Sigma)

				n =	50
Stock	Final		Component	x 1	x n
10	0.2	muM	primer for	0.50	25.00
10	0.2	muM	primer rev	0.50	25.00
4000	100000		SYBR	1.00	50.00
10	1	x	10xBuffer B	2.50	125.00
2	0.2	mM	dNTP mix	2.50	125.00
25	4	mM	MgCl2	4.00	200.00
625	20	µg	BSA	0.80	40.00
1	0.005	u	Taq	0.13	6.25
			H2O	12.08	603.75
			DNA	1.00	50.00
scale:	25		EV	25.00	1250.00

Table 9. Scheme for master mix preparation.

cDNA samples were thawed on ice and dilutions for establishing a standard curve were prepared. Usually starting the standards with a 1:1000 diluted qPCR product followed by seven 1:10 dilutions worked best. A master mix was prepared as

described in Table 9 in a separate room in order to avoid contaminations. Master mix was aliquoted to the 96-well plate using a Multipette (Xstream, Eppendorf). Finally, 1 µl cDNA was added in triplicats, the plate was centrifuged to spin down droplets followed by running the qPCR using a qPCR system (Stratagene MX3000P, Agilent technologies) with applying a program with 40 cycles: Denaturation for 10 min. at 95°C, 95°C for 00:30 min, decreasing temperature for 1 min to 58°C for annealing followed by extension for 1 min at 72°C.

gene	primer	sequence
haxin	fwd	CATGACGGACAGCAGTGTAGATGGAA
	rev	CTCGTAGCTGCCGGAGGGCAGTAG
ß-catenin	fwd	CAATGGCTTGGAATGAGACTGCTGATCTT
	rev	GGTCAGTATCAAACCAGGCCAGCTGATT
GAPDH	fwd	GGAAGGTGAAGGTCGGAGTCAA
	rev	ACCAGAGTTAAAAGCAGCCCTG
C-Myc	fwd	TCGGGTAGTGGAAAACCAGC
	rev	TTCCTGTTGGTGAAGCTAACGTT

Table 10. Sequences of qPCR primers.

6.7 Western blot

Reagents and buffers

Resolving mix 12% (100 mL)	Acrylamide (40%) (Roth)	30 mL
	3x Gel buffer (Roth)	33 mL
	Water	37 mL
Stacking mix 5% (50 mL)	Acrylamide (40%) (Roth)	6.25 mL
	3x Gel buffer (Roth)	16.5 mL
	Water	27.25 mL
3x Gel buffer	Bis – Tris pH 6.5 (Roth)	1 M
1x MOPS running buffer	EDTA (Serva)	1 mM
	MOPS (Sigma)	50 mM
	SDS (Roth)	0.1%
	Tris (Roth)	50 mM
200x Reducing agent	Sodium metabisulfite (Sigma)	0.5 M
1x Transfer buffer	Glycine (Roth)	150 mM
	Isopropanol (Roth)	15%
	Tris (Roth)	25 mM
1x TBS-T	EDTA pH 8.0 (Serva)	1 mM

(Tris buffered saline + Tween)	NaCl (5M Stock) (Roth)	150 mM
	Tris-Cl pH 7.4 (Roth)	10 mM
	Tween 20 (Roth)	0.1%

Whole cell protein extracts from SW480 cells were made 48 h after electroporation with 32 µM morpholino oligonucleotide by scraping cells in medium and washing the well with1 ml ice-cold 1x PBS, followed by centrifuging 5 min at 900 rpm at 4°C. Medium and PBS were aspirated and cells re-suspended in 1 ml ice-cold 1x PBS, transferred to a pre-cooled 2 ml reaction tube and centrifuged at 2800 rpm 5min at 4°C. Supernatant was evacuated and pellets were re-suspended in 100 µl lysis buffer containing 20 mM HEPES pH 7.9, 400 mM NaCl, 1 mM EDTA, 0.2% NP-40, 1 µM DTT and 0.5 µM PMSF. Bradford assay (Biorad) was used, following the manufacturer's instructions, for determination of protein concentrations within samples. 5 and 20 µg of each sample was diluted with Lämmli buffer (378 mMTris-Cl, pH 6.8, 12% SDS, 60% glycerol, 600 mM DTT and 0.02% bromphenol blue) and run on an SDS page with stacking gel (5% acrylamide) and running gel (12% acrylamide) in 1x MOPS running buffer (50 mM Tris, 50 mM MOPS, 1 mM EDTA, 0.1% SDS) with 30 mA (80 V increases to 160 V during run) per gel for 90 min. Gels were transferred on membranes by blotting in 1x transfer buffer (150 mM glycine, 25 mM tris and 15% isopropanol) for 1 to 2 h at 100 mA. Membranes were blocked 1-2 h in 5% milk powder (Roth) in 1x TBS-T (10 mM Tris-Cl, pH 7.4, 150 mM NaCl, 1 mM EDTA, pH 8.0, 0.1% Tween20) on a shaker. Membranes were washed 3x with 1x TBS-T for 10 min at RT shaking. Primary antibodies were diluted 1:500 (ß-catenin) or 1:10000 (GAPDH) and incubated O/N at 4°C shaking. After washing membranes 3x 10 min with 1x TBS-T, secondary antibody goat anti-rabbit was added in a 1:5000 dilution with 5% BSA in 1x TBS-T and incubated 1 h at RT shaking. Subsequently membranes were washed 3x with 1x TBS-T for 10 min shaking followed by detection with ECL solutions (Santa Cruz) and a ChemiDoc (Protein Simple) station. Finally, quantification was done using Image J.

6.8 Melting point analysis of catemer oligonucleotides

6.8.1 Melting point analysis with DNA oligonucleotides

Melting points were determined using fluorescing EvaGreen dye (Biotium). Oligonucleotide annealing in a PCR cycler (Thermo Scientific, Arktik) was followed by measurement in a real time PCR cycler (Stratagene MX3000P, Agilent technologies).
First samples were prepared with a total volume of 25 µl containing 4 pmol of the two oligonucleotides tested (see Table 11), as well as buffer SB+tween with 1.5 mM $MgCl_2$.

For annealing the following thermal profile was applied:

95°C 10:00 min
91x (1° reduction per min)
04°C ∞

After annealing 1.25 µl EvaGreen (Biotium) was added on ice and measurement was conducted using a real time PCR cycler (Stratagene MX3000P, Agilent technologies)

start: 25°C 00:30 min
Measurement during heating (2°C increase per minute)
95°C 00:30 min

Reagents and buffers

Buffer SB+tween:	Tris (Roth) 66.7 mM (pH 8.8)
	$(NH_4)_2SO_4$ (Roth) 16.6 mM
	Tween20 (Roth) 0.01%
EvaGreen dye (Biotium,):	1x: 1.25 µl from 20x company stock in 25 µl

6.8.2 Determination of ideal distance between catemer subunits

For these experiments the same annealing and measurement conditions were used as above under 6.8.1.
Concentrations of PNAs varied though. In experiments comparing two PNAs 80 pmol were added to the reaction and the target oligonucleotide was added at 40 pmol/25µl.

6.9 PNAs and morpholino oligonucleotides

All PNAs used for experiments were synthesised by ugichemGmbH and are listed with the morpholino oligonucleotides from Gene tools, LLC below (Table 11).

PNA name	target description	sequence
PNA327	SD basis	FluPac-Alkin-ATACTTACCTGAGAGT
PNA328	SD mut	FluPac-Alkin-CAATTTACCTCGGAGT
PNA329	Tcf3	FluPac-Alkin-CAATTTACCTCGGAGT
PNA330/393	ß-catenin	FluPac-Alkin-TTCCCTACCTCATTCC
PNA383	ß-catenin transcription start	FluPac-Alkin-AAGCCGCTGTATCCT
PNA384	ß-catenin translation start	FluPac-Alkin-GAGTAGCCATTGTCC
PNA385	ß-catenin exon 4 SD, -0 bp	FluPac-Alkin-TTGCTTACCTGGTCCT

PNA386	ß-catenin exon 4 SD, -2 bp	FluPac-Alkin-GCTTACCTGGTCCTCG
PNA387	ß-catenin exon 5 SD, -0 bp	FluPac-Alkin-TTTCTTACCCAAGCAT
PNA388	ß-catenin exon 5 SD, -2 bp	FluPac-Alkin-TCTTACCCAAGCATTT
PNA389	ß-catenin exon 6 SD, -0 bp	FluPac-Alkin-TCTCTTACCTTGCTTT
PNA390	ß-catenin exon 6 SD, -2 bp	FluPac-Alkin-TCTTACCTTGCTTTCT
PNA391	ß-catenin exon 12 SD, -0 bp	FluPac-Alkin-TTACTTACCCACACCT
PNA392	ß-catenin exon 12 SD, -2 bp	FluPac-Alkin-ACTTACCCACACCTTC
PNA330/393	ß-catenin exon 13 SD, -0 bp	FluPac-Alkin-TTCCCTACCTCATTCC
PNA394	ß-catenin exon 13 SD, -2 bp	FluPac-Alkin-CCCTACCTCATTCCAA
PNA117	SD basis, catemer	Ac-Alkin-AGTTTGAACGCG-Lys (Fluorescein)
PNA355	SD basis, catemer	Ac-TTGATACTTACC-Lys (atto612Q)
PNA356	SD basis, catemer	Ac-Alkin (atto594)-AGTTTGAACGCG-Lys (Fluorescein)
morpholino oligonucleotide name	target description	sequence
SD-MO	SD basis	TCGTAGCCTTGATACTTACCTGAGA
Tcf3-MO	SD Tcf3	GCATTGAATAACAATTTACCTCGGA
ßcat-MO	SD ß-catenin	AACTGCTCACATTTCCCTACCTCAT

Table 11. Sequences and target descriptions for PNAs and morpholino oligonucleotides.

Oligonucleotide name	description	sequence
TC1416	Catemer basis1 = DNA template +4	CGCGTTCAAACTCTCAGGTAAGTATCAAGGCTACGAGACAGGTTAGC
TC1417	Catemer Amin	AGAGTTTGAACGCG
TC1418	Catemer Bmin	GCCTTGATACTTACCTG
TC1419	Catemer Cmin	GCTAACCTGTCTCGTA
TC1420	Catemer Bcompl	GGATGCCTAAGCGTGCCTTGATACTTACCTGGAGTCGTGAGTGCT
TC1421	Catemer A6	CGACTCAGAGTTTGAACGCG
TC1422	Catemer A10	CTCACGACTCAGAGTTTGAACGCG
TC1423	Catemer C6	GCTAACCTGTCTCGTAACGCTT
TC1424	Catemer C10	GCTAACCTGTCTCGTAACGCTTAGGC
TC1432	together with catemer basis1 TC1416 for SD Mlu-Bpu	TGAGCTAACCTGTCTCGTAGCCTTGATACTTACCTGAGAGTTTGAA
TC1439	Catemer A14	AGCACTCACGACTCAGAGTTTGAACGCG
TC1440	Catemer C14	GCTAACCTGTCTCGTAACGCTTAGGCATCC
TP1687	DNA template for catemer oligos + BHQ1	TAMRA-CGCGTTCAAACTCTCAGGTAAGTATCAA
TP1688	DNA template +4 for catemer oligos	CGCGTTCAAACTCTCAGGTAAGTATCAA
TP1689	DNA template +3 for catemer oligos	CGCGTTCAAACTCTAGGTAAGTATCAA
TP1690	DNA template +2 for catemer oligos	CGCGTTCAAACTCAGGTAAGTATCAA
TP1709	DNA template +1 for catemer oligos	CGCGTTCAAACTAGGTAAGTATCAA
TP1710	DNA template 0 for catemer oligos	CGCGTTCAAACTGGTAAGTATCAA
TP1711	DNA template -2 for catemer oligos	CGCGTTCAAACTTAAGTATCAA
PNA name	description	sequence
Ugi117	targeting SD basis, catemer	Ac-Alkin-AGTTTGAACGCG-Lys (Fluorescein)
Ugi355	targeting SD basis, catemer	Ac-TTGATACTTACC-Lys (atto612Q)
Ugi356	targeting SD basis, catemer	Ac-Alkin (atto594)-AGTTTGAACGCG-Lys (Fluorescein)

Table 12. Sequences and description of PNAs and DNA oligonucleotides for the catemer project.

7 Results

7.1 Splice based reporter assay for testing antisense reagents

In order to develop a splice based reporter assay capable of quantifying antisense effects a variation of different approaches were tested. First I used an ideal target to see if the principle works. I compared different promoters and then I tested another target (tcf3) for which functional antisense molecules were already available. In order to optimise the signal a new type of luciferase (Nluc) was compared to Fluc and established with our constructs. For details according to the principle of the assay see Appendix I: Vonbrüll et al. 2018.

7.1.1 Constructs for reporter assay – proof of principle

7.1.1.1 Transient transfections

In order to test which levels of induction are possible with our reporter system, three different constructs were cloned. wt basis included a consensus splice site and was mainly used for testing the assay together with the morpholino oligonucleotide (SD-MO) targeting its splice donor. For experiments with SD-MO a stable cell line was generated. It was designed not to give a signal, unless antisense reagents were applied to block splicing. A second version represented the fully spliced state (spliced basis) giving only a background signal. A third version was generated for which splicing is impossible due to a mutation within the splice donor (blocked basis). That simulates a splice block with an antisense reagent and leads to highest possible reporter signal. After transient transfection into HeLa cells the wt basis and spliced basis showed 7% and 4% activation respectively, compared to the highest possible signal of blocked basis (Fig. 20). Furthermore, the CMV promoters of the reporter constructs were also compared with other promoters commonly used in the lab (Fig. 21) and showed good activation levels compared to the EF1α and other CMV promoters.

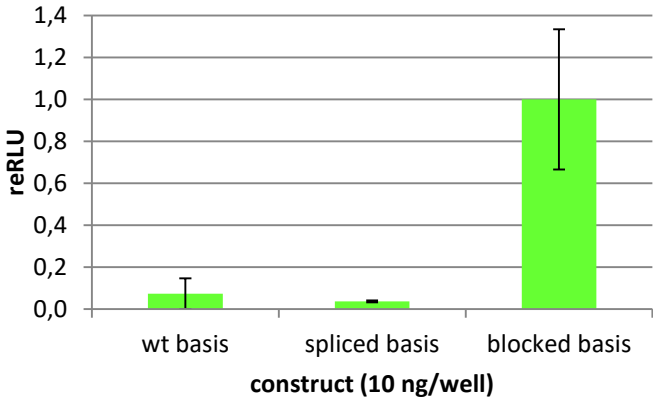

Figure 20. **Reporter activation of basis1 splice donor constructs.** HeLa cells were transiently transfected with wt basis (pKCFintron basis1), spliced basis (pKCFintron SD spliced) and blocked basis (pKCFintron SDmut). All values were normalised to the blocked basis values. Data represent mean values of at least 2 independent experiments, error bars indicate standard deviation.

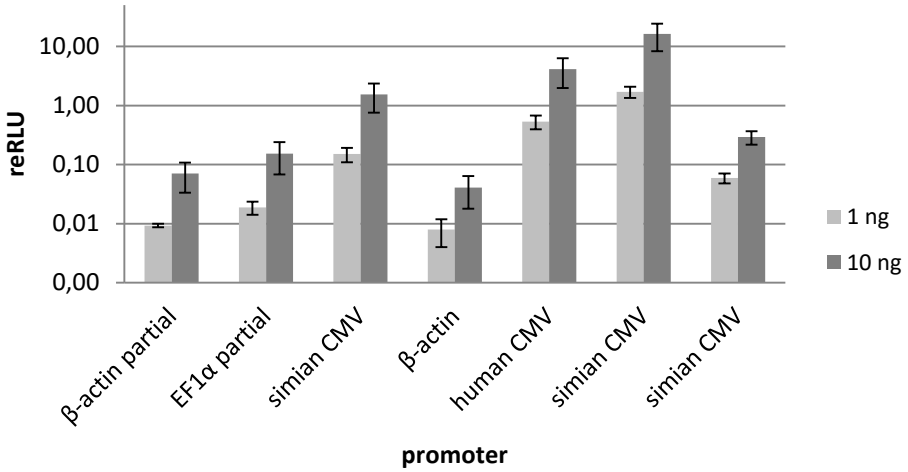

Figure 21. **Reporter activation of different promoters compared.** HeLa cells were transiently transfected with 2 ng/well pMCGlucS as an internal reference, 1 or 10 ng of reporter and up to 90 ng/well total DNA volume with pBsMhistone H4. Tested promoters were β-actin partial (pMA part luc), EF1α partial (pEF1α part luc), simian CMV (pKCFintron luc), β-actin (pMA luc), human CMV (pKC 2 luc 2a), simian CMV (pMC luc), simian CMV (pKCFintron SDmut). Values were normalised to the internal reference. Data represent mean values of 3 independent experiments. Error bars indicate standard deviation.

After these first promising results we wanted to test if the principle also works for another splice donor. Therefore, constructs including a splice donor from tcf3 were generated. wt tcf3 (1% activation), spliced tcf3 (0% activation), and blocked tcf3 (100% activation) also showed expected luciferase expression (Fig. 22).

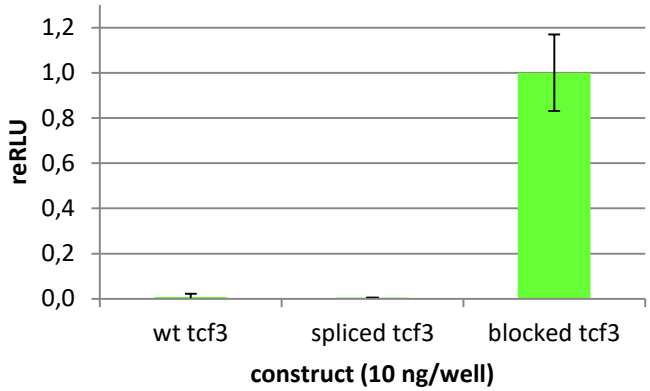

Figure 22. **Reporter activation of tcf3 splice donor based constructs.** HeLa cells were transiently transfected with wt tcf3 (pKCTcf3), spliced tcf3 (pKCTcf3 intron spliced) and blocked tcf3 (pKCTcf3intron mut). All values were normalised to the blocked tcf3 values. Data represent mean values of at least 2 independent experiments, error bars indicate standard deviation.

Transient experiments within HeLa were also conducted to test constructs with Nluc[163]. Nluc has been shown to have advantageous characteristics compared to Fluc[110] therefore constructs were recloned using Nluc. Comparing wt basis Nluc with a blocked basis Nluc version the basis version showed 7% reporter activation compared to full activation of the mutated one. A version including a specific β-catenin splice donor - wt βSD Nluc showed a 2% reporter activation compared to the fully activated blocked βSD Nluc construct (Fig. 23).

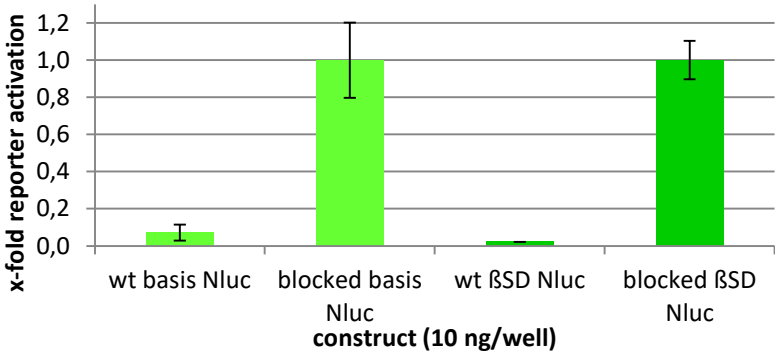

Figure 23. **Reporter activation with transiently transfected Nluc splice assay constructs.** wt basis Nluc (pSplice3 basis1), blocked basis Nluc (pSplice3SDmut), β-catenin constructs: wt βSD Nluc (pSplice3βcat ex13SD) and blocked βSD Nluc (pSplice3βcat ex13SDmut). Data represent mean values of at least 2 independent experiments, error bars indicate standard deviation.

Hence, these experiments could only help to test the possible levels of induction, but not whether a block with actual antisense reagents is detectable. Therefore wt basis (100 ng/well) construct with a consensus sequence was transiently transfected. Subsequently cells were scraped with 4μM SD-MO and increasing concentrations of PNA SDbasis (PNA327). SD-MO resulted in a 3.5-fold reporter induction at a 4μM concentration compared to controls whereas the PNA SDbasis showed a 1.5-fold effect at 64μM. But, nonetheless this gave a hint that the reporter assay works.

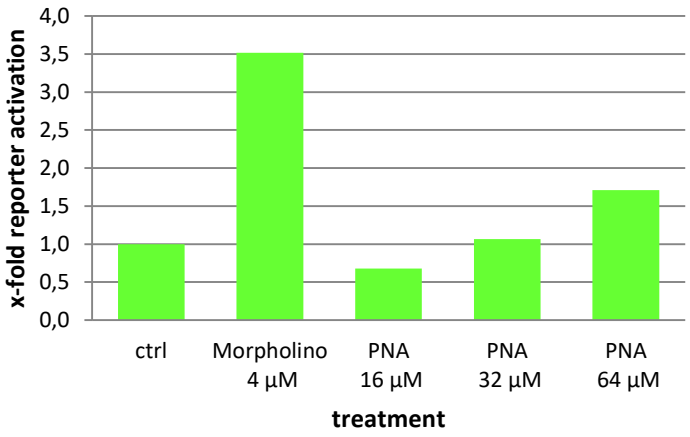

Figure 24. **Reporter activation after splice block through antisense treatment.** HeLa cells were transiently transfected with 100 ng/well pKCFintron basis1 and scraped with 4µM SD MO and 16, 32 and 64µM of PNA SDbasis. All values were normalised to control cells scraped without addition of antisense molecules (ctrl). Data represent values of one experiment.

7.1.2 Stable cell lines

After providing evidence that the principle for the splice based assay worked, stable cell lines were generated. Therefore a setup including PiggyBac transposase was used[162]. Originating from *Trichoplusia Ni* the transposable PiggyBac element consists of an internal repeat, spacer and a terminal repeat as well as a single open reading frame. The transposon-specific inverted terminal repeats are recognised by the transposase. It subsequently removes these sites efficiently and integrates them into chromosomal insertion sites[164,165]. Hence a typical DNA transposon system includes the expression plasmid with the transposase as well as the donor plasmid including the construct aimed to be integrated being flanked by cis-acting transposase sequences[166]. Although the specificity of its insertion site (TTAA) is low the 2472 bp element shows several advantages. It can carry cargo up to 14 kb without affecting transposition unlike other transposon systems as *Sleeping Beauty* or *Tol2.* Further the efficiency of transposition is less affected by transposase levels and its excision is precise without leaving a trace[167].
For the stable cell lines generated within this project, different reporter genes were compared. The assays were designed as dual luciferase assays enabling correction for varying cell number as well as transfection efficiency[168]. pSplice2 basis1 constructs included Fluc as a reporter gene showing the antisense effect following the splice block and Rluc as a second, constitutively expressed reporter used as a reference. All pSplice3 versions used Nluc as a reporter indicating the antisense effect and Fluc constitutively expressed reference.
Using the piggy bac insertion system a number of single clones were generated. Figure 25 is an example for basal Nluc and luc values measured from a variety of

single clones (pSplice3βcat ex13SD). Favourites should have a good Fluc signal (at least 10-fold above the background, as well as a measureable Nluc signal. It is important that the basal Nluc signal is not too high in order to get a strong increase of the signal upon splice block. Here the clones 1_3, 1_11 and 1_15 fulfilled these criteria best, and were further tested.

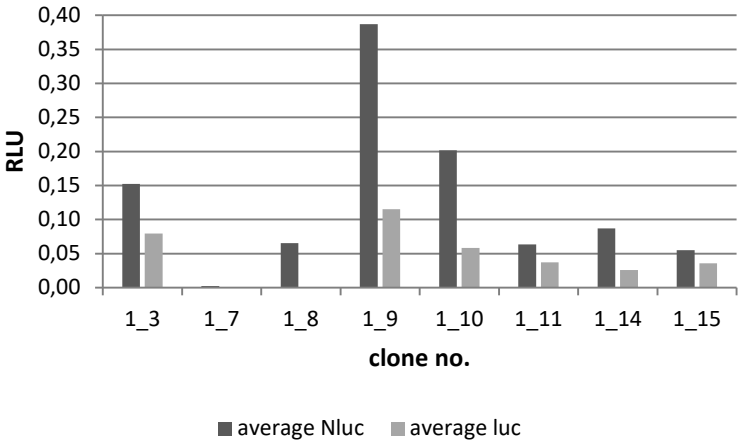

Figure 25. **Example for single clone testing.** After seeding HeLa pSplice3βcat ex13SD single clones in a 24-well plate basal (non-induced) Nluc and Fluc values (average from 6 wells) were determined in order to choose favorites. Data represent values from one experiment.

Next experiments to test the stable cell lines were conducted by delivering morpholino oligonucleotides to HeLa cells via scraping. Within the pSplice2 basis1 cell line including the test splice donor, PNA SDbasis caused concentration dependent reporter activation up to 4-fold at a concentration of 64µM. Using this concentration in the Nluc cell line with the same splice donor (pSplice3 basis1) could elevate activation up to 9-fold (Fig. 26).

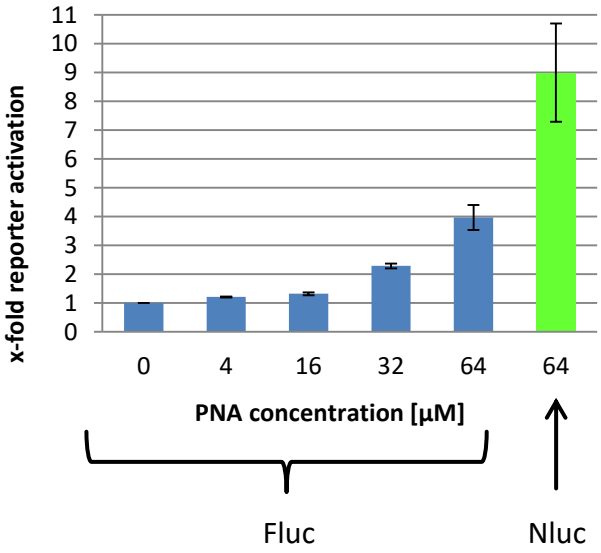

Figure 26. **Reporter activation in stable HeLa cell lines with Fluc or Nluc.** Cell lines pSplice2 basis1 (Fluc, blue) and pSplice3basis1 (Nluc, green) were scraped with PNA SDbasis targeting splice donor basis1 at 4, 16, 32 and 64 µM PNA. All values were normalised to the only scraped non-treated (0) values. Further Fluc values were normalized to Rluc and Nluc values to Fluc. Data

represent mean values of at least 3 independent experiments, error bars indicate standard deviation.

Taken together we could establish a reliable reporter assay for the detection of antisense effects. After showing proof of principle with transient transfection of constructs mimicking the outcome of a splice block, we could show that the design also works in combination with different antisense molecules. Especially the introduction of Nluc into our stable cell lines could further improve the sensitivity of the assay. After having established a powerful assay, since intracellular delivery of antisense reagents represents a major problem within antisense research, it was critical to next test different delivery methods.

7.2 Intracellular delivery methods

7.2.1 Incubation of cells with PNAs

In order to test if the modifications of the PNAs would enable unaided intracellular delivery, HeLa cells stably transfected with the splice based reporter constructs were incubated with suitable PNAs. Simply incubating the stable splice based reporter cell line pSplice2 basis1 with PNA 327 at 4, 8, 16, 32 and 64 µM concentrations for 1, 2 or 3 days did not result in significant reporter activation compared to control cells incubated only with medium (Fig. 27).

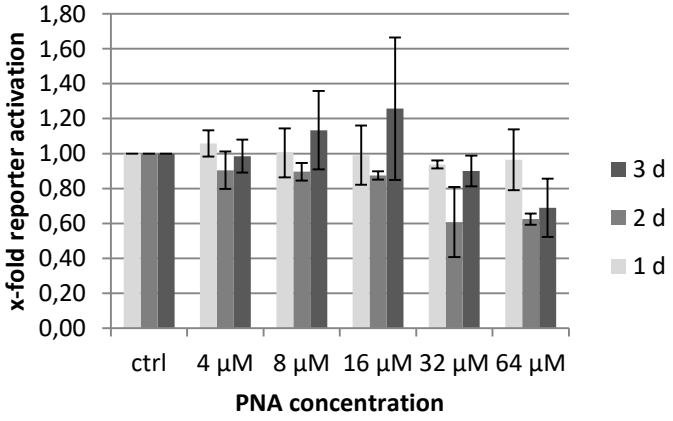

Figure 27. **Effect of PNA incubation on the Hela reporter cell line.** 0.5 x 10^4 cells/well of HeLa pSplice2 basis1 were seeded. Next day PNA327 was incubated with 4, 8, 16, 32 and 64 µM concentration for 1, 2 or 3 days. All values were normalised to cells incubated in normal DMEM (ctrl) values. Data represent mean values of at least 2 independent experiments, error bars indicate standard deviation.

The notion that intracellular delivery will not work by simply incubating cells was also noticed within HepG2 cells. Although antisense effects on β-catenin will be discussed in more detail later (chapter 7.3 “Targeting β-catenin with splice based antisense molecules”) these experiments are shown in advance, because they

demonstrate the effect of PNAs after intracellular delivery via incubation. HepG2 cells were incubated with different PNAs at a 64µM concentration for 3 days. On axin mRNA level there was no significant reduction of mRNA with any PNA tested (Fig. 28A). ß-catenin levels were only affected with PNAs targeting translation initiation (PNA383 and 384) (Fig. 28B), however the high standard deviations show that incubation of the PNAs does not work reliable enough for a consistent delivery.

A)

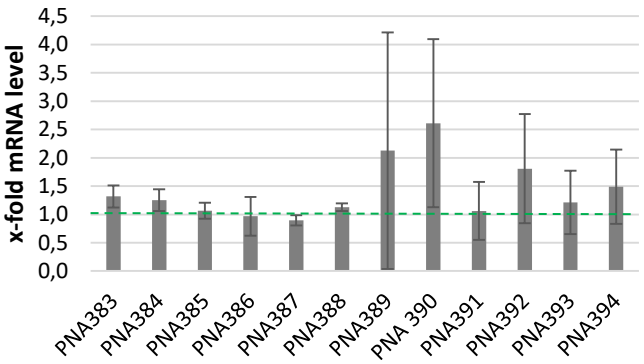

B)

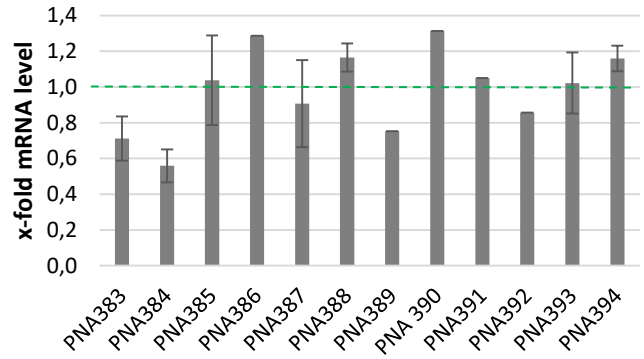

Figure 28. **Effect of PNA incubation on HepG2 cells.** 0.5 x 10^6 cells/well of HepG2 cell line cells were seeded on 6-well plates and incubated for 3 days with 64 µM of indicated PNAs. qPCR was performed using **A)** axin or **B)** ß-catenin primers. All values were normalised to the housekeeping gene GAPDH and further normalised to values of control cells without PNA treatment. Data represent mean values of at least two independent experiment (ones without error bars are single determinations). Error bars indicate standard deviation.

Taken together with the results from the reporter assay the search for a reliable, reproducible delivery method was indispensable.

7.2.2 Scraping

Several experiments using the scraping method have already been presented in chapter 7.1.1 and 7.1.2 Here a more quantitative analysis of scraping was performed.

First experiments were conducted to test scraping (as described in Material and Methods) with a buffer called loading solution (10 mM KH_2PO_4, D-glucosemonohydrate 1 mg/ml, EDTA 0.5 M, KCl 140 mM)[38] compared to DMEM. As shown exemplary in Fig. 29 usage of the loading solution results in better efficiency for FITC delivery by cell scraping. Hence, we decided to use the loading solution for all later experiments.

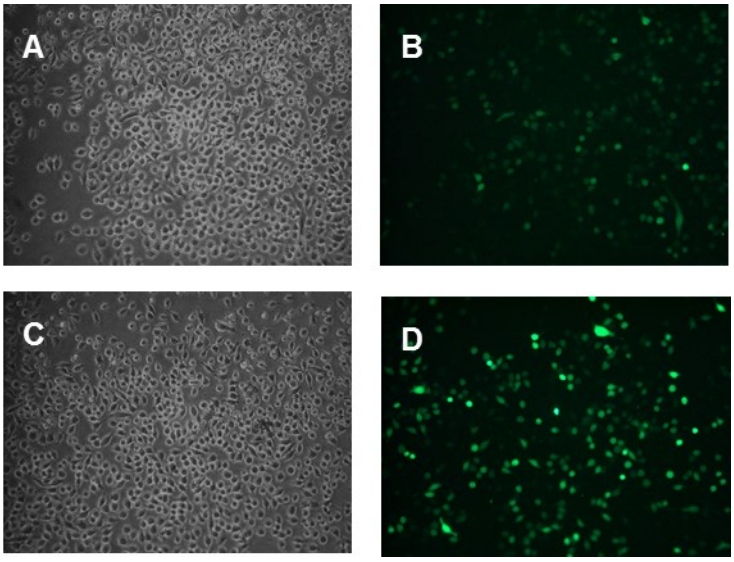

Figure 29. **Scraping efficiency DMEM compared to loading solution.** Example of delivery efficiency within HeLa cells 1 d after scraping with 0.1 mg/ml FITC dextran with either DMEM (A, B) or loading solution (C, D).

For final tests cells were scraped with 0.1 mg/ml FITC dextran and analysed using a fluorescence microscope and a flow cytometer. For determination of viability cells were stained with 7-AAD. With HeLa scraping worked fine for intracellular delivery, with about 57% FITC positive, living cells (Fig. 30). Contrary to that, SW480 were building clumps in the 24-well plate (Fig. 31). Scraping was hindered, resulting in efficiencies around 9%.

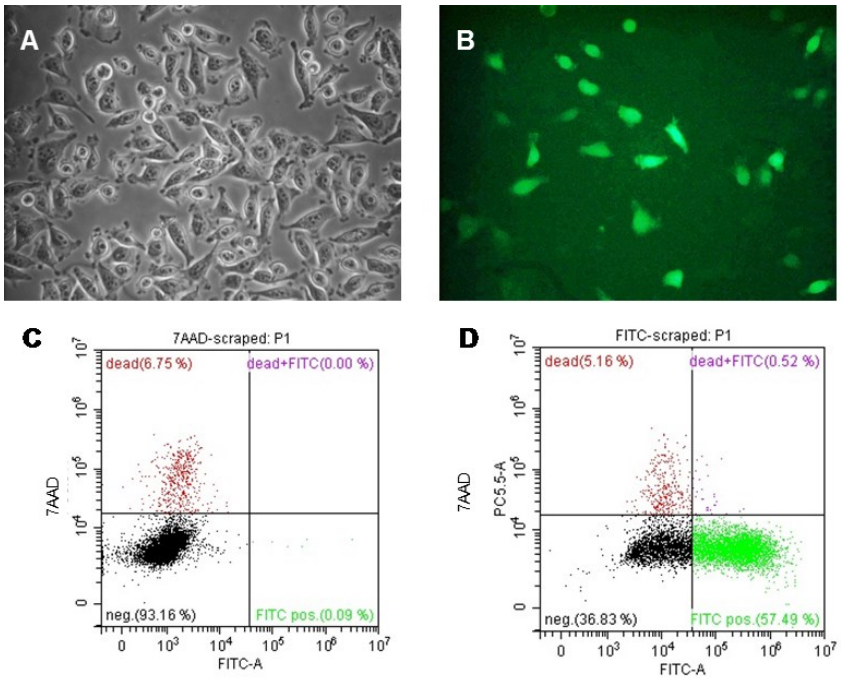

Figure 30. **HeLa cells scraped with FITC dextran.** Morphology of HeLa cells 1 d after scraping with 0.1 mg/ml FITC dextran A) bright field B) fluorescence image. Scraping leads to 57% positive, living cells D). Analysis of cell survival and efficacy by 7AAD (2 ng/µl) staining and cytometry. Cell survival being comparable for cells scraped without FITC shown in C).

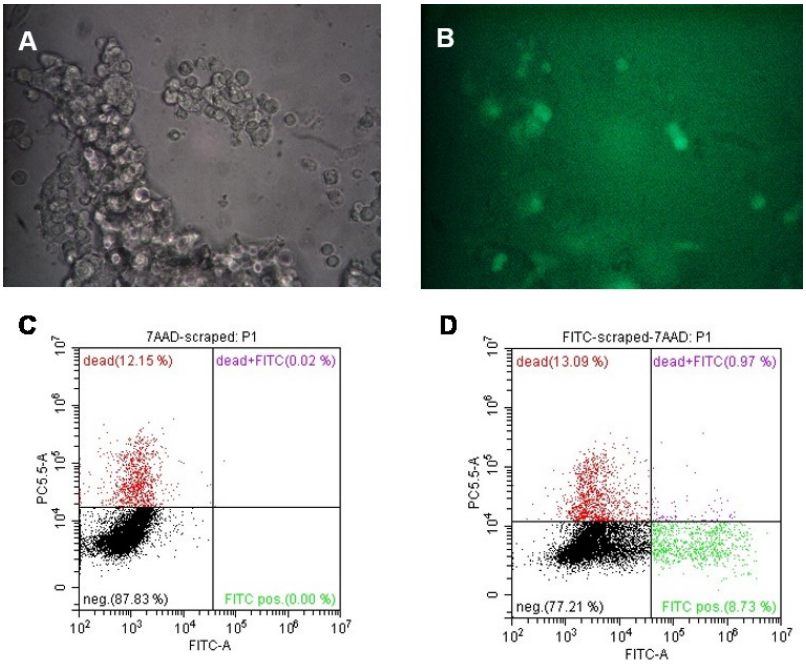

Figure 31. **SW480 cells scraped with FITC dextran.** SW480 cells 1 d after scraping with 0.1 mg/ml FITC dextran A) bright field B) fluorescence image. Cells tend to aggregate in clumps A). Scraping leads to 9% positive, living cells D). Analysis of cell survival and efficacy by 7AAD (2 ng/µl) staining and flow cytometry. Cell survival was comparable in cells without FITC shown in C).

We next tested cell scraping together with PNAs as a means to compare PNAs. HeLa cells were pre-treated with 50 mM LiCl in order to evaluate the β-catenin level upon activated Wnt signalling. After cell scraping with different PNAs at 64

µM axin mRNA levels were determined screening for reduced β-catenin levels. Whereas scraping worked fine together with the reporter assay it could not deliver the PNAs reproducible enough to quantify differences on mRNA level (Fig. 32). One main issue here was that we wanted to show the effect of the ß-catenin targeting PNAs ideally on a cancer cell line as SW480. These cells overexpress the gene, but as shown above the cell scraping protocol cannot be applied to them. In the HeLa cells we activated the pathway by LiCl treatment, but the axin levels of the cells showed very high standard deviations.

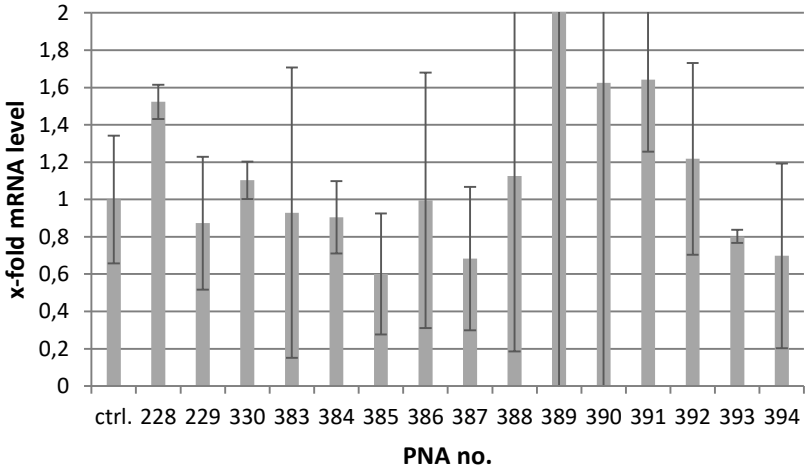

Figure 32. **Effect of PNAs after cell scraping of HeLa cells.** PNAs were scrape-delivered with different PNAs (as indicated) at 64 µM. Axin mRNA levels were determined by qPCR. All values were normalised to the housekeeping gene GAPDH and further normalised to values of control cells with 50 mM LiCl, but without PNA treatment. Data represent mean values of at least two independent experiments. Error bars indicate standard deviation.

7.2.3 Co-transfection of PNAs with annealed oligonucleotides

This principle has been successfully used for PNA delivery by Hamilton et al. [46] and we used the PNA/oligonucleotide ratios described therein for our first experiments.
For PNA/oligonucleotide co-transfections a number of parameters were varied for optimisation. For transfections with Turbofect a total DNA content of 90 ng/well is optimal. We tested different total amounts of a neutral plasmid (pBsMhistone H4) to evaluate optimal conditions for co-transfection (Fig. 33). Applied with 400 nM PNA or 400 nM oligonucleotide filling up the reaction with 90 ng/well worked best.

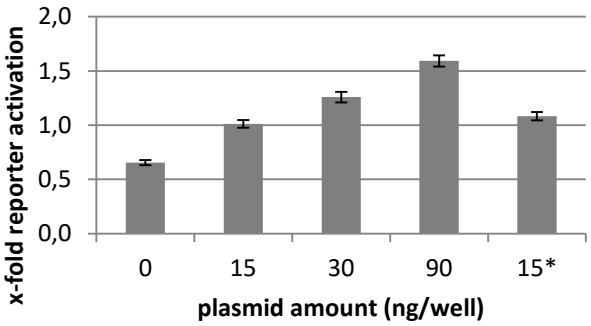

Figure 33. HeLa pSplice3 basis1 were seeded with 0.5 x 10^4 cells/well on a PEI coated 96-well plate, and transfected with 400 nM PNA327 annealed to 400 nM oligonucleotide 1821 (12 bp overlap) or 1822 (11 bp overlap, [*]) and varying amounts of 15, 30 or 90 ng/well neutral DNA (pBsMhistone H4). All values were normalised to controls only transfected with the respective oligonucleotide. Data represent 12 technical replicates from one experiment.

Next step was to test different PNA concentrations, showing that 400 and 800 nM worked best, but none of them showed sufficient reporter activation (Fig. 34).

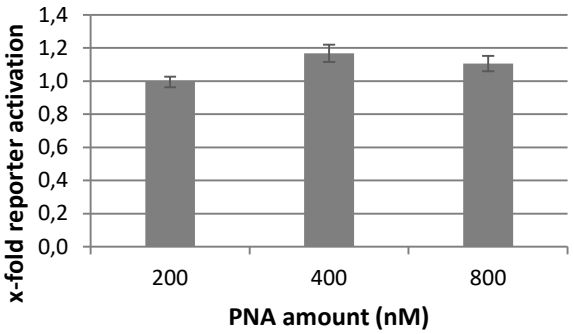

Figure 34. HeLa pSplice3 basis1 were seeded with 0.5 x 10^4 cells/well on a PEI coated 96-well plate, and transfected with 200, 400 or 800 nM PNA327 annealed to 400 nM oligonucleotide 1821 (12 bp overlap) and 90 ng/well pBsMhistone H4. All values were normalised to controls only transfected with the respective oligonucleotide. Data represent 12 technical replicates from one experiment.

Finally, oligonucleotides with a different number of nucleotides overlapping with the annealed PNA were compared. Since a combination of 800 nM oligonucleotide 1824, with 800 nM PNA327 showed up to 2-fold effects, we used similar conditions with other oligonucleotides. Lower (200 nM) and higher concentrations (1600 nM) could not improve the effect. Neither did oligonucleotides with less or more overlap than the 12 bp tested with oligonucleotide1824 and 1825. Taken together the method did not aid delivery efficiency to a feasible extent in these experiments (Fig. 35).

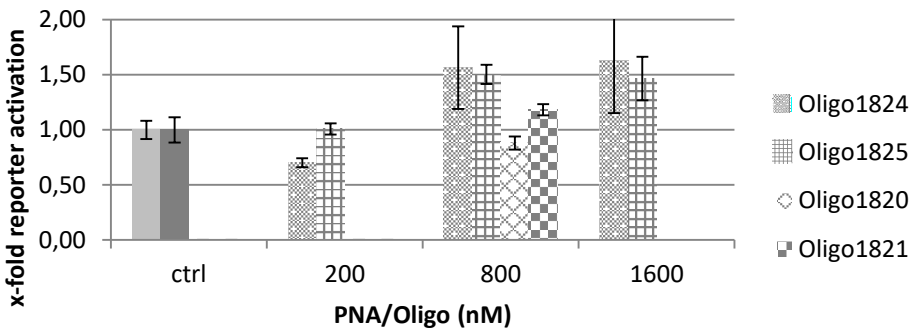

Figure 35. **PNA/oligonucleotide co-transfections.** HeLa pSplice3 basis1 were seeded with 0.5 x 10^4 cells/well on a PEI coated 96-well plate, and transfected with PNA u327 annealed to different oligonucleotides as indicated: Oligo1824 (12 bp overlap), oligo1825 (12 bp overlap), oligo1820 (13 bp overlap) and oligo 1821 (12 bp overlap). All values were normalised to controls only transfected with the respective oligonucleotide (ctrl). All values were normalised to controls only transfected with the respective oligonucleotide. Data represent mean values of 12 technical replicates, error bars indicate standard deviation.

7.2.4 Electroporation

In order to establish electroporation conditions suitable for different cell lines a variety of conditions were tested. First experiments were done using 0.1 mg/ml FITC dextran in varying volumes (data not shown). Presented here are results with the standard conditions that were used for later experiments.
Electroporation efficiency of FITC dextran delivery was tested by subsequent flow cytometer analysis. Being electroporated with 0.1 mg/ml FITC dextran using a pulse interval of 20 msec, pulse width of 12 ms, train duration 0.25 seconds, voltage 60 V at a frequency of 1 kHz (Fig. 36) HeLa cells showed sufficient delivery efficiencies of about 43% positive, alive cells. With that efficiency experiments to quantify and compare the effect of PNAs with our reporter assay were possible. SW480 cells were electroporated with the same conditions as HeLa except for applying a longer train duration of 0.5 seconds. SW480 showed values at about 23% positive, living cells after being incubated 48 h for recovery. This recovery made sense contrary to HeLa, because SW480 grow slower, enabling extended incubation without risking overgrowth. Compared to incubation, scraping

or co-transfection with oligonucleotides, electroporation showed best efficiencies and reproducibility.

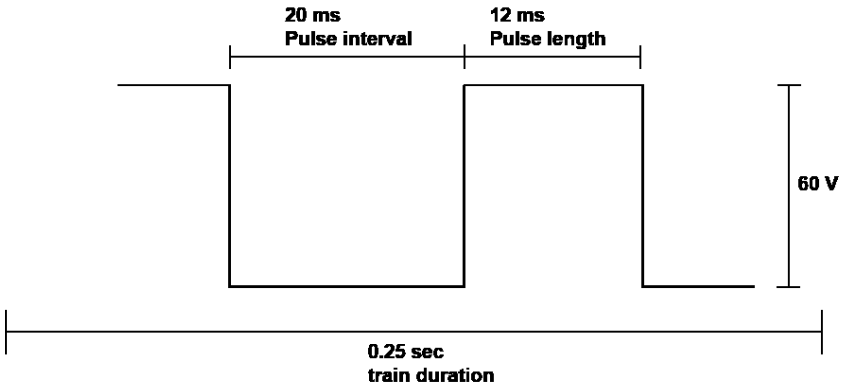

Figure 36 **Adjustments for electroporation.** Pulse length defines the duration of one pulse with a certain voltage. A pulse interval is the duration between two pulses. Train duration defines the duration multiple pulses are supposed to take.

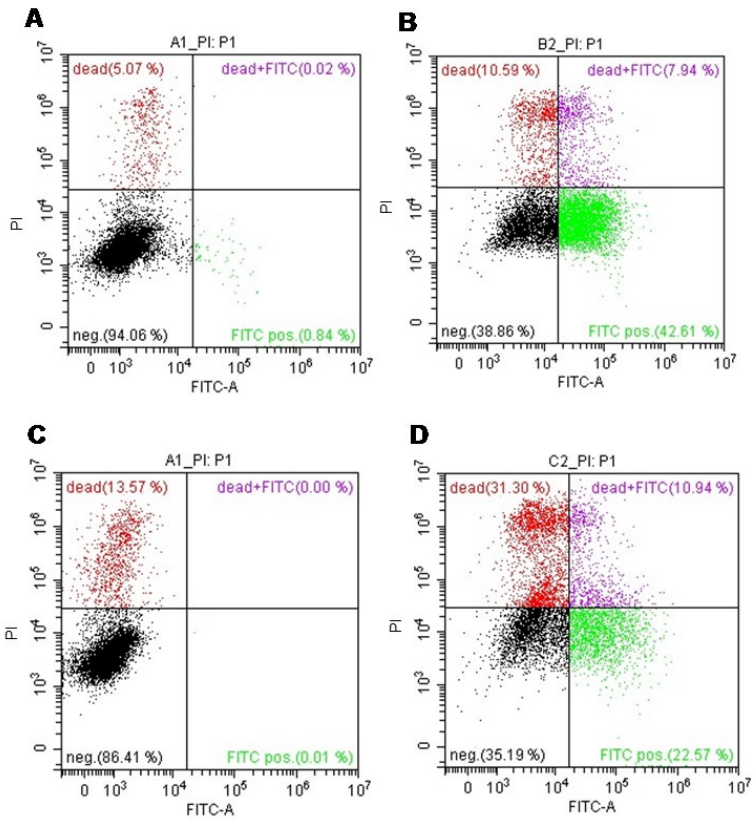

Figure 37. **Transfection efficiency within** electroporated **cells.** Cells were electroporated with 0.1 mg/ml FITC dextran using a pulse interval of 20 msec, pulse width of 12 ms, train duration 0.25 seconds for HeLa or 0.5 sec for SW480, voltage 60 V at a frequency of 1 kHz. Or same conditions without FITC for control cells (ctrl). A) HeLa ctrl cells without FITC, B) Hela cells with FITC, C) SW480 ctrl cells and D) SW480 cells with FITC.

7.3 Targeting β-catenin with splice based antisense molecules

Due to the crucial role of Wnt signalling in many forms of cancer it was suggested as a target for therapeutical approaches (Introduction 5.2). Hence, we chose to develop a splice based antisense strategy. Since β-catenin has a central role in the Wnt pathway (Introduction 5.2), we selected it as a target gene. After successful development of an assay that could help us to quantify the antisense effect of antisense molecules on specific splice sites it was important to develop a strategy specifically for β-catenin. Since the appearance of cryptic splice sites can negatively influence any splice-based strategy (Introduction 3.4.5.3) the first step was to do in-silico analysis that helped to detect these sites. Subsequently we chose splice sites that fulfilled the criteria not to be neighboured by cryptic sites and designed PNAs. These were screened for their efficiency and favourites were further analysed.

7.3.1 In-silico analysis for cryptic splice sites

Planning our splice based assay or designing PNAs targeting splice sites it was crucial to locate cryptic splice sites next to our target sequence first. A strong cryptic splice site could be recognised by the splice apparatus and restore splicing[93]. This could restore the reading frame in an unpredictable and unwanted fashion, especially for an antisense strategy. Therefore we decided to test our selected target sites with two detection programs ASSP[169] and NetGene[170]. Alternative and cryptic splice sites are weaker than constitutive ones, hence they cannot be determined using current gene finding programs that search for optimal splice sites and gene structures. Therefore specific alternative splice site detection programs were developed. These predict potential splice sites based on the information from alternative splice site sequences. Quantitative models are used to recognise the site and assign a score. Depending on the level of the score compared to a cut-off value a classification as a constitutive or alternative splice site is made by the programs[171,169]. But there are also new approaches (as NetGene) using knowledge apart from the sequence, like protein coding potential, exon and intron length predicted, strength of neighbouring splice sites and average GC content[170]. Hence it depends a lot on the algorithm of the program, therefore we ran the predictions with both ASSP and NetGene in order to double check the results. Exemplary NetGene and ASSP results for ß-catenin exon 10 to exon 14 are shown in the appendix (Appendix II, p. 97). Compared to the NetGene results ASSP finds far more alternative sites. Important to note, that it has been shown that ASSP often predicted authentic splice sites as alternative ones with a confidence of more than 0.88 [171]. Which may be an explanation for the different results. For us it was sufficient to avoid splice sites with high confidence levels next to exon junctions. Based on this information, we planned our antisense strategies. Finally, we could show that splicing took place in the expected manner

at the chosen sites - for both our splice based assay and the strategy for targeting exon13 of ß-catenin (Appendix I: Vonbrüll et al. 2018).

7.3.2 Screening of antisense molecules for targeting of β-catenin

After choosing splice sites ideal for a blocking strategy, avoiding complications with cryptic sites, PNAs and morpholino oligonucleotides targeting different positions of ß-catenin were designed and synthesised. Subsequently, as shown in Vonbrüll et al. 2018 these were screened (Appendix: Vonbrüll et al. 2018, Fig. 2A). Therefore, a variety of PNAs were delivered to SW480 cells by electroporation and analysed by qPCR unveiling favourites (Appendix I: Vonbrüll et al. 2018, Table S3). PNAs targeting the splice donor of exon 13 were identified as the most promising ones. In order to verify the impression of this first screen and further determine a favourite target site these were as well compared with our newly developed splice based assay (Appendix I: Vonbrüll et al. 2018, Fig. 2B). HeLa cells of our stable pSplice3βcat Ex13 SD cell line were electroporated with 128 µM PNA. PNA18 showed highest efficiencies and were chosen for experiments targeting ß-catenin within SW480 cells, which overexpress the protein. A splice block of exon13 using PNA18 affected splicing most strongly. Further, the protein level of ß-catenin was reduced and mRNA levels of the target genes Axin, Myc and VEGF were reduced (Appendix I: Vonbrüll et al. 2018, Fig. 3 A-C). After finding a good targeting site on β-catenin we were curious to find out more about the exact way that the splice block at this exon affected the resulting protein according to its interactions with potential interaction partners.

7.3.3 β-catenin truncations induced by splice blocking

Mammalian-two-hybrid analysis

In order to evaluate how a block at the splice site induced by PNA18 does influence the resulting protein we set up a series of experiments comparing shortened versions of ß-catenin. These included mammalian-two-hybrid analyses (Appendix I: Vonbrüll et al. 2018). For these experiments, an optimal transfection efficiency is critical. Therefore, we performed a series of experiments in order to improve transfections in different cell lines.

7.3.4 Transfection efficiency of different cell lines

It has been documented that transfection efficiencies can strongly vary among different cell lines[172]. Aiming at an optimal readout for reporter assays with shortened β-catenin versions (Appendix: Vonbrüll et al. 2018) we tested different cell lines. SW480 with naturally elevated Wnt signalling were compared to A2780, PC-3 and LNCaP cell line cells. All were transfected with equal amounts of three

different Wnt reporters including pMlucF6lefcons[173] (lef cons), pMlucM6lefmyc (lef myc) and pMlucF[173]. The luciferase values were acceptable for SW480 cells, all other cell lines showed low activity (Fig. 38).

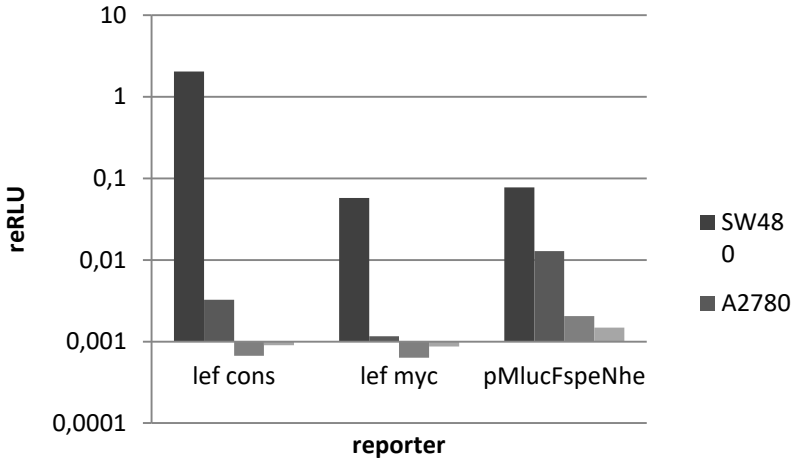

Figure 38. SW480, A2780, PC-3 and LNCaP cells were transfected with 70 ng/well reporter pMlucF6lefcons (lef cons) or pMlucM6lefmyc (lef myc) or pMlucF Spe Nhe and unspecific DNA (pBsMHisH4) up to 90 ng/well total plasmid amount. Data represent values of one experiment.

7.3.5 Transfection optimisation in HeLa and HEK 293 T-REx cells

Especially for mammalian 2-hybrid experiments high transfection efficiencies were critical. Therefore we tested different concentrations of total DNA amount and Turbofect transfection reagent. Transiently transfecting total plasmid amounts of 70, 90 and 120 ng plasmid (pKC luc) and 1x (corresponds to standardly used 0.14 µl Turbofect prepared for 1 well), 1.25x and 1.5x turbofect showed that using the 90 ng/well total DNA amount recommended by the manufacturer a 1.5-fold Turbofect results in best transfection efficiency for HEK 293 T-REx cells (Fig. 39).

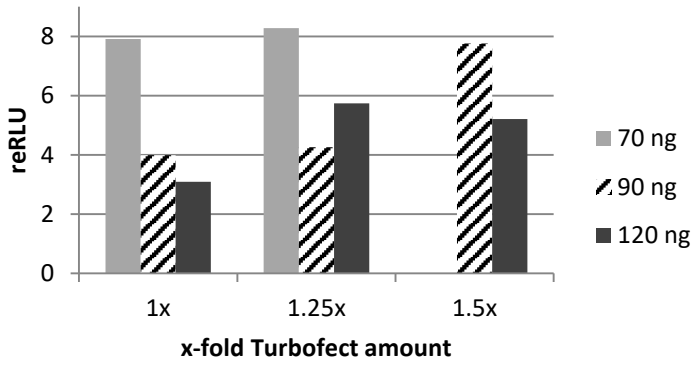

Figure 39. HEK 293 T-REx cells were transiently transfected with 2 ng/well pKC luc, 2 ng/well pMCGlucS, 20 ng/well pMCGFP and varying amounts of unspecific DNA (pBsMHisH4) in order to fill up to total DNA amounts indicated. Data represent mean values of 12-fold determinations from one experiment.

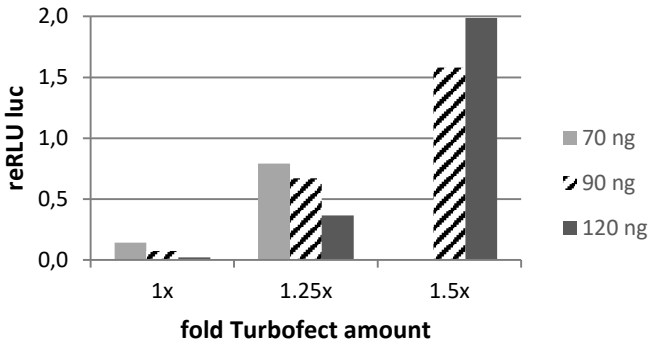

Figure 40. HeLa cells were transiently transfected with 2 ng/well pKC luc, 2 ng/well pMCGlucS, 20 ng/well pMCGFP and varying amounts of pBsMHisH4 in order to fill up to total DNA amounts indicated. Data represent mean values of 12-fold determinations from one experiment.

Within HeLa cells we tested the same conditions as with HEK. Here an increase of Turbofect concentration resulted in stronger efficiencies throughout (Fig. 40). Hence, we wanted to detect the plateau where the maximal efficiency was reached, therefore we repeated the experiment with the same conditions but with one additional DNA amount of 150 ng total DNA/well and also a 2-fold (2x) Turbofect concentration. With HeLa an increase of total plasmid amount resulted in better efficiencies. At 90 ng/well DNA 1.25-fold and 1.5-fold Turofect concentrations improved transfection efficiency. Use of 2-fold Turbofect did not increase luciferase signals at any tested condition (Fig. 41).

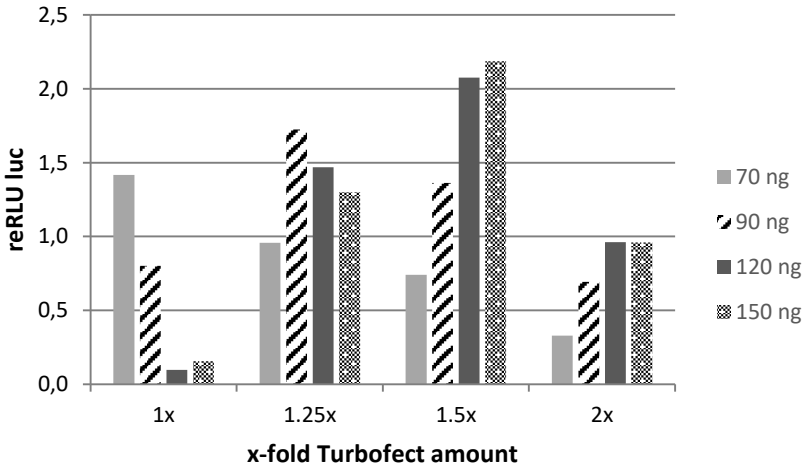

Figure 41 HeLa cells were transiently transfected with 2 ng/well pKC luc, 2 ng/well pMCGlucS, 20 ng/well pMCGFP and varying amounts of unspecific DNA (pBsMHisH4) in order to fill up to total DNA amounts indicated. Data represent mean values of 12-fold determinations from one experiment.

As a result we decided to use 1.25-fold Turbofect amount for mammalian 2-hybrid experiments in order to increase transfection efficiency without pushing costs for reagents too hard.

Using the improved transfection protocol we could conduct the mammalian-two-hybrid analysis. We generated expression constructs according to expected splice products (details Appendix I: Vonbrüll et al. 2018, Fig. 4) and chose Lef1, Tcf3, Cadherin and α-catenin as baits. The shortened versions of exon 13 still showed Tcf/Lef binding we next analysed a potential dominant negative effect. Basis for this idea is the absence of the C-terminally located transactivation domain of β-catenin. Truncated versions of β-catenin which retain the Tcf/Lef interaction could therefore compete with naturally occurring, full length protein and therefore boost the knockdown. In order to get a first impression some constructs already available in the lab were tested. In order to determine levels of Wnt pathway activity a reporter with six Tcf/Lef binding sites [173] was co-transfected with similar amounts of full length and shortened ß-catenin versions. As shown in Fig. 42 compared to the full length version a selection of all shortened ones resulted in decreased activity of ß-catenin. Strongest effects could be observed with the shortest ß-catenin (134-663). Follow-up experiments were done with constructs closely resembling the outcome of a splice block at the splice donor of either exon 13 or exon 6 as a control. The constructs were generated by PCR. Blocking of a splice sites results in the presence of the remaining un-spliced intron or often the exon next to the blocked donor is skipped. For exon 13 we generated ß-catenin(+I13) with intron 13 added, ß-catenin(E13skip) mimicking a skipped exon 13. In order to have a shortened negative control without the armadillo repeats that are important for interactions with co-factors we made controls for exon 6 namely ß-catenin(+I6) and ß-catenin(E6skip), all constructs ending at the first naturally occurring stop codon in the corresponding frame. These showed clearly that a splice block short at exon 13 generated a protein, that could still fully interact with its interaction partners Tcf3 and Lef1 (Appendix I: Vonbrüll et al. 2018, Fig. 4). At the same time the shortened version competed with naturally occurring full-length protein (Appendix I: Vonbrüll et al. 2018, Fig. 5)) leading to a “dominant negative” effect.

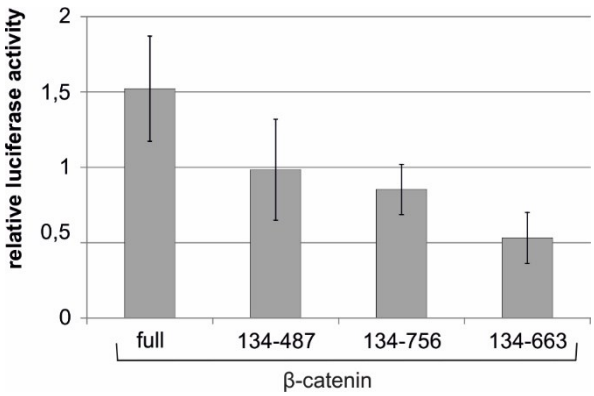

Figure 42. **Dominant negative effect of truncated β-catenin.** Transfection of 1 ng/well full length β-catenin pKCDPβcat (full) together with 70 ng reporter pMlucF6lefcons, 2 ng Rluc control pMCGlucS and 20 ng β-catenin deletion constructs pKCDPβcat(134-487), pKCDPβcat(134-756) or

pKCDPβcat(134-663) as indicated into HeLa cells. Luciferase measurements 24 h after transfection. All values were normalised to samples transfected with empty pKC vector. Data represent mean values of at least 3 independent experiments, error bars indicate SEM.

7.4 Catemer concept

This concept was developed in order to further improve binding affinity of antisense molecules. An extension of oligonucleotides increases the affinity for its target, but also favours unspecific interactions. Therefore binding in a competitive situation within the cell is improved only to a certain degree [9]. A new strategy is to use oligonucleotides that not only bind the targeted mRNA sequence side by side, but are also connected with neighbouring oligonucleotides in a chain-like arrangement as “Catemer oligonucleotides”(Fig. 43). These connecting interactions could be any kind of interaction.

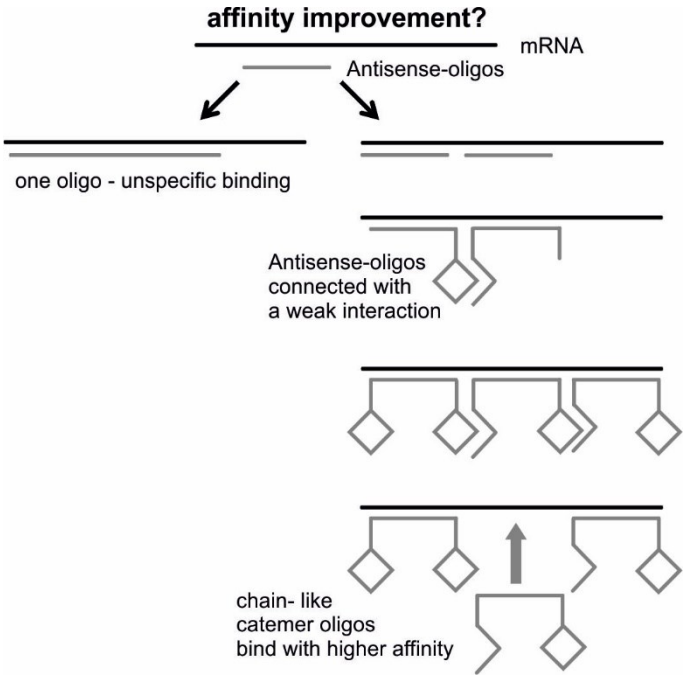

Figure 43. **Catemer principle.** Oligonucleotides are connected via a weak interaction and result in improved affinity by binding a longer target sequence.

7.4.1 Melting point analysis with DNA oligonucleotides

In order to determine binding strength a melting point analysis was performed for a target sequence with different combinations of complementary oligonucleotides (sequences; Table 12). The connecting interactions between the oligonucleotides are here base pair interactions between extensions of the oligonucleotides. In order to get an idea of the necessary strengths of these interactions different lengths of the complementary extensions were tested. The target sequence was called “basis” and resembles that of the test splice donor also used in the stable cell line pSplice3 basis1 (Table 2). Sequences and position of oligonucleotides

binding the target “basis” are depicted in Fig. 44. Combination and length of the chosen interactions are shown in Fig. 45. Melting points resulting from the analysis indicate that, as a result of stronger connecting interactions between neighbouring oligonucleotides the melting point increases (Fig. 46B and C). Even the longest complementary regions (strongest interactions) still increased the overall melting point.

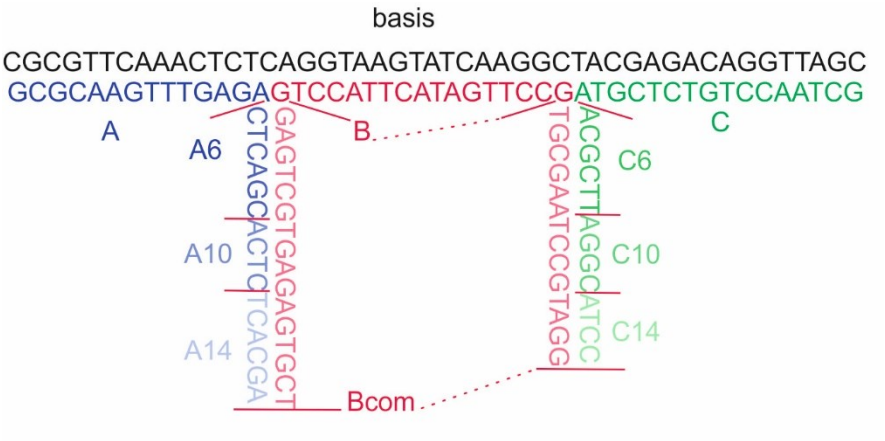

Figure 44. **Catemer principle.** Sequences of tested target and catemer oligo nucleotides. A6, A10, A14 are extended versions of A; additional nucleotides indicated. Same principle for B and C units.

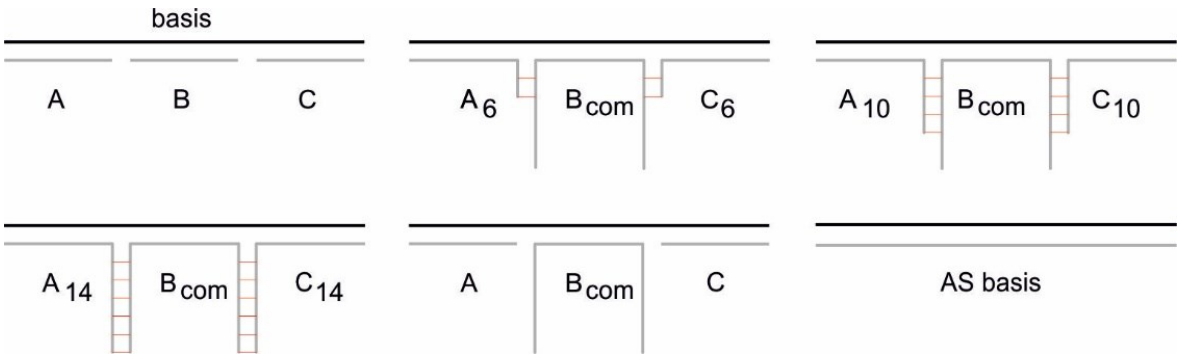

Figure 45. **Combinations of catemer oligonucleotides.** These combinations were tested via melting point analysis.

A)

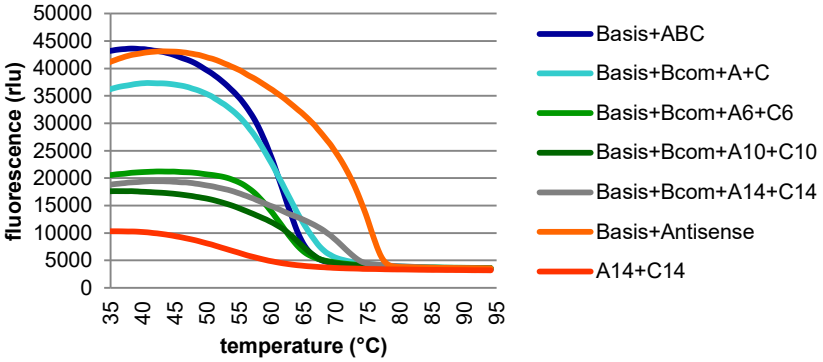

B)

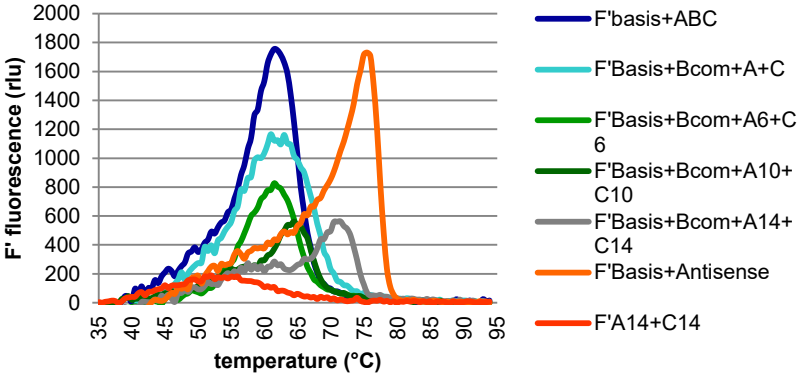

C)

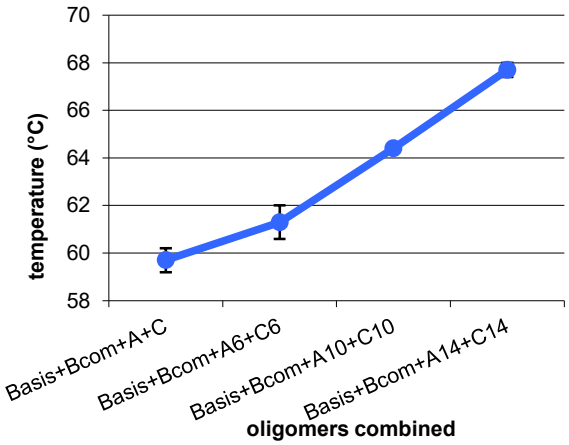

Figure 46. **Melting point analysis.** A) The oligonucleotides were analysed in a reaction containing 4 pmol of each oligonucleotide combined as described in Fig. 44. B) First derivatives of the curves in A). C) Melting points of curves shown in B). EvaGreen dye binds double stranded DNA meaning increased binding affinity results in a stronger signal.

7.4.2 Determination of the ideal distance between catemer subunits

Next, we determined what the optimal distance between the single oligonucleotides within the catemer-chain would be. Therefore, a set of fluorescein labelled PNAs was designed (Table 11). These were annealed to a DNA target sequence in different distances to one another. PNAs were designed with lysine residues that could carry a quencher. One PNA carrying a fluorescing Atto594 would be quenched by the neighbouring PNA carrying an Atto612 quencher (Fig. 47). By using target oligonucleotides with different lengths between the binding sites of the two PNAs the distance of the neighbouring PNAs could be varied and tested via fluorescence measurement. Once the binding distance between the PNAs would be reduced to a level where they would start to interfere with each other, this would result in reduced quenching (Fig. 47). First experiments were done using only a fluorescently labelled PNA (PNA117, Table 11) for determination of the lowest concentration that could be easily detected within a qPCR cycler (Fig. 48A). Then an oligonucleotide with an atto 612 quencher (PNA355) was added to establish conditions that show the quenching effect (Fig. 50B). These experiments show that the signal from the PNA alone is strongly dependent on the temperature already (Fig. 48A), but adding the oligonucleotide with the quencher does decrease measured fluorescence (Fig. 48B). Different concentrations of the quencher were tested, revealing that using the double amount of PNA compared to the oligonucleotide resulted in the best effect (Fig. 49). This was also obvious after determination of the melting points. With double PNA amount (P4OQ2) compared to the oligonucleotide, the melting point could be shown most accurately (Fig. 49B).

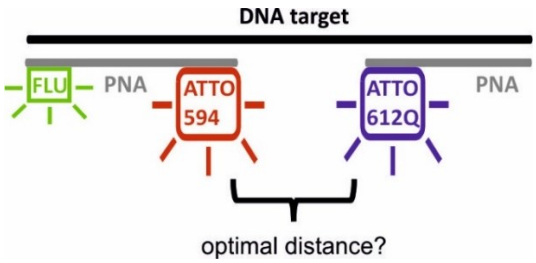

Figure 47. Principle for optimisation of distance between catemer subunits. Details see text.

A)

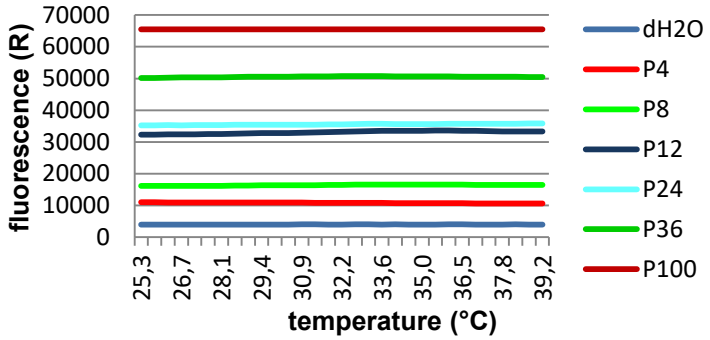

B)

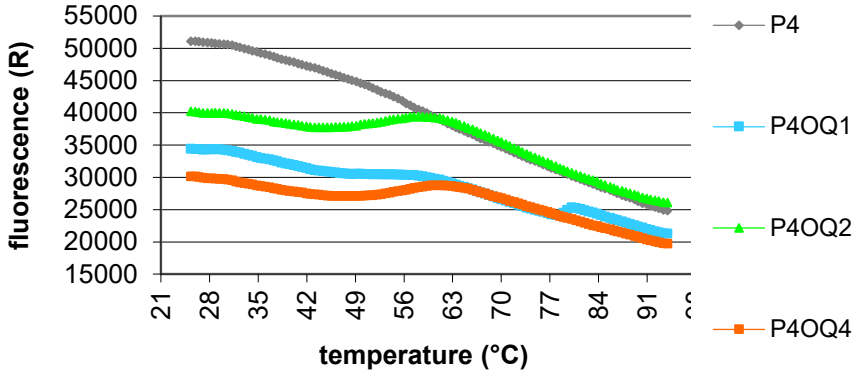

Figure 48. **Melting point analysis** Determination of the detection limits at increasing temperature (starting at 25.3°C to 39.2°C) within the qPCR cycler A) Fluorescence of 0 (dH2O), 4 (P4), 8 (P8), 12 (P12), 24 (P24), 36 (P36) and 100 (P100) pmol PNA117. First experiments adding a quencher B) Fluorescence of 4 pmol PNA117 (P4) or combined with 1 pmol (P4OQ1), 2 (P4OQ2) pmol and 4 pmol (P4OQ4) PNA355.

A)

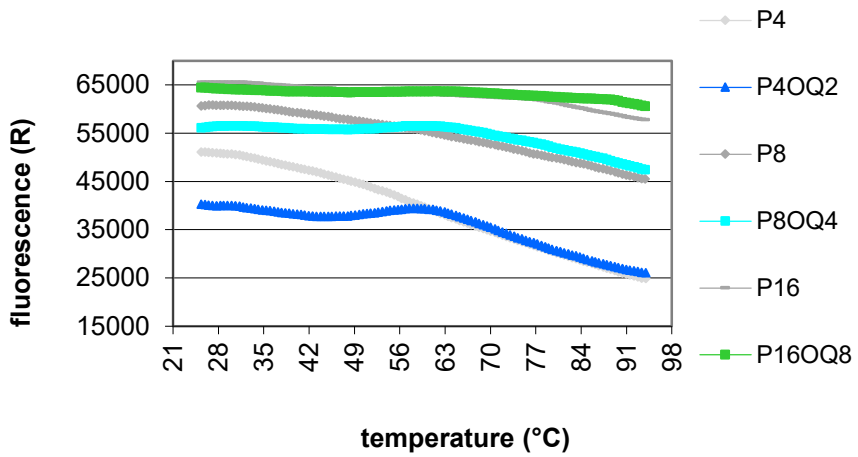

B)

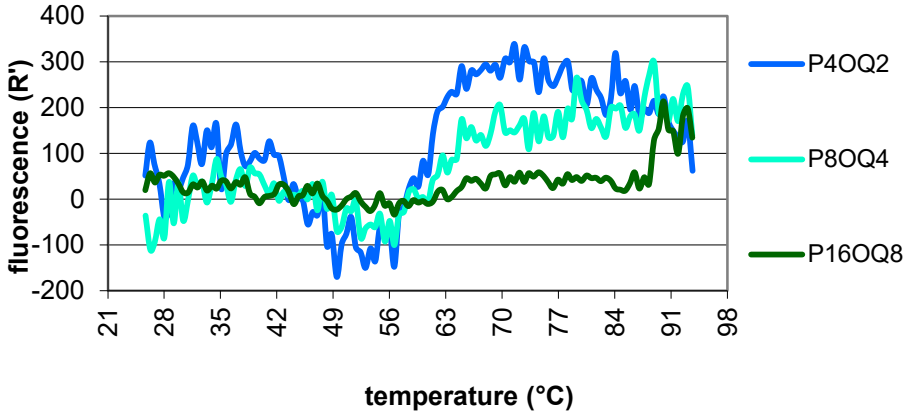

Figure 49 **Melting point determination** A) Fluorescence of 4 (P4), 8 (P8) and 16 (P16) pmol PNA117 alone or combined with 2 pmol (P4OQ2), 4 pmol (P8OQ4) and 8 pmol (P16OQ8) PNA355. B) First derivativs of selected combinations described in A).

As a next step varying lengths of the target sequence were included in order to determine the optimal distance between neighbouring oligonucleotides. After testing a variety of target lengths it was obvious that only after an overlap of 6 nucleotides the melting point shifted to a lower temperature (Fig. 49). Indicating there is not much steric hindrance between the Lys residues of the PNAs.

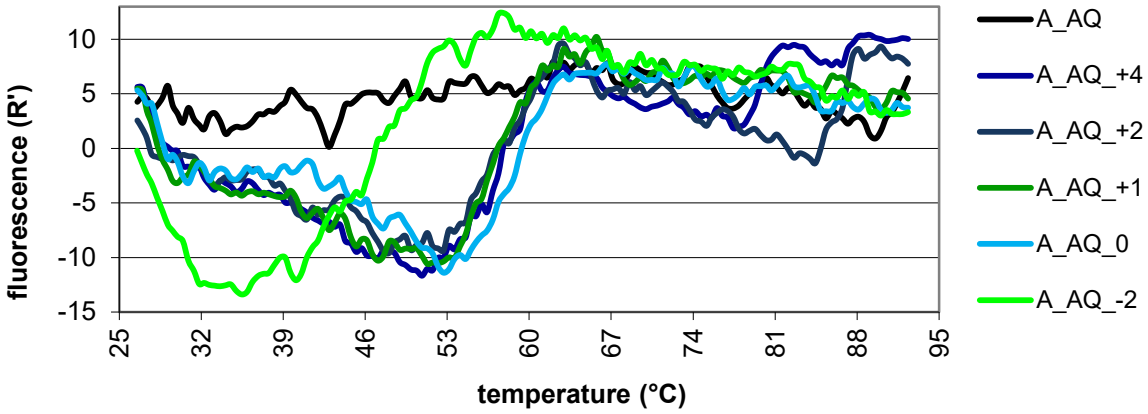

Figure 50 Melting points of 80 pmol PNA356 (A) and 80 pmol PNA355 (AQ) combined with 40 pmol of different target oligonucleotide lengths, leaving space between the PNAs of plus 4 bases (+4; oligonucleotide TP1688), plus 2 bases (+2; TP1690), plus 1 base (+1; TP1709), zero (0; TP1710) or an overlap of 2 bases (-2; TP1711). For sequences, see Table 12.

These experiments showed that the distance between catemer subunits would not be that critical for good binding affinity. Since the catemer concept itself looked promising in the first experiments it would have been necessary to test if these effects also provide an advantage in cell culture experiments. But since the company providing us with the PNAs (our collaboration partner ugichem GmbH) went bust we could not bring this project to an end.

8 Discussion

During the last decade there have been many attempts to optimise antisense molecules for therapeutic use [5]. FDA approved use of Fomivirsen [2], Pegaptanib [3] and Mipomersen [4] highlighted the potential of these reagents. Nonetheless, progress has been hampered due to a variety of reasons. Besides intracellular delivery it is important to find safe targeting strategies for different diseases. The main goal of this project was to successfully target Wnt signalling in tumor cells with antisense molecules. In order to reach this point we first designed a splice based reporter assay to quantify the effects of antisense molecules and subsequently select favourite target sites for a successful knock down. Furthermore, in a side project a completely new idea of combining antisense oligonucleotides for a more efficient targeting strategy was tested.

8.1 Splice based reporter assay

A variety of splice based reporter assays have been successfully used for the quantification of antisense effects resulting from splice targeting molecules [118,119].

First designs were based on a setup including the sequence of a ß-thalassemia related β-globin point mutation combined with GFP [120,174] or luciferase[175]. Efficient binding of an antisense molecule led to a successfully restored reading frame resulting in luciferase or GFP expression [174,175]. We chose a design where potentially any splice donor can be put into an artificial surrounding including a luciferase reporter enabling experiments with any sequence of interest (Appendix: Vonbrüll et al. 2018; Fig. 1A). The construct includes restriction sites, therefore donor sequences of interest can be easily introduced with one cloning step. In order to test the principle a series of constructs was made containing different splice sites. First experiments were conducted via transient transfection of the constructs into HeLa cells. As a target a Tcf3 ("tcf3" constructs) splice donor was blocked as well as an ideal consensus splice donor sequence ("basis1" constructs). Since these already showed good activation (Appendix: Vonbrüll et al. 2018; Fig. S1
) we could proceed on improving the assay. Therefore we introduced Nluc instead of Fluc, resulting in a 2.25-fold improved reporter activation compared to the Fluc construct (Results: Fig. 26, p. 61). The increased sensitivity is in good agreement with other studies using this new luciferase [176,177]. Within the stable cell lines Nluc constructs, tested via scrape delivered PNAs showed 9-fold reporter activation (Results: Fig. 26, p.61), comparable to previously published work [175]. This is sufficient, although similar assays showed up to 20-fold increase in reporter activation [118,178]. It is important to mention that a direct comparison is difficult, because these groups used different PNAs as well as delivery methods. Irrespective of that we could use the assay in order to quantify differences in efficiency of different PNAs targeting a similar position of β-catenin (Appendix: Vonbrüll et al. 2018; Fig. 2b). Beside good luciferase activation it was important to verify that the splice block would affect the target site in an expected manner. This was achieved using primers specific for the blocked splice donor - resulting in a typical splice switch (Appendix: Vonbrüll et al. 2018; Fig. 1C) as documented for other genes before [97,179]. Taken together these experiments showed that the assay could be used for its purpose to sensitively quantify the effect of splice blocking antisense reagents.

8.2 PNAs

Despite partially unsolved challenges with delivery and solubility - once in the cell - PNAs are able to bind target strands of DNA or RNA with high affinity. That explains ongoing efforts to improve these issues. As described in the introduction (p. X) a variety of modifications has been tested successfully for improved delivery. Among promising backbone modifications (p. 17) pePNAs were excessively tested within Medaka by our group. These experiments show improved solubility compared to non-modified PNAs as well as selective mRNA binding [88]. Therefore it was expected that the good target specificity should work

well for a splice based assay within HeLa. Compared to morpholino oligonucleotides overall shorter PNA oligonucleotides can be designed specific for a certain splice donor. While water solubility with the pePNAs used in this project was good, according to antisense efficiency PNAs did not reach the level of the morpholino oligonucleotides. Using scraping as a means of delivery for both PNAs and morpholino oligonucleotides, the efficiency determined with our reporter assay was higher with the morpholino oligonucleotides. These showed 3.5-fold reporter activation at 4 µM compared to 1.5-fold activation at 64 µM PNA concentration (Fig. 24, p. 53). For morpholino oligonucleotides these values are within the expected range [180,181]. Other studies show similar reporter activation at lower PNA concentrations [119,182,183]. There is no way to exactly name the reason for these differences, but they may be owed to variations in PNA backbone modifications, delivery methods as well as the use of different cell lines. Nonetheless the efficiencies were sufficient for testing different PNA sequences with the assay. It was however necessary to use comparably high PNA concentrations in order to see strong effects.

8.3 Intracellular delivery of PNAs

In order to test optimal PNAs for our ß-catenin targeting strategy our aim was to reproducibly deliver as much PNA as possible to the cells. For in-vitro experiments an intracellular delivery by incubation would be ideal. Since there have been some groups successfully delivering side chain modified PNAs solely by incubating them with cells [82,84,85,183] we also thoroughly tested this approach. A 1.2-fold reporter activation after incubating HeLa cells transfected with our reporter constructs with 16 µM PNA for 3 days showed that incubation did not provide sufficient delivery efficiency. Compared to this Delgado et al. incubated a HepG2 cell line with 5µM γGPNA for 1 day and showed 5-fold reductions using a reporter assay with a negative readout [183]. We gained further insight by also incubating HepG2 cells. Since a concentration of 64 µM had shown good effects in previously conducted scrape delivery experiments (Results: Fig. 26, p. 61) we incubated HepG2 at 64 µM for 3 days and determined mRNA levels of the target genes axin and ß-catenin that have been shown reduced at γGPNA delivery [183]. The results showed very high standard deviations and weak effects on mRNA levels compared to control cells (Results: Fig. 27 p. 62). Once again it's critical to directly compare the outcome with other papers, because the other groups used varying conditions including different PNAs [82,84,85,183] and/or cell lines [82,84,85].
Scraping has been previously described delivering macromolecules [36] as morpholino oligonucleotides [181] and we successfully used it for PNA delivery. Cell scraping brought good results with low standard deviation combined with stable HeLa cell lines including constructs for the splice based reporter assay in good

agreement with Summerton et al. who successfully used scraping to deliver morpholino oligonucleotides to HeLa cells [181]. Screening PNAs targeting “native” β-catenin within HeLa cells scraping was not efficient and reproducible enough. Subsequent analysis by qPCR showed that standard deviations were too high for a comparison of effects (Fig. 32, p. 66). Part of the problem were the high fluctuations of the axin levels of control cells making a comparison to treated cells difficult. Since scraping did not work with SW480 cells we could only test HeLa cells, which don’t naturally overexpress β-catenin - hence not being ideal for the knock-down experiments.

Experiments with co-transfection of PNAs with annealed oligonucleotides were designed according to two publications that successfully used it [46,47]. But tested with our assay we could not optimise the delivery method to a sufficient level - showing only 2-fold reporter activation. This could be owed to a variety of reasons. Mainly the length of the oligonucleotides is crucial, but we tested different combinations without finding an optimal combination. Further, other groups [46,47] did not use the same PNAs. Meaning that the lysine-phosphonic-ester modifications of the PNAs that should initially improve cell entrance after incubation may as well hinder successful co-transfection.

Electroporation has been widely used for delivery of antisense reagents to cell culture cells [43]. After our experience with scraping the main goal was to get higher reproducibility and a delivery method compatible with SW480 cells. Finally with delivery efficiencies of 23 to 43% our setup could not match the to 90% [39,42] documented before, but reproducibility was high and the main advantage of this delivery method was that we could also deliver PNAs to SW480 cells that were not accessible with the cell scraping protocol. Therefore, we chose electroporation for the PNA screening and experiments targeting naturally occurring β-catenin presented in the Appendix: Vonbrüll et al. 2018; Fig. 3).

8.4 Targeting β-catenin with splice based antisense molecules

As mentioned before ß-catenin overexpression does play a major role in different types of cancer [6]. There have been recent publications showing decreased tumour burden after targeting ß-catenin with different approaches. Successful ß-catenin knock-down was possible with PNAs in hepatocellular carcinoma (HCC) [183] or oligodeoxynucelotides (ODNs) in SW480 colon carcinoma cells within xenograft mice [184] as well as Prodigiosin [185], RNAi [186] or siRNA [187] all being examples that highlight the potential of ß-catenin as a target for antisense based therapies. Nonetheless the crucial role of ß-catenin in cell-cell adhesion [188] should be considered for these approaches. Our strategy was to compare PNAs targeting different splice donors of ß-catenin, starting from the transcription start, to the

ARM repeats (Appendix I: Vonbrüll et al. 2018; Fig. 2A). PNAs targeting exon13 turned out to be most successful. In part the success of this targeting site is based on the intact interaction of the truncated protein with Tcf/Lef [157] an assumption we verified later (Appendix I: Vonbrüll et al.2018; Fig. 4B). Lack of the C-terminal transactivation domain therefore enables a dominant negative effect on the wild type β-catenin (see below). Further, according to the results of our in-silico analysis (Appendix II) we could exclude the presence of neighbouring, strong cryptic splice sites. Thereby a potential activation of cryptic splice sites which would impair the knockdown strategy could be avoided [96]. PNA18 showed specific effects on ß-catenin splicing and protein level (Appendix I: Vonbrüll et al. 2018; Fig. 3B) in agreement with previous work using splice modifying AS molecules [97,179]. Although this comparison does only apply for the effect of PNAs on the splicing, because these groups targeted different genes in other cell lines. But the principle of targeting a splice site remains the same. Further, the mRNA level of the target genes Axin and Myc was reduced [183]. Effects on VEGF were controversial as discussed before, since blocking of ß-catenin with AS oligonucleotides caused VEGF inhibition contrary to an increase of VEGF mRNA level after anti-ß-catenin siRNA treatment [8]. After these experiments showed this targeting strategy to be successful within SW480 we wanted to learn more about the interaction of resulting shortened ß-catenin with its main interaction partners. Therefore, we used a mammalian-two-hybrid analysis. Control versions resulting from exon6 splice block (ß-catenin(+I6) and ß-catenin(E6skip)) showed clearly reduced interaction with Tcf/Lef. Contrary to this the exon13 block (ß-catenin(+I13) and ß-catenin(E13skip)) still showed interaction similar to the full length molecule (Appendix I: Vonbrüll et al. 2018; Fig. 4B). That fits together nicely with previous work on the subject, where Tcf/Lef interactions with ß-catenin require intact armadillo repeats of ß-catenin [157,159]. After establishing that these exon 13 versions could still properly interact with Tcf/Lef the next step was to use reporter assay experiments to directly show a potential dominant negative effect.

8.5 Dominant negative effect

A first detailed definition of dominant negative mutations was offered by Herskowitz in 1987. They were defined as prone to produce proteins able to interfere with the activity of their wild-type counterpart upon overexpression [189]. Besides natural dominant negative mutations playing a critical role in human diseases these effects have since been investigated for their potential use for therapeutic applications [190,191] also in combination with morpholino oligonucleotides [62]. Targeting ß-catenin this means that a shortened molecule resulting from the treatment would ideally compete with naturally occurring full-length ß-catenin. Due to the fact that the transactivation domain is located at the C-terminus, all C-terminally truncated proteins could potentially act in a dominant negative fashion. As expected C-terminally truncated β-catenin proteins retaining the Tcf/Lef-interaction substantially

reduced the activity of full length protein (Appendix I: Vonbrüll et al. 2018; Fig. 5A). This so-far unique ß-catenin targeting strategy is particularly interesting, because by maintaining major properties of the molecule it should retain important functions within cell-cell adhesion.

8.6 Catemer

Considering improved antisense reagents and strategies the binding affinity plays a critical role. Increasing the length of the antisense oligonucleotides does increase affinity only to a certain limit. For longer molecules the affinity decreases due to competition with other RNA molecules which unspecifically bind to the antisense molecules [192]. For improved binding affinity we therefore developed a novel strategy connecting oligonucleotides to chain-like catemer structures. In order to test the improvements we analysed melting point curves [193]. Our analyses indeed showed improvements towards higher melting points for oligonucleotides with stronger interactions between neighbouring catemer subunits (Results: Fig. 45, p.75/76). Follow up experiments for determination of ideal distance between subunits showed that PNAs can be positioned on the template directly next to each other (no space) without disturbing proper binding (Results: Fig, 48 and 49, p. 78/79). Therefore, first experiments indicate a potential of the strategy to improve the affinity of antisense molecules. Further experiments will be necessary to test this strategy within cells or *in vivo* models.

9 References

1. Mansoor, M. & Melendez, A. J. Advances in Antisense Oligonucleotide Development for Target Identification, Validation, and as Novel Therapeutics. 275–295 (2008).
2. Perry, C. M. & Balfour, J. A. Fomivirsen. *Drugs* **57,** 375–80; discussion 381 (1999).
3. Lundin, K. E., Gissberg, O. & Smith, C. I. E. Oligonucleotide Therapies: The Past and the Present. *Hum. Gene Ther.* **26,** 475–485 (2015).
4. Moreno, P. M. D. & Pego, A. P. Therapeutic antisense oligonucleotides against cancer: hurdling to the clinic. *Front. Chem.* **2,** 87 (2014).
5. Warren, T. K., Shurtleff, A. C. & Bavari, S. Advanced morpholino oligomers: a novel approach to antiviral therapy. *Antiviral Res.* **94,** 80–8 (2012).
6. Polakis, P. The many ways of Wnt in cancer. *Curr. Opin. Genet. Dev.* **17,** 45–51 (2007).
7. Roh, H. *et al.* Suppression of β -Catenin Inhibits the Neoplastic Growth of APC -Mutant Colon Cancer Cells Suppression of ß-Catenin Inhibits the Neoplastic Growth of APC -Mutant Colon. *Cancer Res.* **61,** 6563–6568 (2001).
8. Luu, H. H. *et al.* Wnt/beta-catenin signaling pathway as a novel cancer drug target. *Curr. Cancer Drug Targets* **4,** 653–671 (2004).
9. Pedersen, L., Hagedorn, P. H., Lindholm, M. W. & Lindow, M. A Kinetic Model Explains Why Shorter and Less Affine Enzyme-recruiting Oligonucleotides Can Be More Potent. *Mol. Ther. Nucleic Acids* **3,** e149 (2014).
10. Aartsma-Rus, A. New Momentum for the Field of Oligonucleotide Therapeutics. *Mol. Ther.* **24,** 193–194 (2016).
11. Wittrup, A. & Lieberman, J. Knocking down disease: a progress report on siRNA therapeutics. *Nat Rev Genet* **16,** 543–552 (2015).
12. Siwkowski, A. M. *et al.* Identification and functional validation of PNAs that inhibit murine CD40 expression by redirection of splicing. *Nucleic Acids Res.* **32,** 2695–706 (2004).
13. Ivanova, G. D. *et al.* Improved cell-penetrating peptide-PNA conjugates for splicing redirection in HeLa cells and exon skipping in mdx mouse muscle. *Nucleic Acids Res.* **36,** 6418–6428 (2008).
14. Hamilton, A. J. & Baulcombe, D. C. Structural basis for double-stranded RNA processing by Dicer. *Science* **29,** 950–952 (1999).
15. Kole, R., Krainer, A. R. & Altman, S. RNA therapeutics: beyond RNA interference and antisense oligonucleotides. *Nat. Rev. Drug Discov.* **11,** (2012).
16. Navarro, Gemma, Essex Sean, Sawant Rupa R., Biswas Swati, Nagesha Dattatri, Sridhar Srinivas, Tros de ILarduya Conchita, T. V. P. Phospholipid-modified polyethylenimine-based nanopreparations for siRNA–mediated gene silencing: Implications for transfection and the role of lipid components.

Nanomedicine **10,** 411–419 (2014).

17. Dudek, H. *et al.* Knockdown of β-catenin with dicer-substrate siRNAs reduces liver tumor burden in vivo. *Mol. Ther.* **22,** 92–101 (2014).
18. Varkouhi, A. K., Scholte, M., Storm, G. & Haisma, H. J. Endosomal escape pathways for delivery of biologicals. *J. Control. Release* **151,** 220–228 (2011).
19. Ohyama, A., Higashi, T., Motoyama, K. & Arima, H. In Vitro and In Vivo Tumor-Targeting siRNA Delivery Using Folate-PEG-appended Dendrimer (G4)/α-Cyclodextrin Conjugates. *Bioconjug. Chem.* acs.bioconjchem.5b00545 (2016). doi:10.1021/acs.bioconjchem.5b00545
20. Bäumer, N. *et al.* Antibody-coupled siRNA as an efficient method for in vivo mRNA knockdown. *Nat. Protoc.* **11,** 22–36 (2016).
21. Kole, R., Krainer, A. R. & Altman, S. RNA therapeutics: beyond RNA interference and antisense oligonucleotides. *Nat. Rev. Drug Discov.* **11,** 125–40 (2012).
22. Zamecnik, P. C. & Stephenson, M. L. Inhibition of Rous sarcoma virus replication and cell transformation by a specific oligodeoxynucleotide. **75,** 280–284 (1978).
23. Vinores, S. A. Pegaptanib in the treatment of wet, age-related macular degeneration. *Int. J. Nanomedicine* **1,** 263–268 (2006).
24. Mologni, L., Nielsen, P. E. & Gambacorti-Passerini, C. In vitro transcriptional and translational block of the bcl-2 gene operated by peptide nucleic acid. *Biochem. Biophys. Res. Commun.* **264,** 537–543 (1999).
25. Peacey, E., Rodriguez, L., Liu, Y. & Wolfe, M. S. Targeting a pre-mRNA structure with bipartite antisense molecules modulates tau alternative splicing. *Nucleic Acids Res.* **40,** 9836–9849 (2012).
26. Cartegni, L. & Krainer, A. R. Correction of disease-associated exon skipping by synthetic exon-specific activators. *Nat. Struct. Biol.* **10,** 120–125 (2003).
27. Sonenberg, N. & Hinnebusch, A. G. Regulation of Translation Initiation in Eukaryotes: Mechanisms and Biological Targets. *Cell* **136,** 731–745 (2009).
28. Hinnebusch, A. G. & Lorsch, J. R. The mechanism of eukaryotic translation initiation: New insights and challenges. *Cold Spring Harb. Perspect. Biol.* **4,** 1–25 (2012).
29. Jackson, R. J., Hellen, C. U. T. & Pestova, T. V. The mechanism of eukaryotic translation initiation and principles of its regulation. **10,** (2010).
30. Summerton, J. & Weller, D. Morpholino Antisense Oligomers: Design, Preparation, and Properties. **195,** 187–195 (1997).
31. Dosaka-akita, H., Akie, K., Hiroumi, H., Small, H. & Lung, C. Inhibition of Proliferation by L- myc Antisense DNA for the Translational Initiation Site in Human Small Cell Lung Cancer. 1559–1564 (1995).
32. Summerton, J. Morpholino antisense oligomers: The case for an RNase H-independent structural type. *Biochim. Biophys. Acta - Gene Struct. Expr.* **1489,** 141–158 (1999).
33. Stein, D., Foster, E., Huang, S. Ben, Weller, D. & Summerton, J. A Specificity Comparison of Four Antisense Types: Morpholino, 2’-0-Methyl

RNA, DNA, and Phosphorothioate DNA. **157,** 151–157 (1997).

34. Scotti, M. M. & Swanson, M. S. RNA mis-splicing in disease. *Nat. Rev. Genet.* **17,** 19–32 (2015).
35. Buratti, E. *et al.* Aberrant 5' splice sites in human disease genes: mutation pattern, nucleotide structure and comparison of computational tools that predict their utilization. *Nucleic Acids Res.* **35,** 4250–63 (2007).
36. McNeil, P. L., Murphy, R. F., Lanni, F. & Taylor, D. L. A method for incorporating macromolecules into adherent cells. *J. Cell Biol.* **98,** 1556–1564 (1984).
37. Partridge, M. *et al.* A simple method for delivering morpholino antisense oligos into the cytoplasm of cells. *Antisense Nucleic Acid Drug Dev.* **6,** 169–175 (1996).
38. Fechheimer, M. *et al.* Transfection of mammalian cells with plasmid DNA by scrape loading and sonication loading. *Proc. Natl. Acad. Sci. U. S. A.* **84,** 8463–8467 (1987).
39. Stroh, T., Erben, U., Kühl, A. a, Zeitz, M. & Siegmund, B. Combined pulse electroporation--a novel strategy for highly efficient transfection of human and mouse cells. *PLoS One* **5,** e9488 (2010).
40. Weaver, J. C. & Chizmadzhev, Y. A. Theory of electroporation : A review. **41,** 135–160 (1996).
41. Tsong, T. Y. Electroporation of cell membranes. *Biophys. J.* **60,** 297–306 (1991).
42. Pucihar, G., Krmelj, J., Reberˇ, M., Napotnik, T. B. & Miklavˇ, D. Equivalent Pulse Parameters for Electroporation. **58,** 3279–3288 (2011).
43. Canatella, P. J. & Prausnitz, M. R. Prediction and optimization of gene transfection and drug delivery by electroporation. *Gene Ther.* **8,** 1464–1469 (2001).
44. Summerton, J. E. Endo-Porter: a novel reagent for safe, effective delivery of substances into cells. *Ann. N. Y. Acad. Sci.* **1058,** 62–75 (2005).
45. Felgner, P. L. *et al.* Lipofection: a highly efficient, lipid-mediated DNA-transfection procedure. *Proc. Natl. Acad. Sci.* **84,** 7413–7417 (1987).
46. Hamilton, S. E., Simmons, C. G., Kathiriya, I. S. & Corey, D. R. Cellular delivery of peptide nucleic acids and inhibition of human telomerase. *Chem. Biol.* **6,** 343–351 (1999).
47. Rasmussen, F. W. *et al.* Evaluation of Transfection Protocols for Unmodified and Modified Peptide Nucleic Acid (PNA) Oligomers. *Oligonucleotides* **57,** 43–57 (2006).
48. Said Hassane, F., Saleh, A. F., Abes, R., Gait, M. J. & Lebleu, B. Cell penetrating peptides: Overview and applications to the delivery of oligonucleotides. *Cell. Mol. Life Sci.* **67,** 715–726 (2010).
49. Shiraishi, T. & Nielsen, P. E. Peptide nucleic acid (PNA) cell penetrating peptide (CPP) conjugates as carriers for cellular delivery of antisense oligomers. *Artif. DNA PNA XNA* **2,** 90–99 (2011).
50. Rogers, F. A., Lin, S. S., Hegan, D. C., Krause, D. S. & Glazer, P. M. Targeted Gene Modification of Hematopoietic Progenitor Cells in Mice

Following Systemic Administration of a PNA-peptide Conjugate. *Mol. Ther.* **20,** 109–118 (2012).

51. Eckstein, F. Nucleoside Phosphorothioates. **2303,** 4718–4723 (1970).
52. Stein, C. a. Exploiting the potential of antisense: beyond phosphorothioate oligodeoxynucleotides. *Chem. Biol.* **3,** 319–23 (1996).
53. Monia, B. P., Johnston, J. F., Sasmor, H. & Cummins, L. L. Nuclease resistance and antisense activity of modified oligonucleotides targeted to Ha-ras. *J. Biol. Chem.* **271,** 14533–14540 (1996).
54. Eckstein, F. What Is Their Origin and What Is Unique About Them ? Phosphorothi oate. *Antisense Nucleic Acid Drug Dev.* **10,** 117–121 (2000).
55. Summerton, J. E. Morpholino, siRNA, and S-DNA compared: impact of structure and mechanism of action on off-target effects and sequence specificity. *Curr. Top. Med. Chem.* **7,** 651–660 (2007).
56. Morcos, P. A. Achieving efficient delivery of morpholino oligos in cultured cells. *Genesis* **30,** 94–102 (2001).
57. Stein, D. a, Skilling, D. E., Iversen, P. L. & Smith, a W. Inhibition of Vesivirus infections in mammalian tissue culture with antisense morpholino oligomers. *Antisense Nucleic Acid Drug Dev.* **11,** 317–25 (2001).
58. Matter, N. & König, H. Targeted 'knockdown' of spliceosome function in mammalian cells. *Nucleic Acids Res.* **33,** e41 (2005).
59. Chiavacci, E. *et al.* MicroRNA 19a replacement partially rescues fin and cardiac defects in zebrafish model of Holt Oram syndrome. *Sci. Rep.* **5,** 18240 (2015).
60. Macaulay, L. J. *et al.* Developmental toxicity of the PBDE metabolite 6-OH-BDE-47 in zebrafish and the potential role of thyroid receptor ?? *Aquat. Toxicol.* **168,** 38–47 (2015).
61. Munoz, R. *et al.* Regeneration of Xenopus laevis spinal cord requires Sox2/3 expressing cells. *Dev. Biol.* **408,** 229–243 (2014).
62. Blum, M., De Robertis, E. M., Wallingford, J. B. & Niehrs, C. Morpholinos: Antisense and Sensibility. *Dev. Cell* **35,** 145–149 (2015).
63. Obika, S. *et al.* Synthesis of 2′-O,4′-C-methyleneuridine and -cytidine. Novel bicyclic nucleosides having a fixed C3, -endo sugar puckering. *Tetrahedron Lett.* **38,** 8735–8738 (1997).
64. Koshkin, A. A. *et al.* LNA (Locked Nucleic Acids): Synthesis of the adenine, cytosine, guanine, 5-methylcytosine, thymine and uracil bicyclonucleoside monomers, oligomerisation, and unprecedented nucleic acid recognition. *Tetrahedron* **54,** 3607–3630 (1998).
65. Kurreck, J., Wyszko, E., Gillen, C. & Erdmann, V. a. Design of antisense oligonucleotides stabilized by locked nucleic acids. *Nucleic Acids Res.* **30,** 1911–1918 (2002).
66. Wahlestedt, C. *et al.* Potent and nontoxic antisense oligonucleotides containing locked nucleic acids. *Proc. Natl. Acad. Sci. U. S. A.* **97,** 5633–5638 (2000).
67. Braasch, D. A., Liu, Y. & Corey, D. R. Antisense inhibition of gene expression in cells by oligonucleotides incorporating locked nucleic acids:

Effect of mRNA target sequence and chimera design. *Nucleic Acids Res.* **30,** 5160–5167 (2002).

68. Wojtkowiak-Szlachcic, A. *et al.* Short antisense-locked nucleic acids (all-LNAs) correct alternative splicing abnormalities in myotonic dystrophy. *Nucleic Acids Res.* **43,** 3318–3331 (2015).
69. Fluiter, K. *et al.* In vivo tumor growth inhibition and biodistribution studies of locked nucleic acid (LNA) antisense oligonucleotides. *Nucleic Acids Res.* **31,** 953–962 (2003).
70. Ray, a & Nordén, B. Peptide nucleic acid (PNA): its medical and biotechnical applications and promise for the future. *FASEB J.* **14,** 1041–60 (2000).
71. Egholm, M. *et al.* PNA hybridizes to complementary oligonucleotides obeying the Watson-Crick hydrogen-bonding rules. *Nature* **365,** 566–568 (1993).
72. Rozners, E. Recent Advances in Chemical Modification of Peptide Nucleic Acids. *J. Nucleic Acids* **2012,** (2012).
73. Ryoo, S. R. *et al.* Quantitative and multiplexed microRNA sensing in living cells based on peptide nucleic acid and nano graphene oxide (PANGO). *ACS Nano* **7,** 5882–5891 (2013).
74. Ren, B., Zhou, J.-M. & Komiyama, M. Straightforward detection of SNPs in double-stranded DNA by using exonuclease III/nuclease S1/PNA system. *Nucleic Acids Res.* **32,** e42 (2004).
75. Jeong, D. *et al.* BRAF (V600E) mutation analysis in papillary thyroid carcinomas by peptide nucleic acid clamp real-time PCR. *Ann. Surg. Oncol.* **20,** 759–766 (2013).
76. Machnik, G. *et al.* A peptide nucleic acid (PNA)-mediated polymerase chain reaction clamping allows the selective inhibition of the ERVWE1 gene amplification. *Mol. Cell. Probes* **28,** 1–5 (2014).
77. Brandt, O. *et al.* PNA microarrays for hybridisation of unlabelled DNA samples. *Nucleic Acids Res* **31,** e119 (2003).
78. Shi, H. *et al.* A review: Fabrications, detections and applications of peptide nucleic acids (PNAs) microarray. *Biosens. Bioelectron.* **66,** 481–489 (2015).
79. Petersen, K. *et al.* Short PNA molecular beacons for real-time PCR allelic discrimination of single nucleotide polymorphisms. *Mol. Cell. Probes* **18,** 117–22 (2004).
80. Koppelhus, U. & Nielsen, P. E. Cellular delivery of peptide nucleic acid (PNA). *Advanced Drug Delivery Reviews* **55,** 267–280 (2003).
81. Tilani, N., De Costa, S. & Heemstra, J. M. Differential DNA and RNA sequence discrimination by PNA having charged side chains. *Bioorg. Med. Chem. Lett.* (2014). doi:10.1016/j.bmcl.2014.03.059
82. Kumar, P. & Jain, D. R. Cγ-Aminopropylene peptide nucleic acid (amp-PNA): Chiral cationic PNAs with superior PNA:DNA/RNA duplex stability and cellular uptake. *Tetrahedron* **71,** 3378–3384 (2015).
83. Bohländer, P. R., Vilaivan, T. & Wagenknecht, H.-A. Strand displacement and duplex invasion into double-stranded DNA by pyrrolidinyl peptide

nucleic acids. *Org. Biomol. Chem.* **13,** 9223–9230 (2015).

84. Zhou, P. *et al.* Novel Binding and Efficient Cellular Uptake of Guanidine-Based Peptide Nucleic Acids (GPNA). *J. Am. Chem. Soc.* **125,** 6878–6879 (2003).
85. Sahu, B. *et al.* Synthesis of Conformationally Preorganized and Cell-Permeable Guanidine-Based γ-Peptide nucleic acids (γGPNAs). *J. Org. Chem.* **74,** 1509–1516 (2009).
86. Dömling, A., Chi, K. Z. & Barrère, M. A novel method to highly versatile monomeric PNA building blocks by multi component reactions. *Bioorganic Med. Chem. Lett.* **9,** 2871–2874 (1999).
87. Baldoli, C., Maiorana, S., Licandro, E., Zinzalla, G. & Perdicchia, D. Synthesis of chiral chromium tricarbonyl labeled thymine PNA monomers via the Ugi reaction. *Org. Lett.* **4,** 4341–4344 (2002).
88. Dorn, S. *et al.* Side chain modified peptide nucleic acids (PNA) for knock-down of six3 in medaka embryos. *BMC Biotechnol.* **12,** (2012).
89. Lee, Y. & Rio, D. C. Mechanisms and Regulation of Alternative Pre-mRNA Splicing. *Annu. Rev. Biochem.* 1–33 (2015). doi:10.1146/annurev-biochem-060614-034316
90. Berglund, J. a, Chua, K., Abovich, N., Reed, R. & Rosbash, M. The splicing factor BBP interacts specifically with the pre-mRNA branchpoint sequence UACUAAC. *Cell* **89,** 781–787 (1997).
91. Nguyen, T. H. D. *et al.* Cryo-EM structure of the yeast U4/U6.U5 tri-snRNP at 3.7 Å resolution. *Nature* **530,** 298–302 (2016).
92. Wang, Y. *et al.* Mechanism of alternative splicing and its regulation. *Biomed. reports* **3,** 152–158 (2015).
93. Kapustin, Y. *et al.* Cryptic splice sites and split genes. *Nucleic Acids Res.* **39,** 5837–44 (2011).
94. Baralle, D. Splicing in action: assessing disease causing sequence changes. *J Med Genet* **42,** 737–748 (2005).
95. Darman, R. B. *et al.* Cancer-Associated SF3B1 Hotspot Mutations Induce Cryptic 3' Splice Site Selection through Use of a Different Branch Point. *Cell Rep.* **13,** 1033–1045 (2015).
96. Draper, B. W., Morcos, P. A. & Kimmel, C. B. Inhibition of Zebrafish fgf8 Pre-mRNA Splicing With Morpholino Oligos : A Quantifiable Method for Gene Knockdown. **156,** 154–156 (2001).
97. Shiraishi, T., Eysturskarth, J. & Nielsen, P. E. Modulation of mdm2 pre-mRNA splicing by 9-aminoacridine-PNA (peptide nucleic acid) conjugates targeting intron-exon junctions. *BMC Cancer* **10,** 342 (2010).
98. Finotti, A. *et al.* Recent trends in the gene therapy of β-thalassemia. *J. Blood Med.* **6,** 69–85 (2015).
99. Goyenvalle, A. *et al.* Engineering Multiple U7snRNA Constructs to Induce Single and Multiexon-skipping for Duchenne Muscular Dystrophy. *Mol. Ther.* **20,** 1212–1221 (2012).
100. Long, C. *et al.* Postnatal genome editing partially restores dystrophin expression in a mouse model of muscular dystrophy. *Science* **351,** aad5725

(2015).

101. Tabebordbar, M. *et al.* In vivo gene editing in dystrophic mouse muscle and muscle stem cells. *Science (80-.).* **5177,** 1–9 (2015).
102. Garcia-Blanco, M. a, Baraniak, A. P. & Lasda, E. L. Alternative splicing in disease and therapy. *Nat. Biotechnol.* **22,** 535–546 (2004).
103. Thein, S. L. Pathophysiology of beta thalassemia--a guide to molecular therapies. *Hematology Am. Soc. Hematol. Educ. Program* 31–37 (2005). doi:10.1182/asheducation-2005.1.31
104. Sierakowska, H., Sambade, M. J., Agrawal, S. & Kole, R. Repair of thalassemic human beta-globin mRNA in mammalian cells by antisense oligonucleotides. *Proc. Natl. Acad. Sci. U. S. A.* **93,** 12840–12844 (1996).
105. El-Andaloussi, S., Johansson, H. J., Lundberg, P. & Langel, Ü. Induction of splice correction by cell-penetrating peptide nucleic acids. *J. Gene Med.* **8,** 1262–1273 (2006).
106. Chin, J. Y. *et al.* Correction of a splice-site mutation in the beta-globin gene stimulated by triplex-forming peptide nucleic acids. *Proc. Natl. Acad. Sci. U. S. A.* **105,** 13514–13519 (2008).
107. Fairclough, R. J., Wood, M. J. & Davies, K. E. Therapy for Duchenne muscular dystrophy: renewed optimism from genetic approaches. *Nat. Rev. Genet.* **14,** 373–8 (2013).
108. Aartsma-rus, A., Ginjaar, I. B. & Bushby, K. The importance of genetic diagnosis for Duchenne muscular dystrophy. 1–7 (2016). doi:10.1136/jmedgenet-2015-103387
109. Mali, P. *et al.* RNA-Guided Human Genome Engineering via Cas9 Prashant. *Science (80-.).* **339,** 823–826 (2013).
110. Xu, L. *et al.* CRISPR-mediated genome editing restores dystrophin expression and function in mdx mice. *Mol. Ther.* (2015). doi:10.1038/mt.2015.192
111. Alberts, Bruce; Johnson, Alexander; Lewis, Julian; Morgan, David; Raff, Martin; Roberts, Keith; Walter, P. *Molecular Biology of the Cell. 6th edition*. (2015).
112. Thorne, N., Inglese, J. & Auld, D. S. Illuminating Insights into Firefly Luciferase and Other Bioluminescent Reporters Used in Chemical Biology. *Chem. Biol.* **17,** 646–657 (2010).
113. de Wet, J. . R., Wood, K. V., DeLuca, M., Helinski, D. R. & Subramani, S. Firefly luciferase gene: structure and expression in mammalian cells. *Mol. Cell. Biol.* **7,** 725–737 (1987).
114. Lorenz, W. W., McCann, R. O., Longiaru, M. & Cormier, M. J. Isolation and expression of a cDNA encoding Renilla reniformis luciferase. *Proc. Natl. Acad. Sci. U. S. A.* **88,** 4438–42 (1991).
115. Lee, J. Y. *et al.* Development of a dual-luciferase reporter system for in vivo visualization of MicroRNA biogenesis and posttranscriptional regulation. *J. Nucl. Med.* **49,** 285–294 (2008).
116. Hall, M. P. *et al.* Engineered luciferase reporter from a deep sea shrimp utilizing a novel imidazopyrazinone substrate. *ACS Chem. Biol.* **7,** 1848–

1857 (2012).

117. Verhaegen, M. & Christopoulos, T. K. Recombinant Gaussia luciferase: Overexpression, purification, and analytical application of a bioluminescent reporter for DNA hybridization. *Anal. Chem.* **74,** 4378–4385 (2002).
118. Kang, S. H., Cho, M. J. & Kole, R. Up-regulation of luciferase gene expression with antisense oligonucleotides: implications and applications in functional assay development. *Biochemistry* **37,** 6235–9 (1998).
119. Wright, D. G., Zhang, Y. & Murphy, J. R. Effective delivery of antisense peptide nucleic acid oligomers into cells by anthrax protective antigen. *Biochem. Biophys. Res. Commun.* **376,** 200–5 (2008).
120. Sazani, P. *et al.* Nuclear antisense effects of neutral, anionic and cationic oligonucleotide analogs. *Nucleic Acids Res.* **29,** 3965–74 (2001).
121. Younis, I. *et al.* Rapid-Response Splicing Reporter Screens Identify Differential Regulators of Constitutive and Alternative Splicing. *Mol. Cell. Biol.* **30,** 1718–28 (2010).
122. Clevers, H. Wnt/beta-catenin signaling in development and disease. *Cell* **127,** 469–80 (2006).
123. Swarup, S. & Verheyen, E. M. Wnt/wingless signaling in drosophila. *Cold Spring Harb. Perspect. Biol.* **4,** 1–15 (2012).
124. Barker, N. & Clevers, H. Mining the Wnt pathway for cancer therapeutics. *Nat. Rev. Drug Discov.* **5,** 997–1014 (2006).
125. Mohammed, M. K. *et al.* Wnt/β-catenin signaling plays an ever-expanding role in stem cell self-renewal, tumorigenesis and cancer chemoresistance. *Genes Dis.* **3,** 11–40 (2016).
126. Henderson, W. R. *et al.* Inhibition of Wnt/beta-catenin/CREB binding protein (CBP) signaling reverses pulmonary fibrosis. *Proc. Natl. Acad. Sci. U. S. A.* **107,** 14309–14 (2010).
127. Clements, W. M. *et al.* β -Catenin Mutation Is a Frequent Cause of Wnt Pathway Activation in Gastric Cancer ␋ -Catenin Mutation Is a Frequent Cause of Wnt Pathway Activation in. 3503–3506 (2002).
128. Bienz, M. & Clevers, H. Linking colorectal cancer to Wnt signaling. *Cell* **103,** 311–320 (2000).
129. Morin, P. J. *et al.* Activation of beta-catenin-Tcf signaling in colon cancer by mutations in beta-catenin or APC. *Science* **275,** 1787–1790 (1997).
130. Anastas, J. N. & Moon, R. T. WNT signalling pathways as therapeutic targets in cancer. *Nat. Rev. Cancer* **13,** 11–26 (2012).
131. Xu, W. & Kimelman, D. Mechanistic insights from structural studies of beta-catenin and its binding partners. *J. Cell Sci.* **120,** 3337–3344 (2007).
132. Webster, M. T. *et al.* Sequence variants of the Axin gene in breast, colon, and other cancers: An analysis of mutations that interfere with GSK3 binding. *Genes Chromosom. Cancer* **28,** 443–453 (2000).
133. Mao, C. D. & Byers, S. W. Cell-context dependent TCF/LEF expression and function: alternative tales of repression, de-repression and activation potentials. *Crit. Rev. Eukaryot. Gene Expr.* **21,** 207–36 (2011).

134. Cuilliere-Dartigues, P. *et al.* TCF-4 isoforms absent in TCF-4 mutated MSI-H colorectal cancer cells colocalize with nuclear CtBP and repress TCF-4-mediated transcription. *Oncogene* **25,** 4441–4448 (2006).

135. Imbeaud, S., Pilati, C., Nault, J., Couchy, G. & Zucman-, J. Genotype-phenotype correlation of CTNNB1 mutations reveals different ß- catenin activity associated with liver tumor progression. 1–61

136. Ilyas, M., Tomlinson, I. P., Rowan, A., Pignatelli, M. & Bodmer, W. F. β-catenin mutations in cell lines established from human colorectal cancers. *Proc. Natl. Acad. Sci. U. S. A.* **94,** 10330–4 (1997).

137. Okabe, H. *et al.* Diverse Basis of β-Catenin Activation in Human Hepatocellular Carcinoma: Implications in Biology and Prognosis. *PLoS One* **11,** e0152695 (2016).

138. Moreno-Bueno, G. *et al.* Abnormalities of the APC/beta-catenin pathway in endometrial cancer. *Oncogene* **21,** 7981–90 (2002).

139. Maiti, S., Alam, R., Amos, C. I. & Huff, V. Frequent association of ß-catenin and WT1 mutations in Wilms tumors. *Cancer Res.* **60,** 6288–6292 (2000).

140. Mullen, J. T. *et al.* ß-Catenin Mutation Status and Outcomes in Sporadic Desmoid Tumors. *Oncologist* **18,** 1043–1049 (2013).

141. Kahn, M. Can we safely target the WNT pathway? *Nat. Rev. Drug Discov.* **13,** 513–32 (2014).

142. Grossmann, T. N. *et al.* Inhibition of oncogenic Wnt signaling through direct targeting of β-catenin. *Proc. Natl. Acad. Sci. U. S. A.* **109,** 17942–7 (2012).

143. Hahne, G. & Grossmann, T. N. Direct targeting of β-catenin: Inhibition of protein-protein interactions for the inactivation of Wnt signaling. *Bioorg. Med. Chem.* **21,** 4020–6 (2013).

144. Delgado, E. *et al.* Complete response of Ctnnb1-mutated tumours to β-catenin suppression by locked nucleic acid antisense in a mouse hepatocarcinogenesis model. *J. Hepatol.* **62,** 380–7 (2015).

145. Xing, Y. *et al.* Crystal structure of a full-length beta-catenin. *Structure* **16,** 478–87 (2008).

146. Willert, K. & Nusset, R. ß-catenin: a key mediator of Wnt signaling. *Curr. Opin. Genet. Dev.* **8,** 95–102 (1998).

147. Mosimann, C., Hausmann, G. & Basler, K. Beta-catenin hits chromatin: regulation of Wnt target gene activation. *Nat. Rev. Mol. Cell Biol.* **10,** 276–86 (2009).

148. Liu, J., Xing, Y., Hinds, T. R., Zheng, J. & Xu, W. The Third 20 Amino Acid Repeat Is the Tightest Binding Site of APC for ß-Catenin. *J. Mol. Biol.* **360,** 133–144 (2006).

149. Ratheesh, A. & Yap, A. S. A bigger picture: classical cadherins and the dynamic actin cytoskeleton. *Nat.Rev.Mol.Cell Biol.* **13,** 673–679 (2012).

150. Pokutta, S. & Weis, W. Structure of the dimerization and beta-catenin-binding region of alpha-catenin. *Mol. Cell* **5,** 533–543 (2000).

151. Orsulic, S., Huber, O., Aberle, H., Arnold, S. & Kemler, R. E-cadherin binding prevents ß-catenin nuclear localization and ß-catenin/LEF-1-mediated transactivation. *J. Cell Sci.* **112,** 1237–45 (1999).

152. Huber, a H. & Weis, W. I. The structure of the beta-catenin/E-cadherin complex and the molecular basis of diverse ligand recognition by beta-catenin. *Cell* **105,** 391–402 (2001).

153. Ogryzko, V. V, Schiltz, R. L., Russanova, V., Howard, B. H. & Nakatani, Y. The transcriptional activators p300 and CBP are acetyltransferases. *Cell* **87,** 953–959 (1996).

154. Li, J. *et al.* CBP/p300 are bimodal regulators of Wnt signaling. *EMBO J.* **26,** 2284–94 (2007).

155. Takemaru, K. I. & Moon, R. T. The transcriptional coactivator CBP interacts with beta-catenin to activate gene expression. *J. Cell Biol.* **149,** 249–54 (2000).

156. Wallmen, B., Schrempp, M. & Hecht, A. Intrinsic properties of Tcf1 and Tcf4 splice variants determine cell-type-specific Wnt/β-catenin target gene expression. *Nucleic Acids Res.* **40,** 9455–69 (2012).

157. Graham, T. A., Weaver, C., Mao, F., Kimelman, D. & Xu, W. Crystal Structure of a ß-Catenin / Tcf Complex. **103,** 885–896 (2000).

158. Kries, J. P. Von *et al.* Hot spots in β -catenin for interactions with LEF-1, conductin and APC. **7,** 1–8 (2000).

159. Sun, J. & Weis, W. I. Biochemical and Structural Characterization of β-Catenin Interactions with Nonphosphorylated and CK2-Phosphorylated Lef-1. *J. Mol. Biol.* **405,** 519–530 (2011).

160. Heimbucher, T. *et al.* Gbx2 and Otx2 interact with the WD40 domain of Groucho/Tle corepressors. *Mol. Cell. Biol.* **27,** 340–51 (2007).

161. Vancha, A. R. *et al.* Use of polyethyleneimine polymer in cell culture as attachment factor and lipofection enhancer. *BMC Biotechnol.* **4,** 23 (2004).

162. Wang, Hwei-gene, M.J., Fraser, L.C., C. Transposon mutagenesis of baculoviruses: analysis of TFP 3 lepidopteran transposon insertions at the FP locus of nuclear polyhedrosis viruses. *Gene* **81,** 97–108 (1989).

163. Hall, M. P. *et al.* Engineered luciferase reporter from a deep sea shrimp utilizing a novel imidazopyrazinone substrate. *ACS Chem. Biol.* **7,** 1848–1857 (2012).

164. Li, X., Lobo, N., Bauser, C. & Fraser, M. The minimum internal and external sequence requirements for transposition of the eukaryotic transformation vector piggyBac. *Mol. Genet. Genomics* **266,** 190–198 (2001).

165. Zhao, S. *et al.* PiggyBac transposon vectors: the tools of the human gene encoding. *Transl. lung cancer Res.* **5,** 120–125 (2016).

166. Feschotte, C. The piggyBac transposon holds promise for human gene therapy. *PNAS* **103,** 14981–14982 (2006).

167. Chen, Y.-T. *et al.* PiggyBac transposon-mediated, reversible gene transfer in human embryonic stem cells. *Stem Cells Dev.* **19,** 763–71 (2010).

168. Allard, S. T. M., Kopish, K. & Corporation, P. LUCIFERASE REPORTER ASSAYS : POWERFUL , ADAPTABLE TOOLS FOR CELL BIOLOGY RESEARCH. (2008).

169. Wang, M. & Marín, A. Characterization and prediction of alternative splice sites. *Gene* **366,** 219–27 (2006).

170. Hebsgaard, S. M. *et al.* Splice site prediction in Arabidopsis thaliana pre-mRNA by combining local and global sequence information. *Nucleic Acids Res.* **24,** 3439–52 (1996).

171. Xia, H., Bi, J. & Li, Y. Identification of alternative 5'/3' splice sites based on the mechanism of splice site competition. *Nucleic Acids Res.* **34,** 6305–6313 (2006).

172. Horibe, T. *et al.* Transfection efficiency of normal and cancer cell lines and monitoring of promoter activity by single-cell bioluminescence imaging. *Luminescence* **29,** 96–100 (2014).

173. Dorn, S. Interactions between Lef/Tcf and β-catenin for transcriptional activation in Wnt signaling and antisense function of modified peptide nucleic acids in Medaka fish. (Universität Wien, 2011).

174. Lonkar, P. *et al.* Targeted correction of a thalassemia-associated beta-globin mutation induced by pseudo-complementary peptide nucleic acids. *Nucleic Acids Res.* **37,** 3635–44 (2009).

175. Bahal, R. *et al.* In vivo correction of anaemia in β-thalassemic mice by γPNA-mediated gene editing with nanoparticle delivery. *Nat. Commun.* **7,** 13304 (2016).

176. Hall, M. P. *et al.* Engineered luciferase reporter from a deep sea shrimp utilizing a novel imidazopyrazinone substrate. *ACS Chem. Biol.* **7,** 1848–1857 (2012).

177. Loh, J. M. S. & Proft, T. Comparison of firefly luciferase and NanoLuc luciferase for biophotonic labeling of group A Streptococcus. *Biotechnol. Lett.* **36,** 829–834 (2014).

178. Shiraishi, T. & Nielsen, P. E. Peptide nucleic acid (PNA) cell penetrating peptide (CPP) conjugates as carriers for cellular delivery of antisense oligomers. *Artif. DNA PNA XNA* **2,** 90–99 (2011).

179. Pankratova, S., Nielsen, B. N., Shiraishi, T. & Nielsen, P. E. PNA-mediated modulation and redirection of Her-2 pre-mRNA splicing : Specific skipping of erbB-2 exon 19 coding for the ATP catalytic domain. 29–38 (2010). doi:10.3892/ijo

180. Ghosh, C. & Iversen, P. L. Intracellular delivery strategies for antisense phosphorodiamidate morpholino oligomers. *Antisense Nucleic Acid Drug Dev.* **10,** 263–274 (2000).

181. Summerton, J. *et al.* Morpholino and Phosphorothioate Antisense Oligomers Compared in Cell-Free and In-Cell Systems. *Antisense Nucleic Acid Drug Dev.* **7,** 63–70 (1997).

182. Ivanova, G. D. *et al.* Improved cell-penetrating peptide-PNA conjugates for splicing redirection in HeLa cells and exon skipping in mdx mouse muscle. *Nucleic Acids Res.* **36,** 6418–28 (2008).

183. Delgado,Evan, Bahal, Raman, Yang,Jing,Min Lee,Jung,H Ly,P.S. Monga, S. β-Catenin Knockdown in Liver Tumor Cells by a Cell Permeable Gamma Guanidine-based Peptide Nucleic Acid. **13,** 867–878 (2014).

184. Green, D. W., Roh, H., Pippin, J. a & Drebin, J. a. Beta-catenin antisense treatment decreases beta-catenin expression and tumor growth rate in colon carcinoma xenografts. *J. Surg. Res.* **101,** 16–20 (2001).

185. Wang, Z. *et al.* Prodigiosin inhibits Wnt/β-catenin signaling and exerts anticancer activity in breast cancer cells. *Proc. Natl. Acad. Sci. U. S. A.* **113,** 201616336 (2016).

186. Ganesh, S. *et al.* Direct Pharmacological Inhibition of b-Catenin by RNA Interference in Tumors of Diverse Origin. *Mol Cancer Ther* **15,** 1–12 (2016).

187. Tao, J. *et al.* Targeting β-catenin in hepatocellular cancers induced by co-expression of mutant β-catenin and K-Ras in mice. *Hepatology* **0,** (2016).

188. Kahn, M. Can we safely target the WNT pathway? *Nat. Rev. Drug Discov.* **13,** 513–532 (2014).

189. Herskowitz, I. Functional inactivation of genes by dominant negative mutations. *Nature* **329,** 219–222 (1987).

190. Veitia, R. A. Dominant negative factors in health and disease. *J. Pathol.* **218,** 409–418 (2009).

191. Hernandez, J. *et al.* Tumor suppressor properties of the splicing regulatory factor RBM10. *RNA Biol.* **13,** 466–472 (2016).

192. Milligan, J. F., Matteucci, M. D. & Martin, J. C. Current concepts in antisense drug design. *J. Med. Chem.* **36,** 1923–1937 (1993).

193. Liebert, M. A., Mergny, J. & Lacroix, L. Analysis of Thermal Melting Curves ABSTRACT. **537,** 515–537 (2003).

10 Appendix I Published work

All experiments were planned by the author, Elisabeth Riegel and Thomas Czerny and conducted by the author. Michaela Aigner, Holger Bock, Birgit Werner and Thomas Lindhorst developed the chemical synthesis and provided the PNAs. Christian Halter developed and build the electroporator.

Molecular Biotechnology
https://doi.org/10.1007/s12033-018-0058-7

ORIGINAL PAPER

A Dominant Negative Antisense Approach Targeting β-Catenin

Matthias Vonbrüll[1] · Elisabeth Riegel[1] · Christian Halter[2] · Michaela Aigner[3] · Holger Bock[4] · Birgit Werner[5] · Thomas Lindhorst[5] · Thomas Czerny[1]

Abstract
There have been many attempts to unveil the therapeutic potential of antisense molecules during the last decade. Due to its specific role in canonical Wnt signalling, β-catenin is a potential target for an antisense-based antitumour therapy. In order to establish such a strategy with peptide nucleic acids, we developed a reporter assay for quantification of antisense effects. The luciferase-based assay detects splice blocking with high sensitivity. Using this assay, we show that the splice donor of exon 13 of β-catenin is particularly suitable for an antisense strategy, as it results in a truncated protein which lacks transactivating functions. Since the truncated proteins retain the interactions with Tcf/Lef proteins, they act in a dominant negative fashion competing with wild-type proteins and thus blocking the transcriptional activity of β-catenin. Furthermore, we show that the truncation does not interfere with binding of cadherin and α-catenin, both essential for its function in cell adhesion. Therefore, the antisense strategy blocks Wnt signalling with high efficiency but retains other important functions of β-catenin.

Keywords Antisense · β-Catenin · Morpholino · PNA · Wnt signalling

Introduction

In 1978 a synthetic antisense oligonucleotide was successfully used by Zamecnik and Stephensen for targeting of Rous sarcoma virus RNA within chick embryo fibroblasts [1]. Subsequently, a vast variety of new reagents were developed and tested [2], peaking in the FDA approval of Fomivirsen [3], Pegaptanib [4] and Mipomersen [5]. The successful clinical application demonstrated the potential of antisense reagents and motivated scientists to overcome issues with solubility, degradation or cellular delivery [6].

Due to their good affinity for complementary RNA sequences, lack of interactions with natural proteins and excellent water solubility, morpholino oligos became the gold standard for antisense knock-down experiments [7, 8]. They show a characteristic structure with a 6-membered morpholine ring replacing ring sugars present within naturally occurring nucleic acids. Furthermore, negatively charged phosphate linkages of DNA and RNA have been replaced by phosphorodiamidate intersubunit linkages [7].

In year 1991 peptide nucleic acids (PNAs) were developed by Nielsen and colleagues [9]. PNAs contain an artificial backbone made of N-(2-aminoethyl) glycine subunits. The nucleobases are attached to the α-amino group by an acetic acid linker [10]. Lack of negatively charged phosphate residues provides reduced electrostatic repulsion between the PNA strand and a target RNA or DNA strand, causing exceptional thermal stability of the resulting hybrid complexes [9]. In order to improve solubility as well as intracellular delivery, a variety of modifications have been described [11, 12]. Phosphonic ester-modified PNAs (pePNAs) represent a specific modification of the α-carbon atom of the

Electronic supplementary material The online version of this article (https://doi.org/10.1007/s12033-018-0058-7) contains supplementary material, which is available to authorized users.

✉ Thomas Czerny
thomas.czerny@fh-campuswien.ac.at

[1] Department of Applied Life Sciences, University of Applied Sciences, FH Campus Wien, Helmut-Qualtinger-Gasse 2, 1030 Vienna, Austria

[2] Department of Engineering, University of Applied Sciences, FH Campus Wien, Favoritenstrasse 226, 1100 Vienna, Austria

[3] Present Address: Sandoz GmbH, Biochemiestraße 10, 6250 Kundl, Austria

[4] Present Address: CAST Gründungszentrum GmbH, Wilhelm-Greil-Straße 15, 6020 Innsbruck, Austria

[5] Present Address: UGISense AG, c/o Nordwind Capital GmbH, Residenzstrasse 18, 80333 Munich, Germany

Published online: 09 March 2018

glycine and improve the solubility and binding strength of interactions [13, 14].

The evolutionary highly conserved canonical Wnt pathway has shown to be crucial in development and disease [15]. Without binding of Wnt ligand proteins to frizzled/LRP5/6 co-receptors, β-catenin is recognised by a destruction complex including APC, Axin and GSK3β. As a result, β-catenin is degraded. In the active state the destruction complex is not formed; β-catenin accumulates and enters the nucleus where it interacts with members of the Tcf/Lef transcription factor family, such as Tcf3 and Lef1 [16]. During this process, Groucho/TLE proteins are replaced by β-catenin and co-activator proteins are recruited resulting in the activation of target genes [17, 18]. Besides its major role in Wnt signalling, β-catenin is also important for cell adhesion, where it connects cadherin to the cytoskeleton through α-catenin binding [19, 20].

Several components of the Wnt pathway, including APC, Axin, Tcf and β-catenin, have shown mutations relevant for human cancers [21, 22]. β-catenin mutations have been found in human colorectal cancer [23] and human hepatocellular carcinoma [24]. They result in constitutively active Wnt signalling, by uncoupling β-catenin from the degradation pathway [25, 26]. Due to its prominent role in the Wnt pathway, β-catenin has been discussed as a target for therapeutic applications [27, 28]. Targeting β-catenin showed a potential therapeutic benefit in a variety of studies, applying antisense reagents [27], peptides [29] or small molecule drugs [30].

In this study, we show a newly designed splice-based reporter assay for quantification of antisense effects, which allows a positive luminescence read out for successful splice blocking by antisense oligos. Based on this assay, a dominant negative knock-down strategy was developed for β-catenin with specific PNA and morpholino oligos. For this purpose, β-catenin was targeted in a way that the interaction with its main partners Tcf/Lef is still possible; however, interaction with essential coactivators is blocked.

Materials and Methods

Plasmids

For the splice-based reporter assay, a backbone containing a human EF1α short promoter [31] driving reporter gene expression, piggybac terminal repeat sequences for genome integration [32], puromycin resistance and a luciferase internal reference was constructed. Firefly luciferase (Fluc) [33] was used as reporter gene for pSplice2basis1 together with Gaussia luciferase (Gluc) [34] as an internal reference or NanoLuc (Nluc, Promega) [35] for pSplice3basis1 combined with the internal reference Fluc. Internal references were used for normalisation in order to compensate for varying cell number and viability. The consensus SD sequence of pSplice2basis1 and pSplice3basis1 is AGGTAAGT. β-catenin deletion constructs were generated via PCR and integrated into a pKC backbone containing a CMV promoter [36]. Mammalian two-hybrid constructs were all based on the pMC vector [37]. For details see Table S1.

Cell Culture and Statistical Analysis

HeLa, HEK293 T-REx (Invitrogen) as well as SW480 cells were cultured in Dulbecco's modified Eagle's medium (DMEM/GE Healthcare) including 10% foetal bovine serum (Thermo Scientific) and 1% penicillin/streptomycin (Thermo Scientific) in a humidified environment with 5% CO_2. Stable cell lines were generated using the piggybac transposon system [32]. Positive clones were picked after puromycin selection (Santa Cruz 1 µg/mL). Quantification of gels and Western blots was performed with ImageJ. *P* values were calculated by the Student's *t* test. Statistical significance: $*p \leq 0.05$; $**p \leq 0.01$; $***p \leq 0.001$.

Antisense Molecules

The synthesis of the lysine–phosphonic–ester-modified PNAs was performed as described in Jung et al. [14] by ugichem GmbH. Phosphorodiamidate morpholino oligonucleotides (abbreviated here as morpholinos) were manufactured by Gene Tools. All antisense molecules are listed in Table S2 with PNAs showing N-terminal (4-(tri-Fluoromethyl)-phenyl)-acetyl-glycine (phenylacetate-glycine) modifications. The PNAs were dissolved in nuclease free water to 1 mM by repeated shaking and vortexing. Finally, they were gently sonicated for 2 min with repeated pulses. Subsequently, the PNAs were kept at − 80 °C.

Transfection, Luciferase Assay and Mammalian Two-Hybrid Assay

For transient transfection cells were seeded in a PEI-coated [38] 96-well plate at a density of 0.5×10^4 cells/well and grown over night (HeLa) or 48 h (HEK293 T-REx). Transfection was performed using TurboFect (Thermo Scientific) transfection reagent following instructions of the manufacturer. Measurement was performed as described [39]. For the mammalian two-hybrid experiments, 80 ng reporter plasmid (plucF24ZF), 2 ng reference (pMcGlucS) and 2 ng bait construct (see Table S1) were co-transfected per well with 22 ng truncated β-catenin constructs (prey) into HEK293 T-REx cells.

Scraping

Cells were seeded in a 24-well plate with 0.3×10^5 cells/well and incubated overnight. 24 h later medium was removed and 30 µL loading solution [40] including the antisense reagent (morpholino or PNA) as well as 0.1 mg/mL fluorescein–isothiocyanate–dextran (FITC-dextran FD10S, Sigma-Aldrich) was added. Subsequently, cells were scraped off the plate with a rubber policeman 5× clockwise and 5× counter clockwise, and remaining cells were washed off with 500 µL DMEM including 10% foetal bovine serum and 1% penicillin/streptomycin (Thermo Scientific) and transferred into a fresh 24-well plate. Cells were incubated 24 h for recovery until RNA extraction or luciferase measurements were performed.

Electroporation

Cells were trypsinised, counted and diluted in DMEM to 3×10^7 cells/mL and 30 µL transferred to a 1 mm gap electroporation cuvette (VWR) pre-cooled on ice. Adjustments for electroporation (device described in [41]) on the Accupulser were: pulse width 12 ms, pulse interval 20 ms, train duration 250 ms for HeLa or 500 ms for SW480, voltage 60 V at a frequency of 1 kHz. After electroporation, cells were transferred to a fresh pre-warmed 24-well plate by flushing the cuvette with 500 µL DMEM including 10% foetal bovine serum and 1% Penicillin/Streptomycin (Thermo Scientific). Another 500 µL including 10% foetal bovine serum and 1% penicillin/streptomycin (Thermo Scientific) was added, and cells were divided into two wells of a 24-well plate followed by a 48 h recovery under standard cell culture conditions. For determination of cytotoxicity, cells were stained with 2 ng/µL 7AAD (Santa Cruz) followed by analysis with a flow cytometer (CytoFLEX, Beckman Coulter).

RNA Extraction and cDNA Synthesis

For RNA extraction the GeneJET RNA Purification Kit (Thermo Scientific) was used following the instructions of the manufacturer. DNAse I (Thermo Scientific), random hexamer primers (Thermo Scientific) and RevertAid Reverse Transcriptase (Thermo Scientific) for cDNA synthesis were used according to the instructions of the manufacturer.

qPCR

Primer and probe sequences are listed in Table S2. For each reaction 25 µL containing 0.2 µM of each primer, 80 mM Tris, 20 mM $(NH_4)_2SO_4$, 0.02% Tween20, 0.2 µM dNTP mix (Thermo Scientific), 0.005 U Taq polymerase (Agrobiogen) and 1 µL cDNA were used. Additionally, for qPCR 1 µL SYBR green to a final dilution of 1:10 (Sigma), 20 µg bovine serum albumin and 4 mM $MgCl_2$ or for Taqman 0.15 µM Taqman probes and 3.5 mM $MgCl_2$ were added. Measurements were taken in a Stratagene MX3000P (Agilent Technologies).

Western Blot

SW480 cells were electroporated with 32 µM morpholino MO3. After 48-h recovery whole cell protein extracts were made with lysis buffer (20 mM HEPES pH 7.9, 400 mM NaCl, 1 mM EDTA, 0.2% NP-40, 1 mM DTT and 0.5 mM PMSF). 5 µg of the protein extracts (determined by Bradford assay) was run on an SDS page followed by semidry blotting. Membranes were blocked 1–2 h in 5% milk powder (Roth) in 1× TBS-T (10 mM Tris–Cl, pH 7.4, 150 mM NaCl, 1 mM EDTA, pH 8.0, 0.1% Tween20) on a shaker. Primary antibodies were diluted 1:500 (β-catenin sc-1496, Santa Cruz) or 1:10,000 (GAPDH sc-25778, Santa Cruz) and incubated O/N at 4 °C shaking. Secondary antibody (HRP conjugated, goat anti-rabbit sc-2004, Santa Cruz) was added in a 1:5000 dilution with 5% BSA in TBS-T. Signals were detected with ECL solution (Santa Cruz Biotechnology) and a ChemiDoc (Protein Simple) station, and quantification was done with ImageJ.

Results

Sensitive Detection of Antisense Effects with a Splice-Based Reporter Assay

For development of an antisense strategy targeting β-catenin, we decided to apply a splice blocking approach [42, 43]. In order to quantify the efficiency of the antisense molecules, a splice-dependant reporter assay was established. The reporter construct was designed by positioning the AUG in the first exon and an artificial intron before the second exon containing the luciferase sequence. Splicing connects exon1 with exon2 coding for luciferase, but in the wrong reading frame resulting in a non-functional protein (Fig. 1a). On the contrary, blocking of splicing by antisense molecules generates an mRNA including the non-spliced intron, which, however, contains an open reading frame directly combining those of exon 1 and 2, and resulting in a functional luciferase fusion protein. The design of the reporter construct further allows easy introduction of any splice donor (SD) of interest by using restriction sites flanking the SD. In order to test the assay, two stable cell lines containing a consensus SD sequence were generated (HeLa pSplice2basis1 and HeLa pSplice3basis1). Experiments applying the PNA oligo PNA1 (Fig. 1b; for information on the antisense oligos see Table S2) or the morpholino oligo MO1 (Fig. S1) showed a

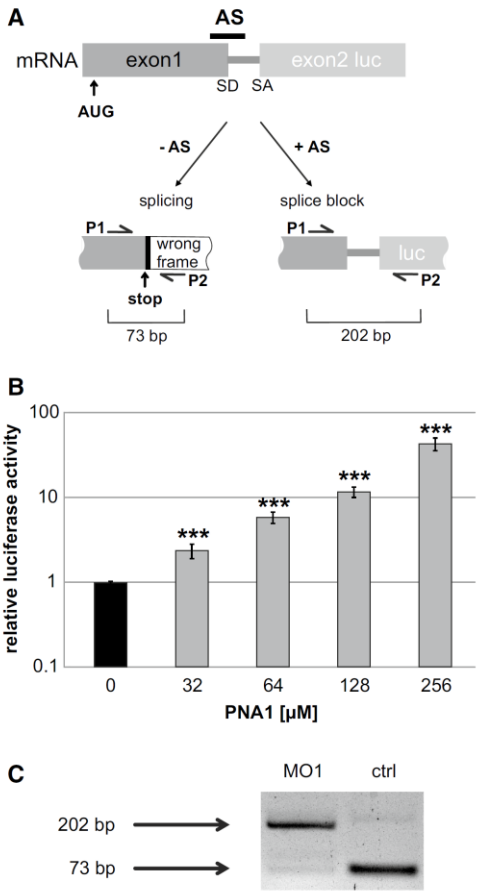

Fig. 1 Splice-based reporter assay. **a** Schematic view of the reporter assay. AS (antisense reagent), SD (splice donor), SA (splice acceptor), P1 and P2 (primers for PCR). **b** HeLa pSplice3basis1 cells were electroporated with the indicated amount of PNA1. After 24 h luciferase activity was determined. Nluc values were divided through internal Fluc reference and normalised to control cells (0) electroporated without PNA. Data represent mean values of at least 3 independent experiments, except for 32 µM (single determination), and error bars indicate SEM. **c** PCR from cDNA of antisense-treated pSplice3basis1 cells treated with 16 µM MO1 compared to equally treated control cells without reagent (ctrl). Scraping was used for delivery, and cells were harvested after 24 h

clear increase in luciferase activity (up to 49- and 13-fold, respectively). A luciferase-based internal reference was used to correct for cell number and to detect toxic effects of the antisense molecules. A concentration-dependent steady increase in luciferase activity was observed and even at the highest amounts of PNAs no drop in activity was observed, indicating no toxicity at the applied concentration range. The low cytotoxicity of the PNAs could be confirmed by flow cytometry. A concentration of 256 µM PNA1 showed no effect on the cell number (Fig. S2A) or the amount of dead cells (7AAD positive; Fig. S2B), compared to control cells electroporated without PNA. However, at 512 µM the total cell number slightly decreased and the number of dead cells increased. To confirm a splice blocking effect cDNA of HeLa pSplice3basis1 cells was analysed with PCR. The expected switch in splicing could be demonstrated using primers (P1 and P2) flanking the intron. A 73 bp product was observed for normal splicing, whereas addition of a splice blocking antisense oligo resulted in a 202 bp PCR fragment including the intron (Fig. 1a, c). The splice blocking efficiency of the morpholino oligo was strong, as indicated by the quantification of the PCR fragments resulting in a 590-fold change of the ratio upon treatment (Fig. 1c).

Splice Blocking Strategy for β-Catenin

In order to develop a strategy for targeting of β-catenin, we first tested multiple PNAs directed against the SD regions of various exons and selected the exon 13 SD for further experiments (Fig. 2a). Similar to the assay presented in Fig. 1, we established a reporter construct containing this SD and generated a stable reporter cell line (HeLa pSplice3βcat Ex13 SD). Using this assay for splice blocking, we tested 4 PNAs targeting the exon 13 SD, all with a length of 16 nucleotides and differing by a 2 nucleotide shift on their target sequences (Table S3). We observed increased luciferase levels for all 4 PNAs, and strongest luciferase induction was observed for PNA18 (Fig. 2b; 6.4-fold induction).

In order to demonstrate that targeting of exon 13 SD reduced the amount of properly spliced β-catenin mRNA, a qPCR assay in SW480 cells was performed. 24 h after electroporation with the antisense molecules, β-catenin mRNA levels were detected with primers in exons 13 and 14, respectively (Table S3). PNA18 showed significant effects also in this assay (reduction to 79%; $p = 0.0011$). Contrary to the luciferase-based assay, PNAs 4, 15 and 19 did not generate a significant reduction in the qPCR assay, whereas a morpholino oligo (MO3) directed to this SD resulted in a reduction of correctly spliced β-catenin mRNA to 59% compared to the mock-treated reference (Table S3). To demonstrate that the reduced detection of β-catenin mRNA was caused by aberrant splicing, an RT-PCR experiment was performed in SW480 cells (Fig. 3a). The appearance of a 304 bp PCR product indicates the presence of intron 13 in the mRNA, whereas a 50-bp fragment appears for correctly processed mRNA, lacking the intron. Electroporation of both PNA18 and MO3 resulted in the appearance of a 304-bp fragment indicating a splice block at exon 13 SD (Fig. 3a). Furthermore, the antisense effect on β-catenin could be verified on the protein level. A Western blot with extracts harvested from SW480 cells showed a reduction of β-catenin protein to 45% compared to non-treated controls (Fig. 3b).

In order to see whether the β-catenin knock-down had an effect on established Wnt target genes, we quantified

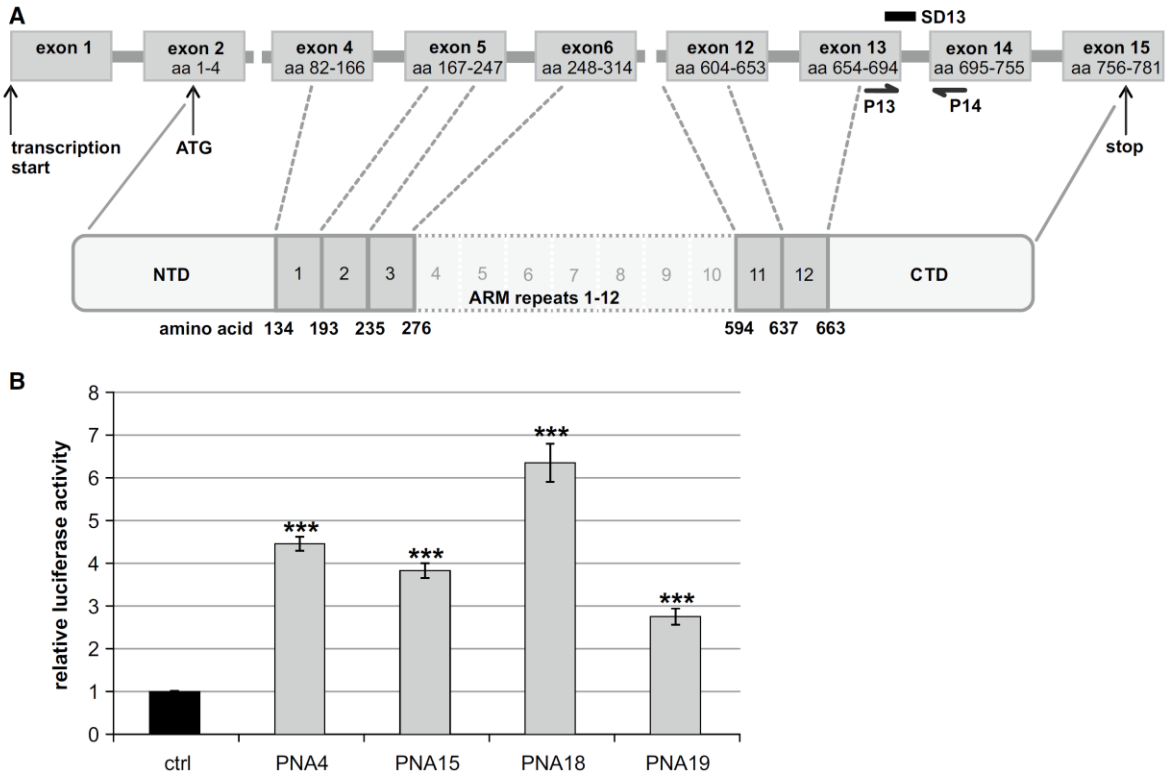

Fig. 2 Targeting β-catenin with PNA and morpholino oligos. **a** Schematic view of the β-catenin gene including exon/intron map with positions of exon 13 SD (SD13) and splice-specific PCR primers (P13, P14), numbering of exons according to NM001904.3. The positions of the exons relative to the armadillo repeats of the protein are indicated. Abbreviations: amino acid (aa), armadillo (ARM), N-terminal domain (NTD), C-terminal domain (CTD). **b** Luciferase assay with different PNAs targeting β-catenin at the SD of exon 13. HeLa pSplice3βcat Ex13 SD cells were electroporated with 128 µM of the indicated PNAs. Nluc values were divided through the internal reference Fluc and normalised to control cells (ctrl) electroporated without PNA. Data represent mean values of at least 3 independent experiments, and error bars indicate SEM

mRNA levels of axin, VEGF and c-myc in SW480 cells after PNA or morpholino treatment. In all cases we observed reduced levels upon antisense molecule application, except for PNA18 which was not effective for VEGF (Fig. 3c). In particular, PNA18 reduced the axin mRNA to 23% and that of c-myc to 55%. Similarly, MO3 reduced axin mRNA to 39%, c-myc to 40% and VEGF to 59%.

Mammalian Two-Hybrid Analysis of β-Catenin Interactions

The experiments so far revealed an effect of splice blocking of exon 13 SD on β-catenin mRNA, protein levels and on Wnt target genes. Splice blocking of an SD typically results in the persistence of the non-spliced intron or less often in skipping of the upstream exon. In both cases the exon 13 SD induced splice block results in a truncated β-catenin protein. The truncation would explain a lack of activity due to loss of interaction with the transcriptional co-activator CBP/p300, which depends on an intact C-terminal domain of β-catenin (Fig. 4a) [44]. To verify the reduced transactivation, we expressed a β-catenin variant truncated after exon 13 in Hela cells and measured its activity in a luciferase reporter assay (Fig. S3). Whereas full-length β-catenin activated the reporter 5.8-fold, the truncated protein resulted in luciferase values close to the basal level (1.4-fold reporter activation compared to the empty expression vector). However, β-catenin not only serves functions in transcriptional regulation, but also plays a critical role in cell adhesion. Ideally, targeting of ß-catenin should block its transcriptional activity, but retain its cell adhesion function. This function depends on protein–protein interactions with cadherin and α-catenin. Whereas the α-catenin interaction has been mapped to the N-terminal domain and armadillo repeat 1 [45], cadherin interacts with the complete central region of β-catenin

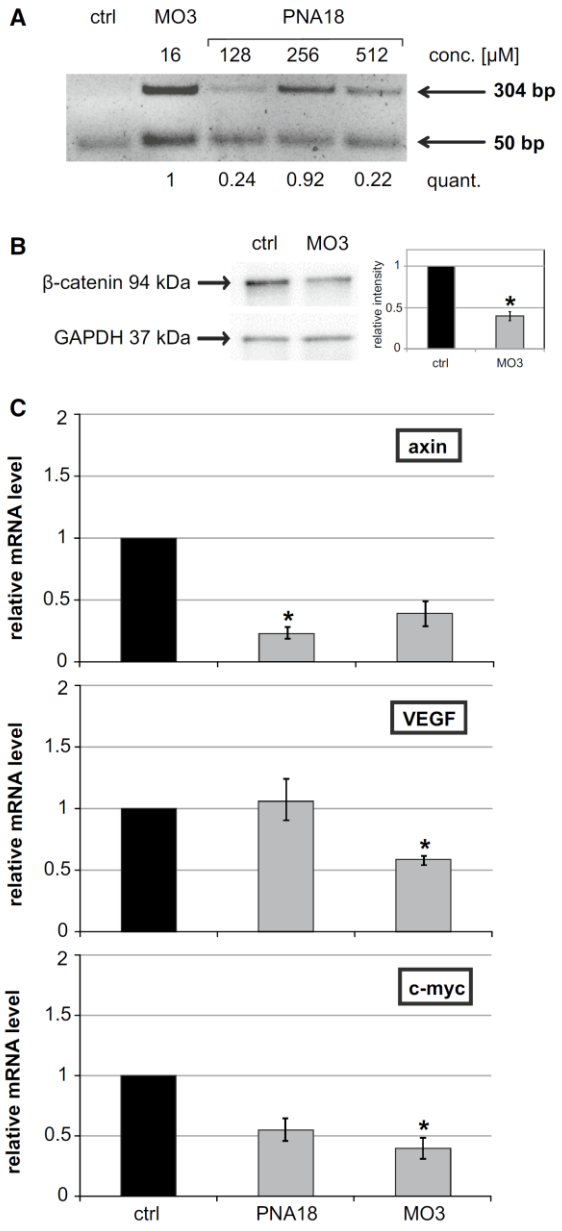

Fig. 3 Effect of splice block at exon 13 of β-catenin in SW480 cells. **a** SW480 cells were electroporated with the indicated amounts of MO3 and PNA18. PCR from cDNA with primers P13 and P14, specific for the presence of intron 13 (304 bp band) as a result of the splice block and 50 bp resulting from normal splicing. Quantification of the band ratio normalised to MO3 is shown below (quant.). **b** Effect on β-catenin protein level in SW480 cells electroporated with 32 μM MO3, extracts prepared after 48 h. Bands for β-catenin and GAPDH are indicated. Quantification is shown for two independent experiments (resulting in a mean protein level of 40% for the MO3-treated samples compared to the control). **c** mRNA levels of the β-catenin target genes axin, VEGF and c-myc determined by qPCR normalised to GAPDH and mock-treated control cells (ctrl). SW480 cells were electroporated with MO3 (16 μM) and PNA18 (256 μM). Data represent mean values of duplicates. Error bars indicate SEM

(Fig. 4a) [46]. The function of β-catenin in cell adhesion could therefore be affected by truncations of the protein upon a splice block.

In order to investigate the effects of the β-catenin truncations on its interactions, we performed a mammalian two-hybrid analysis [39]. We selected blocking of two SD regions for the analysis; in addition to the SD of exon 13 (aa 654–694) we used that of exon 6 (aa 248–314) as a control, which leads to truncations lacking the majority of the armadillo repeats. In both cases we considered the presence of a non-spliced intron or skipping of the upstream exon due to the splice block. In addition, the presence of prominent cryptic splice sites in the vicinity of the SD was excluded [47]. We then generated expression constructs by PCR according to the expected splice products. For exon 6 we generated β-catenin(+I6) (intron 6 added) and β-catenin(E6skip) (exon 6 skipped) and for exon 13 β-catenin(+I13) (intron 13 added) and β-catenin(E13skip) (exon 13 skipped); the constructs were extended until the first in frame stop codon. The four truncated β-catenin versions served as prey in the mammalian two-hybrid assay and were N-terminally fused to the p65 transactivation domain. Tcf3, Lef1, cadherin and α-catenin were used as baits, fused to the DNA binding domain ZFHD [39].

For all baits interactions with full-length β-catenin as prey were clearly detectable (Fig. 4b). Also an interaction of α-catenin was detectable for all baits; however, the interactions of Tcf3 and Lef1 were clearly reduced for β-catenin(+I6) and β-catenin(E6skip), compared to that of β-catenin(+I13), β-catenin(E13skip) and β-catenin full length. Finally, the cadherin interaction was also strongly reduced for the exon 6 truncations (+I6 and E6skip), but the exon 13 truncations (+I13 and E13skip) both showed luciferase activities similar to full-length β-catenin. Therefore, truncations of β-catenin due to splice blocking at exon 13 SD retain the interactions necessary for a function in cell adhesion.

Dominant Negative Effect of β-Catenin Truncations

Loss of the C-terminus is expected to result in a lack of transcriptional activity, but the mammalian two-hybrid experiments revealed binding of Tcf/Lef to the exon 13 truncations of β-catenin. This combination could be the basis for a dominant negative effect, where truncated β-catenin proteins would interfere with binding of wild-type proteins to Tcf/Lef. To test this, we transfected a β-catenin full-length expression construct together with different amounts of those for the truncated β-catenin versions. A co-transfected luciferase reporter construct containing six Tcf/Lef binding sites [49] was used for detection of Wnt pathway activity. Compared to the empty expression vector, all truncated versions resulted

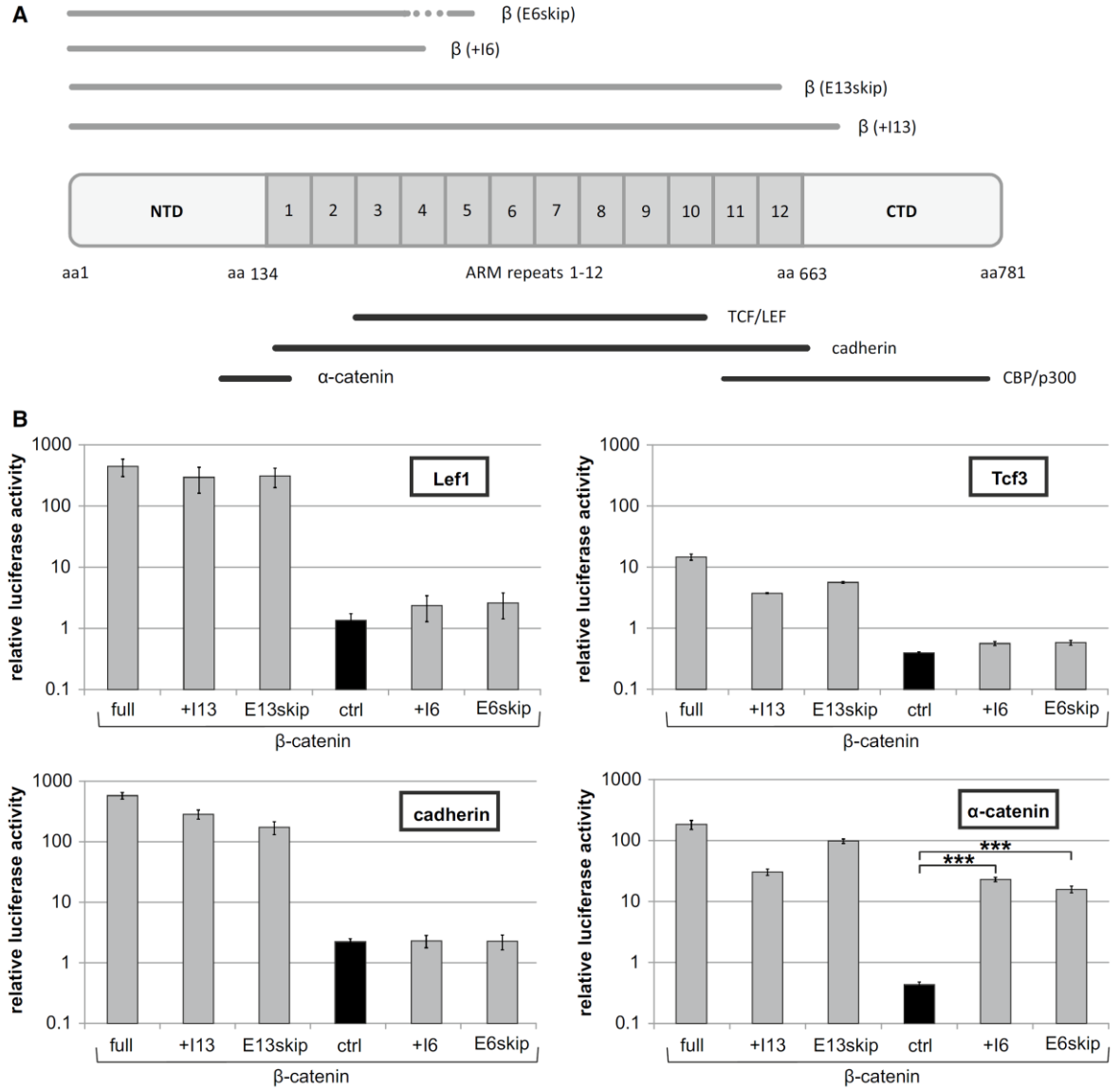

Fig. 4 Protein–protein interactions of truncated β-catenin. **a** Schematic presentation of truncated β-catenin versions. Position of armadillo (ARM) repeats is indicated as well as the interaction sites of known binding partners [45, 46, 48]. aa (amino acids), NTD (N-terminal domain), CTD (C-terminal domain), ARM (armadillo). **b** Mammalian two-hybrid assay with the baits Lef1 (pMCLef1mZFb6), Tcf3 (pMCZFb6Tcf3), cadherin (pMCZFghe-cadherin) or β-catenin (pMCZFg alpha-catenin) together with the preys β-catenin full length (full; pMC65gDPβcat), β-catenin(+I13) (pMC65gDPβcat[1-694]), β-catenin(E13skip) (pMC65gDPβcat[1-653]), β-catenin(+I6) (pMC65gDPβcat[plusintron6]), β-catenin(E6skip) (pMC65gDPβcat[exon6skip]) and no prey (ctrl). All Fluc values were divided through the internal reference Gluc and then normalised to samples lacking bait and prey. Data represent mean values of at least 3 independent experiments, and error bars indicate SEM

in reduced activity of β-catenin. However, strongest effects were seen for the two exon 13 constructs (β-catenin(+I13), reduction to 31% and β-catenin(E13skip), reduction to 23% (Fig. 5a). The most effective truncation of β-catenin(E13skip) showed effects already at low concentrations (3 ng; Fig. 5b), whereas co-transfection of full-length β-catenin had the opposite effect leading to an increase in the luciferase activity of the Wnt responsive reporter. In this experiment the activity of the full-length protein can be directly compared with the dominant

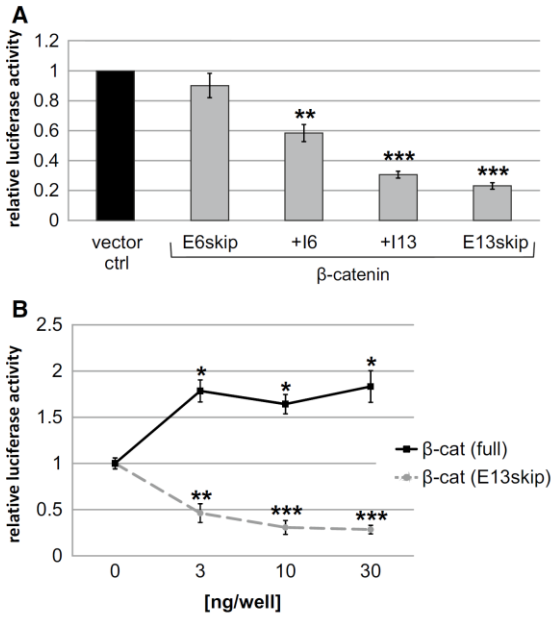

Fig. 5 Dominant negative effect of truncated β-catenin versions. **a** 70 ng pMlucF6lefcons, 2 ng pMCGlucS and 10 ng β-catenin full length [pKCDPβcat] were co-transfected into HeLa cells with 30 ng truncated β-catenin versions: pKCDPβcat(E6skip), pKCDPβcat(+I6), pKCDPβcat(1-694)(+I13), pKCDPβcat(1-653)(E13skip) and empty pKC vector (vector ctrl). Measurements were taken 24 h after transfection. All values were normalised to samples with empty expression vector pKC. Data represent mean values of at least 3 independent experiments, and error bars indicate SEM. **b** Concentration-dependent dominant negative effect of β-catenin(E13skip) (pKCDPβcat[1-653]) compared to β-catenin full length (full; pKCDPβcat). 70 ng pMlucF6lefcons, 2 ng pMCGlucS and 10 ng pKCDPβcat were co-transfected with 3, 10 and 30 ng pKCDPβcat or pKCDPβcat(1-653) into HeLa cells. Values were normalised to controls without expression vector for β-catenin. All Fluc reporter values were divided through Gluc internal reference. Data represent mean values of at least 3 independent experiments, and error bars indicate SEM

negative effect of the truncated version, thus confirming the strict dependence of β-catenin on an intact C-terminus for canonical Wnt signalling.

Discussion

Splice-Based Reporter Assay

Alternative splicing is widely used by nature to extend the repertoire of the proteome, and aberrant splicing has been shown to be the cause for a variety of diseases [50]. Antisense molecules bind to mRNA and thus have the potential to manipulate the access of the splice machinery. Whereas most applications aim to inactivate gene function by generating non-functional proteins, also correction of aberrant splicing has been tested as a therapeutic strategy for diseases like β-Thalassaemia [43, 51], also applying reporter assays [52]. We established a luciferase-based assay which shows several advantages. The splice target sequence is integrated into an otherwise completely artificial surrounding and can easily be exchanged. The specific design of the intron allows a positive readout for the assay, meaning that successful splice blocking results in a luciferase signal above the background (Fig. 1a).

Using this reporter we developed stable cell lines for two different splice sites and in both cases observed sensitive and reliable signals for splice blocking oligos. In the case of β-catenin 4 different PNAs directed against the exon 13 SD resulted in positive signals in the luciferase assay (Fig. 2b; $p \leq 0.02$ for all 4 PNAs). On the other hand, a qPCR-based assay showed a significant reduction of β-catenin mRNA only for PNA18 (Table S3; $p = 0.001$), whereas non-significant values were obtained for the other 3 PNAs ($p \geq 0.3$). Main reason for this discrepancy is the error rates, which are considerably smaller for the luciferase assay (compare Fig. 2b and Table S3). Therefore, the optimisation of conditions for splice blocking works highly efficient with the presented reporter assay. Furthermore, compared to alternatives as qPCR or Western blot this assay is fast and simple.

PNAs show a number of advantageous properties compared to other antisense reagents. Due to the neutral charge of their backbone and the lack of electrostatic repulsion, they bind RNA with high affinity. Consequently, short antisense molecules (13–18 bases) are sufficient for selective binding. The small size makes them ideal for therapeutic applications, and the intracellular delivery can be further boosted using cell penetrating peptides [53], nanoparticles [54], liposomes [55] or modifications of the PNA backbone [56]. Phosphonic ester modifications of the backbone improve both the cellular uptake [57] and the knock-down efficiency [13, 14]. The phosphonic ester PNAs used in this study induced splice blocking (Fig. 1c), comparable to previous studies with PNAs [58, 59].

Targeting β-Catenin with Splice-Based Antisense Molecules

Due to its relevance in cancer development, β-catenin has become a favoured target for nouveau cancer therapy strategies. Recent publications show decreased tumour burden within varying cancer types after targeting β-catenin with different approaches. PNAs have already been used for β-catenin knock-down in liver tumour cells [56] or antisense oligodeoxynucleotides for β-catenin targeting in xenograft mice with SW480 colon carcinoma cells [60]. Furthermore, small molecule inhibitors [61] or siRNA [62] were successfully used within xenograft mouse models. Nonetheless,

rigorous targeting of β-catenin may be problematic due to the essential role of β-catenin in non-cancer related functions as cell–cell adhesion [63].

Antisense-mediated splice blocking as a strategy to reduce β-catenin levels in the cell worked in our approach and resulted in reduced levels of β-catenin mRNA, protein and consequently also of target genes (Fig. 3). A specific advantage of our splice-based antisense strategy is the generation of a dominant negative protein version. Targeting of exon 13 SD results in a C-terminally truncated protein, which lacks transactivation properties, but retains its interaction with Tcf/Lef proteins, thus competing with wild-type β-catenin (Figs. 4, 5). Most importantly, the truncation does not interfere with interactions of β-catenin with α-catenin and cadherin (Fig. 4), both critical for its function in cell adhesion. Therefore, our splice blocking antisense approach generates a truncated protein with the potential to efficiently interfere with Wnt signalling in a dominant negative manner, but at the same time retaining critical functions of β-catenin in cell adhesion. A next step would be to test this approach in an in vivo model.

Conclusion

Herein, we present a splice-based reporter assay for accurate quantification of knock-down effects of antisense molecules. Furthermore, a strategy for targeting β-catenin next to its C-terminal transactivation domain resulted in a dominant negative protein, which efficiently blocks Wnt signalling, but retains interactions with cell adhesion molecules.

Acknowledgements Open access funding provided by FH Campus Wien - University of Applied Sciences. The work was supported by the Austrian Research Promotion Agency (FFG, Grant 836444) and the City of Vienna (MA23—project 18-18).

Authors' Contributions MV and ER were responsible for experimental design, analysis, execution and writing of the manuscript. CH built and maintained the electroporator. MA, HB, BW and TL performed the PNA design and synthesis. TC was responsible for experimental design, analysis, writing, communication and supervising of the project. All authors read and approved the final manuscript.

Compliance with Ethical Standards

Conflict of interest MA, HB, BW and TL were full employees of the company ugichem GmbH that developed PNAs for therapeutic applications. Design and synthesis of the PNAs were performed at the ugichem GmbH, which became insolvent 2015.

References

1. Zamecnik, P. C., & Stephenson, M. L. (1978). Inhibition of Rous sarcoma virus replication and cell transformation by a specific oligodeoxynucleotide. *Proceedings of the National Academy of Sciences, 75*(1), 280–284.
2. Mansoor, M., & Melendez, A. J. (2008). Advances in antisense oligonucleotide development for target identification, validation, and as novel therapeutics. *Gene Regulation and Systems Biology, 2,* 275–295.
3. Perry, C. M., & Barman Balfour, J. A. (1999). Fomivirsen. *Drugs, 57*(3), 375–380.
4. Vinores, S. A. (2006). Pegaptanib in the treatment of wet, age-related macular degeneration. *International Journal of Nanomedicine, 1*(3), 263–268.
5. Moreno, P., & Pego, A. P. (2014). Therapeutic antisense oligonucleotides against cancer: Hurdling to the clinic. *Frontiers in Chemistry, 2*(October), 87.
6. Warren, T. K., Shurtleff, A. C., & Bavari, S. (2012). Advanced morpholino oligomers: A novel approach to antiviral therapy. *Antiviral Research, 94*(1), 80–88.
7. Summerton, J. (2007). Morpholino, siRNA, and S-DNA compared: Impact of structure and mechanism of action on off-target effects and sequence specificity. *Current Topics in Medicinal Chemistry, 7*(7), 651–660.
8. Blum, M., De Robertis, E. M., Wallingford, J. B., & Niehrs, C. (2015). Morpholinos: Antisense and sensibility. *Developmental Cell, 35*(2), 145–149.
9. Egholm, M., Buchardt, O., Christensen, L., Behrens, C., Freier, S. M., Driver, D. A., et al. (1993). PNA hybridizes to complementary oligonucleotides obeying the Watson–Crick hydrogen-bonding rules. *Nature, 365*(6446), 566–568.
10. Nielsen, P. G., Egholm, M., Berg, R. H., & Buchardt, O. (1991). Sequence-selective recognition of DNA by strand displacement with a thymine-substituted polyamide. *Science, 254*(5037), 1497–1500.
11. Kumar, P., & Jain, D. R. (2015). Cγ-Aminopropylene peptide nucleic acid (amp-PNA): Chiral cationic PNAs with superior PNA: DNA/RNA duplex stability and cellular uptake. *Tetrahedron, 71*(21), 3378–3384.
12. Bohländer, P. R., Vilaivan, T., & Wagenknecht, H.-A. (2015). Strand displacement and duplex invasion into double-stranded DNA by pyrrolidinyl peptide nucleic acids. *Organic & Biomolecular Chemistry, 13*(35), 9223–9230.
13. Dorn, S., Aghaallaei, N., Jung, G., Bajoghli, B., Werner, B., Bock, H., et al. (2012). Side chain modified peptide nucleic acids (PNA) for knock-down of six3 in medaka embryos. *BMC Biotechnology, 12*(1), 50.
14. Jung, G., Dorn, S., Aghaallaei, N., Bajoghli, B., Riegel, E., Bock, H., et al. (2018). The function of Tcf3 in medaka embryos: Efficient knock down with pePNAs. *BMC Biotechnology*, *18*, 1.
15. Nusse, R., & Varmus, H. E. (1992). Wnt genes. *Cell, 69*(7), 1073–1087.
16. Mao, C. D., & Byers, S. W. (2011). Cell-context dependent TCF/LEF expression and function: Alternative tales of repression, de-repression and activation potentials. *Critical Reviews™ in Eukaryotic Gene Expression*, *21*(3), 207–236.
17. Henderson, W. R., Chi, E. Y., Ye, X., Nguyen, C., Tien, Y. T., Zhou, B., et al. (2010). Inhibition of Wnt/-catenin/CREB binding

protein (CBP) signaling reverses pulmonary fibrosis. *Proceedings of the National Academy of Sciences, 107*(32), 14309–14314.
18. Clevers, H. (2006). Wnt/β-catenin signaling in development and disease. *Cell, 127*(3), 469–480.
19. Nelson, W. J. (2004). Convergence of Wnt, β-catenin, and cadherin pathways. *Science, 303*(5663), 1483–1487.
20. Valenta, T., Hausmann, G., & Basler, K. (2012). The many faces and functions of β-catenin. *The EMBO Journal, 31*(12), 2714–2736.
21. Polakis, P. (2007). The many ways of Wnt in cancer. *Current Opinion in Genetics & Development, 17*(1), 45–51.
22. Rubinfeld, B. (1997). Stabilization of beta-catenin by genetic defects in melanoma cell lines. *Science, 275*(5307), 1790–1792.
23. Ilyas, M., Tomlinson, I. P. M., Rowan, A., Pignatelli, M., & Bodmer, W. F. (1997). β-catenin mutations in cell lines established from human colorectal cancers. *Proceedings of the National Academy of Sciences, 94*(19), 10330–10334.
24. Okabe, H., Kinoshita, H., Imai, K., Nakagawa, S., Higashi, T., Arima, K., et al. (2016). Diverse basis of β-catenin activation in human hepatocellular carcinoma: Implications in biology and prognosis. *PLoS One, 11*(4), e0152695.
25. Tien, L. T., Ito, M., Nakao, M., Niino, D., Serik, M., Nakashima, M., et al. (2005). Expression of beta-catenin in hepatocellular carcinoma. *World Journal of Gastroenterology, 11*(16), 2398–2401.
26. Bienz, M., & Clevers, H. (2000). Linking colorectal cancer to Wnt signaling. *Cell, 103*(2), 311–320.
27. Roh, H., Green, D. W., Boswell, C. B., Cells, C., Pippin, J. A., & Drebin, J. A. (2001). Suppression of β-catenin inhibits the neoplastic growth of APC-mutant colon cancer cells suppression of ß-catenin inhibits the neoplastic growth of APC-mutant colon. *Cancer Research, 61*(17), 6563–6568.
28. Luu, H. H., Zhang, R., Haydon, R. C., Rayburn, E., Kang, Q., Si, W., et al. (2004). Wnt/β-catenin signaling pathway as novel cancer drug targets. *Current Cancer Drug Targets, 4*(8), 653–671.
29. Grossmann, T. N., Yeh, J. T.-H., Bowman, B. R., Chu, Q., Moellering, R. E., & Verdine, G. L. (2012). Inhibition of oncogenic Wnt signaling through direct targeting of β-catenin. *Proceedings of the National Academy of Sciences, 109*(44), 17942–17947.
30. Hahne, G., & Grossmann, T. N. (2013). Direct targeting of β-catenin: Inhibition of protein–protein interactions for the inactivation of Wnt signaling. *Bioorganic & Medicinal Chemistry, 21*(14), 4020–4026.
31. Wan Kim, D., Uetsuki, T., Kaziro, Y., Yamaguchi, N., & Sugano, S. (1990). Use of the human elongation factor 1α promoter as a versatile and efficient expression system. *Gene, 91*(2), 217–223.
32. Wang, H., Fraser, M. J., & Cary, L. C. (1989). Transposon mutagenesis of baculoviruses: Analysis of TFP 3 lepidopteran transposon insertions at the FP locus of nuclear polyhedrosis viruses. *Gene, 81*(1), 97–108.
33. de Wet, J. R., Wood, K. V., DeLuca, M., Helinski, D. R., & Subramani, S. (1987). Firefly luciferase gene: Structure and expression in mammalian cells. *Molecular and Cellular Biology, 7*(2), 725–737.
34. Verhaegen, M., & Christopoulos, T. K. (2002). Recombinant gaussia luciferase. overexpression, purification, and analytical application of a bioluminescent reporter for DNA hybridization. *Analytical Chemistry, 74*(17), 4378–4385.
35. Hall, M. P., Unch, J., Binkowski, B. F., Valley, M. P., Butler, B. L., Wood, M. G., et al. (2012). Engineered luciferase reporter from a deep sea shrimp utilizing a novel imidazopyrazinone substrate. *ACS Chemical Biology, 7*(11), 1848–1857.
36. Heimbucher, T., Murko, C., Bajoghli, B., Aghaallaei, N., Huber, A., Stebegg, R., et al. (2007). Gbx2 and Otx2 interact with the WD40 domain of groucho/Tle corepressors. *Molecular and Cellular Biology, 27*(1), 340–351.
37. Fink, M., Flekna, G., Ludwig, A., Heimbucher, T., & Czerny, T. (2006). Improved translation efficiency of injected mRNA during early embryonic development. *Developmental Dynamics, 235*(12), 3370–3378.
38. Vancha, A. R., Govindaraju, S., Parsa, K. V., Jasti, M., González-García, M., & Ballestero, R. P. (2004). Use of polyethyleneimine polymer in cell culture as attachment factor and lipofection enhancer. *BMC Biotechnology, 4*(1), 23.
39. Riegel, E., Heimbucher, T., Höfer, T., & Czerny, T. (2017). A sensitive, semi-quantitative mammalian two-hybrid assay. *BioTechniques, 62,* 206–214.
40. Fechheimer, M., Boylan, J. F., Parker, S., Sisken, J. E., Patel, G. L., & Zimmer, S. G. (1987). Transfection of mammalian cells with plasmid DNA by scrape loading and sonication loading. *Proceedings of the National Academy of Sciences, 84*(23), 8463–8467.
41. Jung, G., Hug, M., Halter, C., Friesenhengst, A., Walzer, J., & Czerny, T. (2013). Diffusion of small molecules into medaka embryos improved by electroporation. *BMC Biotechnology, 13*(1), 53.
42. Veltrop, M., & Aartsma-Rus, A. (2014). Antisense-mediated exon skipping: Taking advantage of a trick from Mother Nature to treat rare genetic diseases. *Experimental Cell Research, 325*(1), 50–55.
43. Kole, R., Krainer, A. R., & Altman, S. (2012). RNA therapeutics: Beyond RNA interference and antisense oligonucleotides. *Nature Reviews Drug Discovery, 11*(2), 125.
44. Vleminckx, K., Kemler, R., & Hecht, A. (1999). The C-terminal transactivation domain of beta-catenin is necessary and sufficient for signaling by the LEF-1/beta-catenin complex in Xenopus laevis. *Mechanisms of Development, 81*(1–2), 65–74.
45. Pokutta, S., & Weis, W. (2000). Structure of the dimerization and beta-catenin-binding region of alpha-catenin. *Molecular Cell, 5*(3), 533–543.
46. Orsulic, S., Huber, O., Aberle, H., Arnold, S., & Kemler, R. (1999). E-cadherin binding prevents beta-catenin nuclear localization and beta-catenin/LEF-1-mediated transactivation. *Journal of cell science, 112*(Pt 8), 1237–1245.
47. Hebsgaard, S. M., Korning, P. G., Tolstrup, N., Engelbrecht, J., Rouzé, P., & Brunak, S. (1996). Splice site prediction in Arabidopsis thaliana pre-mRNA by combining local and global sequence information. *Nucleic Acids Research, 24*(17), 3439–3452.
48. Xing, Y., Takemaru, K.-I., Liu, J., Berndt, J. D., Zheng, J. J., Moon, R. T., et al. (2008). Crystal Structure of a Full-Length β-Catenin. *Structure, 16*(3), 478–487.
49. Hsu, S. C., Galceran, J., & Grosschedl, R. (1998). Modulation of transcriptional regulation by LEF-1 in response to Wnt-1 signaling and association with beta-catenin. *Molecular and Cellular Biology, 18*(8), 4807–4818.
50. Scotti, M. M., & Swanson, M. S. (2015). RNA mis-splicing in disease. *Nature Reviews Genetics, 17*(1), 19–32.
51. Sierakowska, H., Sambade, M. J., Agrawal, S., & Kole, R. (1996). Repair of thalassemic human-globin mRNA in mammalian cells by antisense oligonucleotides. *Proceedings of the National Academy of Sciences, 93*(23), 12840–12844.
52. Bahal, R., Ali McNeer, N., Quijano, E., Liu, Y., Sulkowski, P., Turchick, A., et al. (2016). In vivo correction of anaemia in β-thalassemic mice by γPNA-mediated gene editing with nanoparticle delivery. *Nature Communications, 7,* 13304.
53. Ivanova, G. D., Arzumanov, A., Abes, R., Yin, H., Wood, M. J. A., Lebleu, B., et al. (2008). Improved cell-penetrating peptide-PNA conjugates for splicing redirection in HeLa cells and exon skipping in mdx mouse muscle. *Nucleic Acids Research, 36*(20), 6418–6428.
54. Beavers, K. R., Werfel, T. A., Shen, T., Kavanaugh, T. E., Kilchrist, K. V., Mares, J. W., et al. (2016). Porous silicon and polymer nanocomposites for delivery of peptide nucleic acids as anti-MicroRNA therapies. *Advanced Materials, 28*(36), 7984–7992.

55. Avitabile, C., Accardo, A., Ringhieri, P., Morelli, G., Saviano, M., Montagner, G., et al. (2015). Incorporation of naked peptide nucleic acids into liposomes leads to fast and efficient delivery. *Bioconjugate Chemistry, 26*(8), 1533–1541.
56. Delgado, E., Bahal, R., Yang, J., Lee, J. M., Ly, H., & PS Monga, S. (2014). β-Catenin knockdown in liver tumor cells by a Cell permeable gamma guanidine-based peptide nucleic acid. *Current Cancer Drug Targets, 13*(8), 867–878.
57. Posch, W., & Piper, S. (2012). Inhibition of human immunodeficiency virus replication by cell membrane-crossing oligomers. *Molecular Medicine, 18*(1), 1.
58. Chin, J. Y., Kuan, J. Y., Lonkar, P. S., Krause, D. S., Seidman, M. M., Peterson, K. R., et al. (2008). Correction of a splice-site mutation in the beta-globin gene stimulated by triplex-forming peptide nucleic acids. *Proceedings of the National Academy of Sciences, 105*(36), 13514–13519.
59. Wright, D. G., Zhang, Y., & Murphy, J. R. (2008). Effective delivery of antisense peptide nucleic acid oligomers into cells by anthrax protective antigen. *Biochemical and Biophysical Research Communications, 376*(1), 200–205.
60. Green, D. W., Roh, H., Pippin, J. A., & Drebin, J. A. (2001). β-catenin antisense treatment decreases β-catenin expression and tumor growth rate in colon carcinoma xenografts. *Journal of Surgical Research, 101*(1), 16–20.
61. Wang, Z., Li, B., Zhou, L., Yu, S., Su, Z., Song, J., et al. (2016). Prodigiosin inhibits Wnt/β-catenin signaling and exerts anticancer activity in breast cancer cells. *Proceedings of the National Academy of Sciences, 113*(46), 13150–13155.
62. Ganesh, S., Koser, M. L., Cyr, W. A., Chopda, G. R., Tao, J., Shui, X., et al. (2016). Direct pharmacological inhibition of β-catenin by rna interference in tumors of diverse origin. *Molecular Cancer Therapeutics, 15*(9), 2143–2154.
63. Kahn, M. (2014). Can we safely target the WNT pathway? *Nature Reviews Drug Discovery, 13*(7), 513–532.

11 Appendix II Results of in-silico splice site analysis

********** NetGene2 v. 2.4 **********

The sequence: has the following composition:

Length: 3938 nucleotides.
28.6% A, 18.0% C, 20.9% G, 32.6% T, 0.0% X, 38.8% G+C

Donor splice sites, direct strand

pos 5'->3'	phase	strand	confidence	5' exon	intron 3'
160	0	+	0.80	GCAATTTGTG	GTAGGTAAAT
164	1	+	0.88	TTTGTGGTAG	GTAAATTCTT H
1153	2	+	0.41	TGGCAACTCG	GTTAGTTTTA
1706	0	+	0.67	GTTTGTGCAG	GTATGTTTTA
2356	1	+	0.91	AGGAATGAAG	GTGTGGGTAA H
2362	1	+	0.93	GAAGGTGTGG	GTAAGTAAAA H
2572	0	+	0.81	TTGGAATGAG	GTAGGGAAAT
2618	1	+	0.53	CCTAGAGCAG	GTATGGCAGC
3341	1	+	0.47	CAAATTACCA	GTGAGTAGTG
3666	0	+	0.31	GAACAAGTCA	GTGAGTATTT

Donor splice sites, complement strand

pos 3'->5'	pos 5'->3'	phase	strand	confidence	5' exon	intron 3'
3434	505	2	-	0.54	GTGAAAACAG	GTTTGTGGAA
3420	519	1	-	0.57	GTGGAAGGGG	GTAGGTGGAG
1926	2013	0	-	0.34	GGCAGCCCAG	GTCAGCTCTC
1321	2618	0	-	0.36	CTTTCCTACA	GTAAGGGCAC
1292	2647	2	-	0.32	TGGGTAAAAG	GTATATAAAA
1061	2878	1	-	0.67	TTTGCAATAT	GTAAGTACCA
508	3431	0	-	0.53	TGAGGCAAGG	GTAAGAGGCT

Acceptor splice sites, direct strand

pos 5'->3'	phase	strand	confidence	5' intron	exon 3'
66	0	+	0.00	GCGTGAGCAG	GGTGCCATTC
111	0	+	0.19	TGCACATCAG	GATACCCAGC
939	0	+	0.43	TCTTTTCTAG	GAAGAAGAGA
1303	0	+	0.43	TTTTACCCAG	AATGATTGGT
1585	0	+	0.94	CTTTTGGCAG	GAGGGGGTCC
1588	0	+	0.14	TTGGCAGGAG	GGGGTCCGCA
2242	2	+	0.19	ACATCCAAAG	AGTAGCTGCA
2244	1	+	0.19	ATCCAAAGAG	TAGCTGCAGG
2247	1	+	0.20	CAAAGAGTAG	CTGCAGGGGT
2253	1	+	0.20	GTAGCTGCAG	GGGTCCTCTG
2276	0	+	0.47	ACTTGCTCAG	GACAAGGAAG
2282	0	+	0.17	TCAGGACAAG	GAAGCTGCAG
2286	1	+	0.07	GACAAGGAAG	CTGCAGAAGC

2425	1	+	0.14	TTTCCTCAAG^GGCCTTTTTC
2449	1	+	0.96	TGTCTCTTAG^CGACATATGC
2461	1	+	0.25	ACATATGCAG^CTGCTGTTTT
2713	1	+	0.33	TGCTGTCTAG^CAACTGCTCT
2969	2	+	0.16	TTTTCTTCAG^CATTTGTCCT
3051	1	+	0.26	CATTCTATAG^AGATCATTGA

Acceptor splice sites, complement strand

---

pos 3'->5'	pos 5'->3'	phase	strand	confidence	5' intron exon 3'
3229	710	1	-	0.16	GTCTCCCCAG^TAGCTAGGAC
3226	713	1	-	0.26	TCCCCAGTAG^CTAGGACTAT
2745	1194	2	-	0.07	CTCTTTAAAG^CTTGTATTAT
2733	1206	2	-	0.18	TGTATTATAG^TTCTTCCTCA
2722	1217	1	-	0.34	TCTTCCTCAG^AGCAGTTGCT
2720	1219	0	-	0.19	TTCCTCAGAG^CAGTTGCTAG
2717	1222	0	-	0.25	CTCAGAGCAG^TTGCTAGACA
2710	1229	1	-	0.17	CAGTTGCTAG^ACAGCATAAA
2706	1233	2	-	0.07	TGCTAGACAG^CATAAAGAAG
2483	1456	1	-	0.14	TTGTCCTCAG^ACATTCGGAA
2344	1595	2	-	0.48	TCATTCCTAG^AGTGAAGTAA
2337	1602	0	-	0.07	TAGAGTGAAG^TAACTCTGTC
2325	1614	0	-	0.18	ACTCTGTCAG^AGGAGCTGTG
2323	1616	2	-	0.18	TCTGTCAGAG^GAGCTGTGGC
2320	1619	2	-	0.19	GTCAGAGGAG^CTGTGGCTCC
2305	1634	2	-	0.19	GCTCCCTCAG^CTTCAATAGC
2296	1643	2	-	0.18	GCTTCAATAG^CTTCTGCAGC
2287	1652	2	-	0.17	GCTTCTGCAG^CTTCCTTGTC
1909	2030	0	-	0.33	TCCCCTCTAG^GCACCCATAA
1679	2260	0	-	0.17	TGGTATTTAG^TCCTCTGATA
1644	2295	2	-	0.18	ACATCCCGAG^CTAGGATGTG
1640	2299	0	-	0.07	CCCGAGCTAG^GATGTGAAGG
936	3003	1	-	0.33	TTCTTCCTAG^AAAAGAGATT
593	3346	0	-	0.25	ATATTCTTAG^GTCCATGAAA
315	3624	1	-	0.43	TTCTCTGCAG^CCATAGAAAT
272	3667	2	-	0.36	TTGTCATTAG^CTCTTCAGGA
264	3675	1	-	0.23	AGCTCTTCAG^GAAGACGGAT

CUTOFF values used for confidence:

Highly confident donor sites (H): 95.0 %
Nearly all true donor sites: 50.0 %

Highly confident acceptor sites (H): 95.0 %
Nearly all true acceptor sites: 20.0 %

ASSP Results

Sequence length: 3938 bp
Acceptor site cutoff: 2.2
Donor site cutoff: 4.5

					Activations**		
Position (bp)	Putative splice site	Sequence	Score*	Intron GC*	Alt./Cryptic	Constitutive	Confidence**
58	Alt. isoform/cryptic donor	GCACCTTTGCgtgagcaggg	5.235	0.557	0.878	0.095	0.892
67	Alt. isoform/cryptic donor	CGTGAGCAGGgtgccattcc	5.752	0.557	0.905	0.071	0.922
112	Alt. isoform/cryptic acceptor	tgcacatcagGATACCCAGC	4.315	0.500	0.752	0.234	0.688
136	Alt. isoform/cryptic donor	ACGTCCATGGgtgggacaca	7.535	0.414	0.757	0.184	0.757
159	Alt. isoform/cryptic donor	GCAATTTGTGgtaggtaaat	9.767	0.371	0.662	0.256	0.613
163	Alt. isoform/cryptic donor	TTTGTGGTAGgtaaattctt	10.089	0.357	0.785	0.149	0.810
270	Alt. isoform/cryptic acceptor	cttcctgaagAGCTAATGAC	6.427	0.443	0.788	0.204	0.741
282	Constitutive donor	TAATGACAAAgtaaataaat	9.298	0.343	0.295	0.617	0.522
321	Alt. isoform/cryptic acceptor	atggctgcagAGAAAATAAG	6.897	0.357	0.776	0.215	0.723
377	Alt. isoform/cryptic donor	CCTTCACATGgtcagtctta	8.625	0.371	0.678	0.257	0.621
392	Alt. isoform/cryptic donor	TCTTACAAAGgttgggttag	7.882	0.386	0.719	0.216	0.700
397	Alt. isoform/cryptic donor	CAAAGGTTGGgttaggtgtt	5.832	0.386	0.905	0.065	0.928
454	Alt. isoform/cryptic acceptor	acttccttagGAAGAGGTAG	5.075	0.371	0.502	0.482	0.040
459	Alt. isoform/cryptic donor	TTAGGAAGAGgtagagtcat	9.396	0.371	0.708	0.218	0.693
499	Alt. isoform/cryptic acceptor	gtaatttcagAGCCTCTTAC	5.913	0.371	0.795	0.191	0.760
568	Alt. isoform/cryptic donor	TATCTTTTCTgtgagttaaa	8.948	0.314	0.810	0.144	0.823
670	Alt. isoform/cryptic donor	TTGATACAAAgtttgtgtct	5.614	0.286	0.831	0.124	0.851
685	Alt. isoform/cryptic donor	TGTCTTAAAAgtagcttcat	6.560	0.300	0.834	0.119	0.857
687	Alt. isoform/cryptic acceptor	gtcttaaaagTAGCTTCATT	2.798	0.329	0.874	0.122	0.861
700	Alt. isoform/cryptic donor	TTCATTAAAAgtatagtcta	8.282	0.286	0.873	0.091	0.896
732	Alt. isoform/cryptic acceptor	gatttctcagACTTTAAGAC	8.976	0.286	0.829	0.164	0.802
740	Alt. isoform/cryptic acceptor	agactttaagACCTTATTAG	2.915	0.286	0.933	0.064	0.932
749	Alt. isoform/cryptic donor	ACCTTATTAGgttagtttag	10.810	0.386	0.775	0.165	0.787
750	Constitutive acceptor	accttattagGTTAGTTTAG	2.291	0.271	0.397	0.580	0.316
820	Alt. isoform/cryptic donor	GTTGCTTTGTgtatgtactc	5.518	0.414	0.833	0.118	0.858
863	Alt. isoform/cryptic donor	ATTTATTACTgttggtattg	5.460	0.400	0.865	0.100	0.885
888	Constitutive donor	TCTCCATGAGgtgacttaat	10.075	0.343	0.405	0.502	0.194
940	Constitutive acceptor	tcttttctagGAAGAAGAGA	7.160	0.386	0.282	0.703	0.599
944	Alt. isoform/cryptic acceptor	ttctaggaagAAGAGAGTTT	4.179	0.400	0.885	0.109	0.877
963	Alt. isoform/cryptic donor	TTGTGTCCTTgtaagaatca	7.545	0.286	0.863	0.091	0.894
969	Alt. isoform/cryptic acceptor	tccttgtaagAATCAAGTTA	3.409	0.357	0.682	0.296	0.566

974	Alt. isoform/cryptic donor	TAAGAATCAAgttatttata	4.752	0.314	0.923	0.054	0.942
997	Alt. isoform/cryptic donor	GCTGCTAAATgtagcagaat	5.364	0.343	0.900	0.069	0.924
1053	Alt. isoform/cryptic donor	GAAACAGATGgtacttacat	8.008	0.386	0.718	0.215	0.700
1121	Alt. isoform/cryptic donor	TCTTGGAAGAgtgaggagtg	7.981	0.414	0.775	0.171	0.779
1152	Alt. isoform/cryptic donor	TGGCAACTCGgttagtttta	8.184	0.314	0.861	0.106	0.877
1164	Alt. isoform/cryptic acceptor	ttagttttagCAGTTGGTGC	3.198	0.443	0.753	0.237	0.685
1167	Alt. isoform/cryptic acceptor	gttttagcagTTGGTGCTAA	3.258	0.443	0.810	0.183	0.774
1304	Alt. isoform/cryptic acceptor	ttttacccagAATGATTGGT	6.290	0.314	0.660	0.327	0.504
1322	Alt. isoform/cryptic donor	TGCCCTTACTgtaggaaagt	4.572	0.529	0.917	0.057	0.937
1327	Alt. isoform/cryptic acceptor	cttactgtagGAAAGTTGTC	6.332	0.371	0.545	0.441	0.191
1349	Alt. isoform/cryptic acceptor	tgggattcagCGCTGTATGG	3.221	0.386	0.780	0.211	0.729
1415	Alt. isoform/cryptic acceptor	gtgctgccagGAGGCCTCTT	2.380	0.543	0.730	0.256	0.649
1430	Constitutive acceptor	ctcttttcagTGACATTCAA	3.920	0.543	0.439	0.544	0.193
1494	Alt. isoform/cryptic donor	GGAACTTCGGgtatataatg	6.542	0.300	0.658	0.263	0.601
1503	Alt. isoform/cryptic donor	GGTATATAATgtaaataatt	7.504	0.329	0.835	0.111	0.867
1546	Alt. isoform/cryptic acceptor	aactttacagAGGAGAATGC	5.029	0.314	0.832	0.162	0.806
1586	Alt. isoform/cryptic acceptor	cttttggcagGAGGGGGTCC	10.286	0.371	0.508	0.480	0.055
1644	Constitutive acceptor	cacatcctagCTCGGGATGT	6.194	0.514	0.434	0.552	0.214
1705	Constitutive donor	GTTTGTGCAGgtatgtttta	14.433	0.271	0.135	0.814	0.834
1706	Constitutive acceptor	gtttgtgcagGTATGTTTTA	8.096	0.429	0.371	0.611	0.393
1755	Alt. isoform/cryptic acceptor	aaatttccagATTGTAATGA	2.843	0.343	0.584	0.398	0.319
1757	Alt. isoform/cryptic donor	TTTCCAGATTgtaatgacta	4.613	0.257	0.868	0.091	0.895
1780	Alt. isoform/cryptic acceptor	aacatttcagAAAATTAGGG	2.397	0.286	0.917	0.080	0.913
1842	Alt. isoform/cryptic donor	ACATTTTTTGgtcagtaaga	8.894	0.414	0.806	0.149	0.816
1846	Alt. isoform/cryptic donor	TTTTTGGTCAgtaagagaaa	6.546	0.429	0.824	0.130	0.843
1848	Alt. isoform/cryptic acceptor	ttttggtcagTAAGAGAAAC	3.244	0.300	0.748	0.242	0.676
1986	Alt. isoform/cryptic acceptor	caaatcttagATCAGTTAGA	5.819	0.557	0.768	0.220	0.713
1989	Alt. isoform/cryptic donor	TCTTAGATCAgttagagctg	5.047	0.386	0.938	0.043	0.954
2054	Alt. isoform/cryptic acceptor	agtgctccagAGCATTAAAC	2.487	0.386	0.745	0.243	0.674
2102	Alt. isoform/cryptic donor	ATTTACTACAgtgtgaatgc	5.037	0.500	0.828	0.130	0.843
2104	Alt. isoform/cryptic acceptor	tttactacagTGTGAATGCC	6.346	0.357	0.679	0.308	0.547
2147	Alt. isoform/cryptic donor	TTGCACCACAgtgggggct	5.999	0.386	0.736	0.200	0.728
2149	Alt. isoform/cryptic acceptor	tgcaccacagTGGGGGGCTT	4.558	0.386	0.948	0.048	0.949
2171	Alt. isoform/cryptic acceptor	catgttttagCTTTAGATTT	4.840	0.500	0.764	0.230	0.699
2177	Alt. isoform/cryptic acceptor	ttagctttagATTTAATTAG	6.039	0.486	0.551	0.440	0.201
2186	Alt. isoform/cryptic donor	ATTTAATTAGgttttgtttg	5.347	0.414	0.949	0.033	0.965
2187	Alt. isoform/cryptic acceptor	atttaattagGTTTTGTTTG	2.925	0.429	0.785	0.203	0.742
2211	Constitutive acceptor	ttctccttagCTGCTTTATT	8.757	0.400	0.356	0.630	0.436
2277	Alt. isoform/cryptic acceptor	acttgctcagGACAAGGAAG	2.875	0.457	0.551	0.424	0.230
2332	Alt. isoform/cryptic acceptor	cctctgacagAGTTACTTCA	5.045	0.529	0.900	0.096	0.893
2348	Constitutive acceptor	ttcactctagGAATGAAGGT	7.239	0.500	0.342	0.640	0.466
2355	Alt. isoform/cryptic donor	AGGAATGAAGgtgtgggtaa	9.086	0.400	0.852	0.109	0.872

2357	Alt. isoform/cryptic donor	GAATGAAGGTgtgggtaagt	6.381	0.414	0.924	0.054	0.942
2361	Alt. isoform/cryptic donor	GAAGGTGTGGgtaagtaaaa	11.108	0.400	0.769	0.167	0.783
2426	Alt. isoform/cryptic acceptor	tttcctcaagGGCCTTTTTC	7.368	0.400	0.951	0.044	0.953
2450	Constitutive acceptor	tgtctcttagCGACATATGC	8.193	0.414	0.306	0.680	0.550
2547	Constitutive acceptor	ctctcttcagAACAGAGCCA	8.572	0.471	0.218	0.774	0.718
2552	Alt. isoform/cryptic acceptor	ttcagaacagAGCCAATGGC	4.937	0.471	0.702	0.286	0.593
2571	Alt. isoform/cryptic donor	TTGGAATGAGgtagggaaat	8.898	0.429	0.620	0.293	0.528
2581	Alt. isoform/cryptic donor	GTAGGGAAATgtgagcagtt	8.103	0.414	0.962	0.026	0.973
2600	Alt. isoform/cryptic donor	TATTTATCTGgtagtttcct	7.373	0.400	0.846	0.113	0.867
2605	Alt. isoform/cryptic acceptor	tatctggtagTTTCCTAGAG	4.964	0.443	0.876	0.114	0.869
2613	Alt. isoform/cryptic acceptor	agtttcctagAGCAGGTATG	3.977	0.429	0.823	0.165	0.800
2617	Alt. isoform/cryptic donor	CCTAGAGCAGgtatggcagc	10.905	0.400	0.846	0.109	0.871
2618	Alt. isoform/cryptic acceptor	cctagagcagGTATGGCAGC	4.100	0.443	0.686	0.301	0.562
2714	Alt. isoform/cryptic acceptor	tgctgtctagCAACTGCTCT	4.946	0.357	0.723	0.268	0.630
2858	Alt. isoform/cryptic donor	TCAAAAGGATgtaaggaaag	7.951	0.300	0.731	0.201	0.725
2970	Alt. isoform/cryptic acceptor	ttttcttcagCATTTGTCCT	7.246	0.200	0.717	0.266	0.629
2983	Alt. isoform/cryptic acceptor	ttgtcctcagTACAGGTGGT	4.222	0.257	0.721	0.269	0.627
2987	Alt. isoform/cryptic donor	CTCAGTACAGgtggttcctt	7.733	0.300	0.709	0.225	0.682
2988	Alt. isoform/cryptic acceptor	ctcagtacagGTGGTTCCTT	7.983	0.271	0.548	0.438	0.201
3052	Alt. isoform/cryptic acceptor	cattctatagAGATCATTGA	6.858	0.314	0.613	0.369	0.398
3063	Alt. isoform/cryptic donor	ATCATTGATGgtacacagac	5.783	0.371	0.736	0.205	0.721
3194	Constitutive acceptor	ccatctttagCTGGGCATGG	2.230	0.471	0.468	0.513	0.086
3226	Alt. isoform/cryptic acceptor	atagtcctagCTACTGGGGA	3.228	0.500	0.880	0.111	0.874
3266	Alt. isoform/cryptic acceptor	ttgaacccagGAGTTAACAG	4.278	0.586	0.843	0.150	0.822
3340	Constitutive donor	CAAATTACCAgtgagtagtg	12.949	0.357	0.165	0.777	0.788
3347	Alt. isoform/cryptic donor	CCAGTGAGTAgtgtgttact	5.761	0.386	0.833	0.118	0.858
3372	Constitutive acceptor	tttttaatagGCATCTTATT	5.332	0.271	0.405	0.578	0.300
3462	Alt. isoform/cryptic acceptor	tctgtcttagTTAATGTCAG	8.382	0.457	0.656	0.330	0.498
3466	Alt. isoform/cryptic donor	CTTAGTTAATgtcagctttg	5.022	0.443	0.887	0.081	0.908
3472	Alt. isoform/cryptic acceptor	ttaatgtcagCTTTGTCTGT	2.595	0.429	0.950	0.046	0.951
3486	Alt. isoform/cryptic acceptor	gtctgtccagCTGCTCAGGC	7.615	0.457	0.718	0.270	0.625
3494	Alt. isoform/cryptic acceptor	agctgctcagGCTAAAACTT	4.235	0.443	0.639	0.350	0.452
3533	Alt. isoform/cryptic acceptor	ctatcagcagCTCCTGTTTG	3.426	0.400	0.932	0.065	0.931
3541	Alt. isoform/cryptic donor	GCTCCTGTTTgtgggtaggc	4.600	0.300	0.731	0.208	0.715
3545	Constitutive donor	CTGTTTGTGGgtaggcattt	8.332	0.300	0.341	0.569	0.401
3550	Alt. isoform/cryptic acceptor	ttgtgggtagGCATTTTGCC	3.263	0.443	0.782	0.208	0.734
3583	Alt. isoform/cryptic acceptor	ttttttttaaACTGCTATAT	2.902	0.314	0.838	0.148	0.824
3599	Alt. isoform/cryptic acceptor	atatctctagCATGTAGAAC	5.148	0.329	0.678	0.308	0.546
3606	Alt. isoform/cryptic acceptor	tagcatgtagAACAGTGCCT	3.112	0.300	0.801	0.188	0.765
3630	Alt. isoform/cryptic donor	CACATAATAGgtgcttaata	6.386	0.286	0.729	0.206	0.718
3661	Alt. isoform/cryptic donor	GAAAGAACAAgtcagtgagt	7.173	0.329	0.887	0.085	0.904
3665	Alt. isoform/cryptic donor	GAACAAGTCAgtgagtattt	12.053	0.329	0.678	0.256	0.623

3680	Alt. isoform/cryptic donor	TATTTTTAATgtgaggtgca	7.371	0.357	0.941	0.041	0.957
3685	Alt. isoform/cryptic donor	TTAATGTGAGgtgcaaagag	5.148	0.329	0.963	0.026	0.973
3705	Alt. isoform/cryptic donor	AAAAAAAAATgtatctttga	6.133	0.357	0.880	0.081	0.908
3716	Alt. isoform/cryptic donor	TATCTTTGAGgtgtggagtt	9.818	0.343	0.603	0.313	0.482
3750	Alt. isoform/cryptic acceptor	attttctaagCATTTGTGTA	5.333	0.343	0.787	0.210	0.733
3794	Alt. isoform/cryptic donor	TAATCTGAAAgtatgcttta	6.032	0.271	0.910	0.062	0.932
3878	Constitutive acceptor	gtttatctagACTGCTGATC	4.050	0.286	0.453	0.519	0.126
3911	Alt. isoform/cryptic acceptor	tggtgcccagGGAGAACCCC	2.455	0.414	0.528	0.453	0.141

* Scores of the pre-processing models reflecting splice site strength, i.e. a PSSM for putative acceptor sites, and an MDD model for putative donor sites. Intron GC values correspond to 70 nt of the neighbouring intron.

** Activations are output values of the backpropagation networks used for classification. High values for one class with low values of the other class imply a good classification. Confidence is a simple measure expressing the differences between output activations. Confidence ranges between zero (undecided) to one (perfect classification).

Reference: Wang M. and Marin A. 2006. Characterization and Prediction of Alternative Splice Sites. Gene 366: 219-227.

12 Appendix III: Zusammenfassung (deutsch)

Seit der Erfindung der Antisense Moleküle gab es zahlreiche Versuche diese für therapeutische Anwendungen zu verwenden[1]. Die FDA-Zulassung von Fomivirsen[2], Pegaptanib[3] und Mipomersen[4] hebt das große Potential von Antisense Molekülen hervor. Dennoch ist der Erfolg - verglichen mit den Anstrengungen - bescheiden[5]. Da jedoch ständig neue Modifikationen an den Molekülen vorgenommen werden, gibt es einen Bedarf an zuverlässigen Assays um diese zu testen. Außerdem ist es wichtig die Targeting-Strategien zu verbessern. Da es nun theoretisch möglich ist jedes Gen zu blocken, ist es sehr wichtig die besten Möglichkeiten zu kennen sobald ein gutes Antisensemolekül gefunden ist.
In Bezug auf potentielle neue Tumortherapien ist der Wnt-Signalweg von großer Bedeutung, da er zahlreiche interessante Zielgene aufweist[6]. Dabei spielt β-Catenin eine Schlüsselrolle. Neben seiner zentralen Funktion im Wnt-Signalweg ist es bei zahlreichen Krebsarten überexprimiert[7,8]. Wir haben in diesem Projekt einen splicebasierten Reporterassay designed und optimiert, um eine neue Antisense Strategie für die Anwendung von PNAs zum Targeting von β-catenin in Tumorzellen zu testen. Nachdem der Asssay eine zuverlässige Quantifizierung der Antisense-Effekte ermöglichte, wurde er verwendet um zu mehrere PNAs mit verschiedenen Targetsites auf β-catenin zu screenen. Dadurch offenbarte sich eine neue Strategie. Durch Targeting des Splicedonors von Exon 13 von β-catenin entsteht eine verkürzte Version des Proteins, die ihre wichtige Interaktion mit Tcf/Lef Porteinen behält. Dafür konkurriert das verkürzte Molekül mit der Wildtyp-Version von β-catenin, was zu einem dominant negativen Effekt führt. Diese Strategie ist anwendbar für alle Moleküle, die für einen Splice-Block geeignet sind. Darin liegt großes Potential für zukünftige Projekte mit β-catenin als Targetgen.

Eine der größten Herausforderungen in der Optimierung von Antisense Molekülen ist die Verbesserung der Bindungsaffinität. Eine einfache Verlängerung der Oligonucleotide kann die Bindungsaffinität nur bis zu einem bestimmten Grad verbessern[9]. In einem zweiten Projekt habe ich getestet, ob ein neues Design mit verbundenen kurzen Oligonucleotiden (Catemer Subunits) die Bindungsaffinität erhöhen kann, ohne dabei an Spezifität zu verlieren. Das Prinzip wurde mit Hilfe von fluoreszenzmarkierten Oligonucleotiden und Schmelzkurven getestet. Die Bindungsaffinität wurde durchaus mit einem höheren Grad an Interaktion zwischen den Catemer Untereinheiten höher.
Diese Arbeit zeigt einen neuen Reporter Assay für die genaue Detektion von Antisense-Effekten in Tumorzellen, sowie eine interessante Targeting-Startegie für β-catenin, die in zukünftigen Projekten angewendet werden kann. Erste Schritte wurden für die Verbesserung der Bindungsaffinität von Antisensemolekülen

gemacht. Diese zeigen eine interessante Option für zukünftige Forschungsprojekte.